HHS Public Access

Author manuscript

Prog Polym Sci. Author manuscript; available in PMC 2022 December 02.

Published in final edited form as:

Prog Polym Sci. 2019 November ; 98: . doi:10.1016/j.progpolymsci.2019.101147.

Stimuli-responsive hydrogels for manipulation of cell microenvironment: From chemistry to biofabrication technology

Mohamed Alaa Mohamed[a,b], **Afsoon Fallahi**[c,d,e], **Ahmed M.A. El-Sokkary**[b], **Sahar Salehi**[f], **Magda A. Akl**[b], **Amin Jafari**[a], **Ali Tamayol**[g,*], **Hicham Fenniri**[h], **Ali khademhosseini**[i,j,**], **Stelios T. Andreadis**[a,*], **Chong Cheng**[a,*]

[a]Department of Chemical and Biological Engineering, University at Buffalo, The State University of New York, Buffalo, NY 14260, USA

[b]Chemistry Department, Faculty of Science, Mansoura University, Mansoura, 35516, Egypt

[c]Biomaterials Innovation Research Center, Department of Medicine, Brigham and Women's Hospital, Harvard Medical School, Boston, MA 02139, USA

[d]Harvard-MIT Division of Health Sciences and Technology, Massachusetts Institute of Technology, Cambridge, MA 02139, USA

[e]Wyss Institute for Biologically Inspired Engineering, Harvard University, Boston, MA 02115, USA

[f]Department of Biomaterials, Faculty of Engineering Science, University of Bayreuth, Bayreuth 95440, Germany

[g]Department of Mechanical and Materials Engineering, University of Nebraska, Lincoln, NE 68588, USA

[h]Department of Chemical Engineering, Northeastern University, Boston, MA 02115, USA

[i]Department of Chemical and Biomolecular Engineering, Department of Bioengineering, Department of Radiology, California NanoSystems Institute (CNSI), University of California, Los Angeles, CA 90095, USA

[j]Center of Nanotechnology, Department of Physics, King Abdulaziz University, Jeddah 21569, Saudi Arabia

Abstract

Native tissues orchestrate their functions by complex interdependent cascades of biochemical and biophysical cues that vary spatially and temporally during cellular processes. Scaffolds with well-tuned structural, mechanical, and biochemical properties have been developed to guide cell behavior and provide insight on cell-matrix interaction. However, static scaffolds very often fail to mimic the dynamicity of native extracellular matrices. Stimuli-responsive scaffolds have emerged as powerful platforms that capture vital features of native tissues owing to their ability to change chemical and physical properties in response to cytocompatible stimuli, thus enabling on-

*Corresponding authors. atamayol@unl.edu (A. Tamayol), sandread@buffalo.edu (S.T. Andreadis), ccheng8@buffalo.edu (C. Cheng).
**Corresponding author at: Department of Chemical and Biomolecular Engineering, Department of Bioengineering, Department of Radiology, California NanoSystems Institute (CNSI), University of California, Los Angeles, CA 90095, USA. khademh@ucla.edu (A. Khademhosseini).

demand manipulation of cell microenvironment. The vast expansion in biorthogonal chemistries and stimuli-responsive functionalities has fuelled further the development of new smart scaffolds that can permit multiple irreversible or reversible spatiotemporal modulation of cell-directing cues, thereby prompting in-depth studies to interpret the decisive elements that regulate cell behavior. Integration of stimuli-responsive hydrogels with current biofabrication technologies has allowed the development of dynamic scaffolds with organizational features and hierarchical architectures similar to native tissues. This review highlights the progress achieved using stimuli-responsive hydrogels in fundamental cell biology studies, with particular emphasis on the interplay between chemistry, biomaterials design, and biofabrication technologies for manipulation of cell microenvironment.

Keywords

Stimuli-responsive hydrogels; Cellular microenvironment; Cell-biomaterial interaction; Spatiotemporal modulation; Dynamic biomaterials; Biofabrication technology

1. Introduction

Cellular microenvironment plays a crucial role in the regulation of cell behavior. Cells reside within intricate microenvironments consisting of extracellular matrix (ECM), soluble factors, and neighboring cells [1]. They interact dynamically with and reconstitute the surrounding ECM during development, tissue regeneration post-injury or disease, or to maintain tissue homeostasis [2-7]. A variation of composition and structure of ECM by cell-mediated remodeling alters the presentation of signaling molecules and changes biophysical properties spatially and temporally [8]. Cell-mediated cleavage of proteolytic domains of ECM proteins by secretion of matrix metalloproteinases (MMPs), collagenases, plasmin, and elastases is critical for cell migration. For example, endothelial and tumor cell invasion in collagen is governed by activation of MMP-1 and MMP-8 collagenases [9,10]. Moreover, following injury, cells degrade the provisional fibrin matrix by MMP enzymes to allow deposition of new ECM proteins [7]. At the same time, cells also secret MMP inhibitors to regulate ECM degradation and remodeling in order to promote regeneration [11]. Under certain conditions such as chronic wounds, aging or certain diseases, the balance between ECM production and degradation is lost, resulting in overproduction of ECM, excessive ECM crosslinking, and cell contraction, ultimately leading to fibrosis and loss of tissue function [12-14]. For instance, excessive deposition of ECM by the fibroblasts of the heart may result in myocardial fibrosis, the hallmark of hypertrophic cardiomyopathy, a well-known disease that causes arrhythmias and heart failure [15]. Also, matrix overproduction and stiffening during breast cancer progression promote integrin clustering and tumor invasion [16,17].

Besides temporal modulation of ECM stiffness, the spatial physical gradients of ECM properties (e.g. stiffness, porosity, and topography) also play a significant role during tissue development, disease progression, and wound healing [13]. For instance, stiffness gradients at the injured sites guide directional cell migration (durotaxis) to promote wound healing [18]. Bone matrix is characterized by inherent porosity gradients, spanning from compact

(5–30% porosity) to spongy (30–90% porosity) structure [19]. In addition, biophysical forces such as shear stress and strain experienced by blood and vascular cells due to blood flow in vasculature; cyclic tensile stress and strain experienced by cardiac and lung cells; and dynamic compressive stress acting on bone and cartilage cells due to body movement are critical determinants of cell behavior [13]. For example, the application of tensile stress and strain promotes migration of fibroblast and endothelial cells [20-23], differentiation of myoblast into myotubes [24,25], maturation of cardiomyocytes [26], and differentiation of mesenchymal stem cells into smooth muscle cell lineages, [27] while compressive stress induces mesenchymal stem cell differentiation into chondrocytes [28].

Similar to physical cues, biochemical cues such as soluble (e.g., chemokines, cytokines, and growth factors) or insoluble signals (e.g., binding domains of ECM) are constantly regulated spatially and temporally by cells to enable specific cell behavior such as migration, proliferation, and differentiation [7]. For example, in vivo differentiation of human mesenchymal stem cells toward chondrocytes is associated with downregulation of fibronectin (FN) at day 7–12 of differentiation by upregulation of FN-cleavage enzyme, MMP-13 [29]. In addition, the concentration gradient of soluble factors is well-regulated in space and time by on-demand release and sequestration [30]. For instance, vascular endothelial growth factor (VEGF) has been demonstrated to promote endothelial cell proliferation, while VEGF concentration gradient guides the directional growth of vessels toward hypoxic sites [31]. Moreover, chemical gradients of morphogens such as hedgehog, bone morphogenetic protein (BMP), transforming growth factor-β (TGF-β), and fibroblast growth factors (FGFs) control differentiation during embryogenesis [19,32,33]. Similarly, chemical gradients regulate the direction of axonal growth [34], as well as the migration of leukocytes and fibroblasts to sites of injury [19,35]. Collectively, a plethora of biological studies suggest that, in order to mimic the cell microenvironment and engineer tissues that recapitulate the structure and function of their native counterparts, it is necessary to engineer biomaterials whose biophysical and biochemical cues can be modulated in space and time.

The progress toward understanding cell-ECM interaction has long been devoted to studying the cellular behavior in preprogrammed static three-dimensional (3D) scaffolds, which are designed to mimic certain biophysical and biochemical features of native ECMs. However, native ECMs are inherently heterogeneous and constantly undergo dynamic remodeling mediated by cells to enable specific cell event [8,36-38]. Therefore, traditionally developed 3D scaffolds with temporally homogeneous cues are unable to provide sustainable guidance to cells. Indeed, most of the reported 3D scaffolds direct cell fate only at specific time points, and thereafter the scaffolds lose their instructive features because the presented signals are no longer effective in guiding the cells at new time points.

Benefited from the advances in biorthogonal chemistries and the growing library of stimuli-responsive functionalities, there has been a substantial paradigm shift in the design criteria of 3D scaffolds. Accordingly, development of stimuli-responsive scaffolds has attracted increasing attention, because they can emulate to a great extent the dynamic nature of native ECMs by undergoing unidirectional or cyclical structural changes with physiologically benign stimuli. Moreover, stimuli-responsive scaffolds can permit user-defined spatiotemporal modulation of biophysical and biochemical cues to direct cell

behavior, paving the way to understand complex interdependent cell signaling. In addition, integration of stimuli-responsive materials with the state-of-art biofabrication technologies has enabled engineering of complexity of cell microenvironment over multiple length scales, and opened new avenues toward the development of functional tissue-like replacements with clinically relevant importance. Furthermore, scaffolds with tunable sensitivity to pH, temperature, light, mechanical, and electrical stimuli have been widely exploited for sustainable and on-demand delivery of bioactive cues to cells, as well as the generation of biochemical gradients to spatially regulate cell growth. Finally, reversible modulation of biophysical cues, such as mechanical stiffness and stress/strain behavior, has also been achieved using stimuli-responsive 3D platforms.

Stimuli-responsive hydrogels have received great attention in cell biology and tissue engineering (TE) fields because of their capability to change their physical and chemical properties in response to user-defined stimuli, allowing modulation of cell microenvironment. Moreover, hydrophilicity and unique physical properties of hydrogels permit diffusion of oxygen, nutrients, and bioactive molecules. In addition, hydrogels are crosslinked macromolecules that retain large amounts of water, thereby acting as reservoirs of signaling molecules that influence cell fate [39,40]. Hydrogels can be classified into two major categories: chemically crosslinked hydrogels in which polymer chains are crosslinked through covalent bonds; and physically crosslinked hydrogels in which 3D structures are formed via weak forces like hydrogen bonding, hydrophobic and ionic interactions, metal-ligand coordination, host-guest intercalation, and stereocomplexation [41]. The materials used in stimuli-responsive hydrogel formation can be natural, synthetic or hybrids of natural and synthetic. The most common natural materials used for hydrogel formation include polysaccharides (such as chitosan, alginate, hyaluronic acid (HA), dextran, and agarose) and proteins (such as collagen, fibrin, elastin, and gelatin) [42]. Natural materials are usually biocompatible and biodegradable, containing biological signals that affect cell behaviors; however, they typically possess poor mechanical properties, with batch-to-batch variability. Importantly, protein-based materials exhibit a complex myriad of bioactive functionalities, resulting in difficulties in defining which bioactive signal elicits a specific cell response [43]. In contrast, synthetic materials offer reproducible and tunable physical, chemical and mechanical properties, but lack biological cues that promote tissue formation and regeneration [44]. Therefore, combining natural and synthetic materials is an intriguing research area that may open avenues toward fabrication of biomimetic scaffolds with tunable mechanical and biological properties [45].

Integration of stimuli-responsive materials with current biofabrication techniques including lithography, micromolding, microcontact printing, 3D bioprinting modalities, and textile fabrication methods have emerged as promising tools for the construction of 3D scaffolds that mimic the architecture of native tissues [46-49]. Thus, such integration provides an opportunity to manipulate the structural and organizational features of scaffolds to direct cell behavior. Some of these techniques can be linked to imaging modalities to reveal recreated tissue architecture [50,51]. Recent studies have demonstrated the development of 3D constructs with organizational features similar to aortic valve, ear, skin, and blood vessels [52]. However, significant efforts are still needed to improve the spatial resolution and vertical buildup of the scaffolds. Furthermore, the development of new biomaterials

that meet the requirement of biofabrication techniques, such as proper viscosity and rapid crosslinking process, is also important.

The main goal of this review is to summarize the state-of-art stimuli-responsive hydrogels that recapitulate critical features of native ECMs and can be modulated with external and/or internal stimuli to alter cell microenvironment, thereby enabling real-time manipulation of cellular response as well as revealing cell-directing cues. The review highlights the multifaceted perspectives of the stimuli-responsive hydrogel, spanning from biomaterials chemistry to biofabrication technology. Specifically, the Introduction section highlights ECM dynamics and the importance of stimuli-responsive hydrogels in studies to understand complex cellular processes. Then, the next section summarizes the chemistry toolsets employed in fabricating chemically and physically crosslinked scaffolds, as well as imparting bioactivity to the design of the scaffolds. Subsequently, the third section discusses various categories of stimuli-responsive hydrogels including pH-, thermo-, photo-, electro, mechano-responsive platforms, with particular emphasis on the stimuli-responsive functionalities and structure-property relationship. Afterward, the fourth section highlights the vital role of stimuli-responsive hydrogels in the modulation of biochemical and biophysical cell-directing cues. Manipulation of cell attachment using stimuli-responsive two-dimensional (2D) substrates, and controlled modulation of structural, mechanical, and biochemical characteristics in stimuli-sensitive 3D platforms, are reviewed in this section. The fifth section highlights the integration of stimuli-responsive hydrogels with recent biofabrication technologies including microcontact printing, micromolding, lithography, textile fabrication technologies and bioprinting modalities, for building stimuli-responsive constructs in vitro with geometrical and dynamic features similar to native tissue. Given the multidisciplinary nature of the research involving stimuli-responsive scaffolds, it is impossible to include a discussion with specific details on every aspect of such stimuli-responsive platforms in this review.

2. Hydrogels

Native ECMs are mainly composed of two components: 1) proteins, such as collagen, laminin, fibronectin, and elastin; and 2) glycosaminoglycans (GAGs), such as sulfated heparin, chondroitin, and keratin, which bind to the protein backbone to form proteoglycan [53]. The negatively charged GAGs fill the interstitial spaces within ECMs and sequester soluble signaling molecules (e.g., growth factors) via non-covalent ionic interaction and hydrogen bonding [54]. In addition, ECMs incorporate cell binding motifs that are critical for cell adhesion via binding to cell surface integrins, as well as linking the cells' cytoskeleton to ECMs which enable signal transduction between cells and their microenvironment [55,56]. Development of in vitro cell culture platforms that recapitulate many aspects of native ECMs and can be modulated internally or externally is crucial for understanding complex cellular processes. To achieve this goal, hydrogels with tunable network architectures must be developed to mimic structural, mechanical, and biological features of native tissues [57]. In this section, we will first introduce the chemistries involved in the construction of chemically and physically crosslinked hydrogels. In the following section, the development of stimuli-responsive scaffolds will be discussed. After that, the

modulation of physicochemical and biological characteristics of 3D hydrogel scaffolds for manipulation of cell microenvironment will be presented.

2.1. Chemically crosslinked hydrogels

Chemical crosslinking involves the formation of a polymer network via covalent linkages between polymer chains. Various chemical reactions have been employed to synthesize covalently crosslinked hydrogels, such as radical polymerization, click reaction, enzyme-mediated reaction, and Schiff-base chemistry. Fig. 1 includes the most common chemical crosslinking strategies employed in the fabrication of 3D hydrogel scaffolds. The choice of crosslinking strategy and conditions defines the properties of the final products, such as swelling behavior, porosity, mechanical properties, and suitability for further modification [58]. Free radical polymerization is one of the most commonly used methods for the formation of covalently crosslinked hydrogels, generally using vinyl monomers or vinyl-functionalized polymers in the presence of crosslinker and radical initiator for polymerization. Controlling the molar feed ratio of monomers to initiator provides appropriate control over mechanical and physical properties. The main advantage of this strategy is the availability of a wide range of monomers, such as 2-hydroxyethyl methacrylate (HEMA), *N*-isopropylacrylamide (NIPAM), and poly(ethylene glycol) (PEG)-based monomers [59]. Moreover, acrylated/methacrylated natural polymers, such as methacrylated gelatin (GelMA), methacrylated hyaluronic acid (HA-MA), and methacrylated heparin, can be used for hydrogel formation with remarkable bioactivity [60,61]. On the other hand, the requirement of thermal- or photo-stimulation to initiate the crosslinking process can induce cytotoxicity [62]. It is worth to mention that several initiators can be used to initiate crosslinking process at mild conditions [63,64]. Difficulty in achieving well-ordered and homogeneous networks owing to the statistical character of the polymerization is another drawback [65].

Hydrogel formation by Schiff base chemistry involves a reaction between aldehyde and amino groups bearing polymers at mild conditions [66]. Aldehyde-containing natural polymers can be obtained through partial oxidation of polysaccharides (such as HA, dextran, chondroitin sulfate and gum arabic), and their subsequent reaction with amino group-bearing natural or synthetic polymers induces hydrogel formation [66,67]. Similarly, the reaction of aldehyde- or ketone-containing polymers with polymer incorporating hydroxylamine yields hydrogel via oxime bond formation, and the reaction occurs at an appreciable rate without using a catalyst [68]. Additionally, the reaction between isothiocyanate and hydroxyl or amino group of polymers is also used for hydrogel preparation under mild conditions [69].

Click reactions are highly efficient and robust reactions that can allow the formation of hydrogels with well-defined network under mild or even physiological conditions [70]. Click reactions include alkyne-azide cycloaddition, Diels-Alder reaction, thiol-ene reaction, and so on. Copper-catalyzed alkyne-azide cycloaddition is commonly used in bioconjugation, but the cytotoxicity of copper prevents its use in regenerative medicine [71-73]. Copper-free strain promoted alkyne-azide cycloaddition has been developed to synthesize non-cytotoxic PEG-based hydrogel [74]. Diels-Alder reaction is another class of click reaction that occurs between diene and dienophile to form substituted cyclohexene. It is commonly used for

hydrogel formation in aqueous solutions without employing catalysts [75]. However, the slow reaction kinetics prevents its use in processes that require rapidly formed hydrogels, e.g., in situ implantation [76]. Fast inverse electron demand Diels-Alder reaction provides a solution to this problem via the reaction of trans-cyclooctene with tetrazine [77]. “Thio” click chemistry is widely used in hydrogel formation, and it proceeds via base-catalyzed Michael addition or photo-initiated thiol-ene reaction [78]. In particular, the latter reaction is efficient, rapid and generally occurs under mild conditions. Another method of chemical crosslinking at ambient condition is native chemical ligation, which involves the reaction of thiol with thioesters [79].

Enzymatic crosslinking is another strategy for crosslinking of polymer chains at mild gelation conditions. Polymers with enzymatically reactive moieties like tyramine, tyrosine, dopamine, and aminophenol undergo rapid in situ gel formation upon oxidation using hydrogen peroxide in the presence of horseradish peroxidase (HRP) catalyst [80,81].

2.2. Physically crosslinked hydrogels

Several approaches have been employed to prepare physically crosslinked hydrogels, such as hydrogen bonding, metal-ligand coordination, host-guest intercalation, ionic interaction, stereocomplexation, and molecular self-assembly (Fig. 2) [82]. In addition, cooperative physical interactions, such as crystallization and heat triggered crosslinking, can also be employed in the crosslinking process to enhance hydrogel stability [83]. Here, we highlight the non-covalent forces, as essential physical toolsets for imparting dynamicity to hydrogel scaffolds, with particular emphasis on structure-property relationship. The vital role of these forces in the manipulation of cell behavior will be discussed in later sections.

2.2.1. Hydrogen bonding—Hydrogen bonding is the primary force behind the assembly of biological molecules, such as DNA, to form 3D structures with specific orientations. The interactions between hydrogen bonding motifs of nucleotide pairs provide stability of the DNA double helix [84]. In order to form hydrogels, multiple hydrogen bonds are required for crosslinking of the polymer chains [85]. Commonly, motifs with multivalent hydrogen bonding sites are used to form stable networks (Fig. 2A), whose stability often depends on the following factors: 1) type of solvent (it is easier to form hydrogels by hydrogen bonding in organic solvents than in aqueous system, due to the competition of water molecules for hydrogen bonding sites, which in turn, minimizes the interactions between chains); 2) nature of donors and acceptors (aromatic, alkyl), and the angle between them which determines association strength (180° angle allows maximum association); 3) the sequence of donor and acceptor that also affects the association constant [86]. Meijer et al. utilized the quadrupole hydrogen bonding motifs of ureidopyrimidinone to prepare physically crosslinked hydrogels through its conjugation to the terminals of 3-arm poly(propylene oxide-*co*-ethylene oxide). The resulting hydrogel displayed viscoelastic behavior, and its mechanical properties decreased significantly by adding a small amount of water [87]. Similarly, Hu et al. harnessed the strong hydrogen bonding between urethane-urethane linkages and urethane-ester linkages to develop hydrogels of high toughness, strength, and fatigue resistance, as well as water uptake of 75% [88]. Urea and guanine

have also been used as hydrogen bonding motifs, and incorporation of hydrophobic moieties to the polymer chains affects the stability and morphology of the resulting hydrogel [89,90].

2.2.2. Metal-ligand coordination—A supramolecular hydrogel is formed when two or more ligands, incorporated in a polymer chain, interact with metal ions to form coordination bonds (Fig. 2B) [91]. Appropriate choice of metal ion and ligand defines hydrogel stability, as the coordination bond strength varies significantly (0–400 kJ/mol) [86]. Schubert et al. demonstrated that terpyridine-bearing polymer complexed with Fe^{2+} to form a supramolecular hydrogel that was thermally stable up to 160 °C, whereas its complexation with Ru^{2+} increased thermal stability of the resulting hydrogel to 250 °C [86]. Finally, poly(acrylic acid) (PAA) complexation with Fe^{3+} yielded a photo-responsive network that underwent reversible dissolution upon treatment with light in the presence of oxygen [92].

2.2.3. Host-guest complexation—Host-guest complexation is a mode of physical interaction in which a cavity-bearing host molecule binds a guest molecule via a thermodynamically favorable interaction. For instance, α-, β-, γ-cyclodextrins (CDs) have cone-like structures with hydrophilic outer surface and hydrophobic internal cavity that can preferentially bind to hydrophobic molecules. Van der Waal forces and hydrophobic interactions are the major forces in host-guest complexation; however, other forces such as hydrogen bonding, the release of CD ring strain and solvent surface tension may also contribute to the complexation [93,94].

There are two major approaches for hydrogel formation by host-guest interaction. The first approach is threading design, which includes threading of linear polymers (such as PEG and poly(vinyl alcohol) (PVA)) inside the CD cavity, and chain entanglement as a result of sliding of CD ring along the linear polymer backbone [95,96]. For example, Wang et al. prepared pH-responsive hydrogel by complexation of PEG pendant groups of poly(PEG dimethacrylate-*co*-2-(dimethylamino)ethyl methacrylate) (poly(PEGDMA-*co*-DMAEMA)) with α-CD, at high pH (Fig. 2C, left image). The hydrogel network was disrupted at lower pH due to the pH-sensitive nature of DMAEMA [97]. Further studies confirmed that γ-CD could accommodate two chains of PEG in its cavity (Fig. 2C, right image) [98]. The second approach is pendant design, in which polymer backbone is functionalized with pendant CD host molecules so it can complex with other polymers incorporating the complementary guest molecules, such as azobenzene and adamantane [99,100]. Besides CD, Cucurbit[n]urils is another host molecule commonly used for the development of supramolecular host-guest hydrogels for TE [101].

2.2.4. Ionic interactions—Hydrogel formation by ionic interaction involves crosslinking of charged polymer chains by mixing with oppositely charged species, which in turn forms coacervate clusters. For example, negatively charged sodium alginate crosslinks rapidly with positively charged calcium ions to form a stable hydrogel (Fig. 2D). Such physically crosslinked hydrogels might display shear thinning behavior under mechanical stress, and restore its original shape upon stress removal [85]. Jiang et al. prepared injectable hydrogels by mixing (1:1 charge ratio) negatively charged HA and positively charged four-armed PEG-*b*-poly(2-aminoethyl methacrylate) [102]. Aida et al. reported hydrogel formation upon mixing of negatively charged composite of clay nanosheets/poly(acrylate)

with positively charged G3-dendron [103]. In another example, Gong et al. synthesized hydrogels by copolymerization of oppositely charged monomers, such as *p*-styrenesulfonate and [2-(acryloyloxy)ethyl]trimethyl ammonium chloride [104]. Numerous examples for hydrogels formation, from chitosan and alginate, by ionic interactions have been reported in the literature [105-111].

2.2.5. Stereocomplexation—Mixing solutions of optically active polymers, such as stereospecific polylactide (PLA) or poly(methyl methacrylate) (PMMA), usually favors the formation of stereocomplexes (Fig. 2E) [112]. The most obvious example is mixing solutions of D- and L-PLA to produce hydrogel with desirable compatibility and degradability. Multivalent Van der Waal force is the driving force for helix formation upon mixing stereo-regular blocks of PLA [86]. In another example, Hennink et al. prepared hydrogel for protein delivery, through modification of dextran with stereoregular PLA, followed by self-assembly [86,113]. PLA-induced stereocomplex formation concept has been used to promote the thermo-gelling properties of pluronic. The modified pluronic displayed sol-gel transition at lower temperature and concentration, and exhibited enhanced mechanical properties [86,114].

2.2.6. Thermal crosslinking—Thermal crosslinking involves using temperature to physically crosslink polymer chains. For instance, PVA undergoes physical crosslinking by the freeze-thawing process because of crystallization, resulting in hydrogel formation. The degree of crosslinking, mechanical properties, and swelling characteristics can be tuned by running multiple freeze-thaw cycles, which increase the degree of crystallinity and alter the physical characteristics of the resultant hydrogel [115]. In addition, block copolymers with semi-crystalline blocks like poly(*ε*-caprolactone) (PCL) and PLA form hydrogel by the same approach [116,117]. Moreover, thermally-induced hydrogel formation via other mechanisms is also employed for the development of physically crosslinked network. For example, poly(NIPAM) (PNIPAM) and pluronic display thermo-responsive behavior, and form self-assembled hydrogels by raising temperature above the lower critical solution temperature (LCST) [62,118].

Furthermore, cooperative physical interactions, such as coiled coil, β-sheet and triple helix, can provide stability to thermally crosslinked networks. Such cooperative forces are commonly useful for hydrogel formation from collagen and silk [119,120]. In one study by Kiick et al., triple-helix-forming collagen-like peptide was conjugated to thermo-responsive elastin-like peptide, and the resultant conjugate underwent reversible thermal crosslinking at room temperature, due to the structural reorganization of triple-helix crosslinks [121]. Moreover, incorporation of polymers with specific peptide sequences with thermo-sensitive structural changes, e.g. $(AKAAAKA)_2$, promotes the temperature-triggered formation of hybrid hydrogels [122].

2.2.7. Molecular self-assembly—Molecular self-assembly of small supramolecular structures in aqueous solution has been widely used for the formation of supramolecular hydrogels for applications as cell culture platforms (Fig. 2F) [91,123,124]. Such supramolecular hydrogels are constructed by the arrangement of hydrogelators in ordered 3D structures via non-covalent forces [123]. Supramolecular hydrogelators containing self-

assembling motifs, such as small organic molecules [125], peptides [126], metal complexes [127], saccharides [128], and nucleobases [129], self-assemble in aqueous solution at a concentration higher than critical gelation concentration to form hydrogels. The structure and functionality of supramolecular hydrogelators dictate the properties of the resulting hydrogels. Among all hydrogelators, peptide-based hydrogelators have received great attention for the construction of 3D structures to support cell growth. Biocompatibility, bioactivity, and the ability to harness a wide range of ECM-mimicking peptides are among the main advantages of such hydrogelators [130,131].

Several stimuli, such as pH, ionic interactions, temperature, ultrasound, light, ionic strength, chemical reactions, and enzymes, are used to trigger the self-assembly process and promote sol-gel transition [131]. For example, Saiani and co-workers induced the formation of the fibrillar structure of Fmoc-diphenylalanine (Fmoc-FF; Fmoc = (fluoren-9-ylmethoxy)carbonyl) by simply decreasing the solution pH, which triggered protonation/deprotonation of the carboxylic group of phenylalanine, ultimately inducing self-assembly and supramolecular hydrogel formation. In addition, solution pH controlled the hydrogen bond strength between water molecules and hydrogelator [132]. In another study of Xu and co-workers, increasing the temperature of dipeptide Fmoc-D-Ala-D-Ala solution induced hydrogel formation by affecting the strength of hydrophobic interactions and hydrogen bonding as well as increasing entropy to promote self-assembly [133]. Finally, Cao et al. reported the self-assembly of cysteine-containing peptides, i.e. Ac-I_3-CGK-NH_2 (Ac = acetyl), under the oxidative condition to form supramolecular hydrogels which possess tunable mechanical properties, with disulfide bonds incorporated between the self-assembled fibers [134].

Stupp and co-workers studied the influence of photocleavable *o*-nitrobenzyl (oNB) group on the self-assembly process of peptide amphiphiles (PAs) carrying bioactive epitope, Arg-Gly-Asp-Ser (RGDS). TEM results showed that PAs undergo self-assembly to form fibrous network after photo-irradiation and cleavage of oNB group. However, PAs form spherical particles under similar self-assembling conditions in the absence of UV irradiation. The researchers concluded that structural modification of β-sheet peptide domains with oNB group disrupts self-assembly and retards nanofiber formation. NIH 3T3 mouse embryonic fibroblast, cultured on hydrogel of PA-containing RGDS epitope, displayed higher expression level of vinculin as compared to control Arg-Gly-Glu-Ser (RGES) epitope. Cell viability studies showed that the cells maintain their viability and proliferation ability after photo-irradiation [135].

Bond cleavage and formation by enzymes can also induce the formation of 3D supramolecular hydrogels. For instance, Xu and co-workers reported the formation of supramolecular hydrogel upon de-phosphorylation of Fmoc-tyrosine phosphate using alkaline phosphatase enzyme in aqueous solution [136]. Another study by Chen et al. demonstrated that the treatment of FEFKFEpYK peptide with phosphatase, stimulated the rapid formation of FEFKFEYK hydrogelator, which self-assembled into a supramolecular hydrogel that enabled encapsulation of various cell types including HeLa, HepG2, and A549 cells [137]. As demonstrated by Palocci and co-workers, lipase was used to connect two precursors, Fmoc-Phe and Phe_2, and the resulting Fmoc-(Phe_3) hydrogelator promoted

microglial cell proliferation and upregulated expression of neural growth factor (NGF) [138].

3. Stimuli-responsive hydrogels

Stimuli-responsive scaffolds are defined as scaffolds that undergo significant physical or chemical changes upon small alteration of external stimuli or changes within their environment. Depending on the magnitude of the stimulus and the response sensitivity, several kinds of physical, chemical, and biological stimuli have been employed to trigger the changes within scaffolds [139]. Bond cleavage, bond formation, swelling/deswelling, and conformational changes are the most common responses. In recent years, there has been a growing interest in the development of stimuli-responsive hydrogels that can respond to the specific stimuli, rather than the construction of static networks. Consequently, the focus has been shifted to exploring new chemistries to allow the construction of smart hydrogels with optimal control over the hydrogel scaffolds regarding their biological and physicochemical features (such as growth factor presentation, cellular attachment, and spatiotemporal release of bioactives in a controlled fashion, degradability, as well as mechanical and electrical features) [57]. This section largely focuses on the current strategies employed in designing stimuli-responsive scaffolds, which can respond to physical stimuli, such as temperature, light, mechanical stress, and electric signals, as well as chemical stimuli like pH. For the development of smart scaffolds that can respond to biological stimuli, we direct readers to an excellent published review in the literature [140].

3.1. pH-responsive hydrogels

Chemically or physically crosslinked hydrogel can display pH-responsive behavior by incorporation of ionic groups with the polymer backbone. Such ionic pendants undergo protonation/deprotonation process with changing pH, which in turn affects the degree of ionization and hence the net charge on the hydrogels. The ionic groups, typically as weak acidic or basic functionalities, can be introduced to the polymer chains through modification reactions or via appropriate selections of monomers with acid/base characteristics for polymerization. For instance, acrylic acid and methacrylic acid are among the widely used acidic monomers that undergo ionization/deionization by changing pH [141,142]. Under slightly basic conditions, the carboxylic groups of the resulting hydrogels become ionized, and the repulsive force between the adjacent negatively charged groups increases the hydrodynamic volume of the hydrogel, leading to polymer swelling. On the other hand, under acidic condition, deionization of the carboxylic groups causes a collapse of the network. Poly(DMAEMA) is an example of polybase with pH-responsive behavior. Protonation of the amino groups occurs at pH less than the pKa value of monomer, whereas it loses the proton at pH higher than the pKa [143].

For designing hydrogels with pH-responsive behavior for manipulation of cell-directing cues, it is important to choose monomers with pKa close to the physiological pH. An associated strategy is the incorporation of hydrophobic moieties to the polymer backbone, thereby restricting the swelling/de-swelling transition via hydrophobic interaction. It has been demonstrated that hydrophobically modified DMAEMA-based hydrogels displayed

swelling/deswelling transition at lower pH by increasing the length of the hydrophobic side chain [144]. The opposite results were obtained for hydrophobically modified PAA [141].

Biopolymer-based hydrogel (e.g. chitosan and alginate gels) is another class of pH-sensitive hydrogels. Changing the pH of an aqueous medium containing chitosan or alginate hydrogels causes phase transition between swollen and de-swollen states due to protonation/deprotonation of amino and carboxylic groups of chitosan and alginate, respectively. The stiffness, swelling characteristics, and gelation kinetics of PEG-chondroitin sulfate hydrogel can also be controlled by altering pH [145]. In addition, pH-responsive polymers such as poly(ortho ester) and poly(β-amino ester) contain pH-cleavable moieties on their backbone, rendering these polymers pH-degradable. Moreover, pH-responsive behavior of various amino acids, such as glutamic acid, aspartic acid and histidine, makes them suitable candidates of monomers for peptide-based hydrogels that can be stimulated by pH changes [139].

Furthermore, besides ionization of acidic or basic functionalities, hydrogels incorporating dynamic covalent bonds (such as hydrazone bond, thioester bond, and phenyboronate complexation) or dynamic non-covalent bonds (such as hydrogen bonding) shift the equilibrium between two different states in response to pH, resulting in significant changes in mechanical and structural properties [146-150]. Finally, pH can also trigger conformational changes within DNA- and protein-based hydrogels because of the pH-dependent folding/unfolding of pH-sensitive domains [150,151].

It is worth noting that the application of pH-sensitive hydrogels for manipulation of cell-directing cues provides bulk control over properties at specific time points, but their application in tuning the property of interest within specific subvolumes of the hydrogels is limited. Although the reversible swelling/deswelling of pH-sensitive hydrogels can be controlled by changing the medium pH, the narrow pH range around the physiological pH 7.4 allowing for biocompatibility with cellular systems restricts the magnitude of chemical or physical changes (e.g. bond cleavage, protonation/deprotonation, folding/unfolding, etc.), and consequently confines the overall change in cell microenvironment within a narrow window.

3.2. Thermo-responsive hydrogels

Thermo-responsive hydrogels undergo sol-gel transition with temperature change, due to the alteration in the hydrophilic/hydrophobic balance within the networks [152]. The thermo-gelation mechanisms include hydrophobic interaction, coil-helix transition and micellar packing and entanglement. Several interaction events are implicated in the thermal sensitivity of hydrogels: polymer-polymer, water-water, and water-polymer interactions [153]. There are two major categories of stimuli-responsive hydrogels: positive and negative thermo-responsive gels. Positive thermo-responsive gels undergo network collapse by cooling below the upper critical solution temperature (UCST), whereas negative thermo-responsive gels display gelation upon heating above LCST [154].

Several synthetic polymers display thermo-responsive behavior in aqueous solutions. For instance, PNIPAM undergoes sol-gel phase transition above LCST (32 °C), resulting in

more hydrophobic gel [155]. Modulation of LCST can be achieved by controlling the molecular weight of the polymer, use of co-solvents, addition of salts, and alteration of the chemical structure [156]. Dadoo and Gramlich prepared hydrogel with thermo-responsive behavior by reacting dithiol-terminated PNIPAM and norbornene-functionalized HA. The hydrogels displayed significant mass loss at 37 °C (> LCST) because of de-watering of hydrogels, whereas it restored its original weight at 4 °C [157]. Other examples include di- and triblock copolymers, such as PEG-*b*-poly(lactic-*co*-glycolic acid), PEG-*b*-poly(propylene oxide)-*b*-PEG and PEG-*b*-poly(*ε*-caprolactone)-*b*-PEG [158]. Above LCST, water molecules surround the hydrophobic blocks, and subsequently the hydrophobic domains aggregate to minimize the contact with water. In another example, the hybrid hydrogel of PNIPAM and PEG-dimethacrylate was synthesized, and its thermo-response and LCST could be tailored based on the ratio of the two components [159].

Natural polymers like chitosan display thermo-gelation transition upon mixing with β-glycerol phosphate, forming a clear solution at room temperature and gel at 37 °C [160]. On the other hand, gelatin exhibits as sols of random coils above 30 °C and forms gels by decreasing the temperature below 25 °C [161]. Thermo-responsive hydrogels can be good candidates for biomedical applications; however, careful control over the transition temperature, gelation time, and pH at transition is needed for clinical applications [162].

3.3. Photo-responsive hydrogels

The incorporation of photo-activating moieties within hydrogel-forming polymer chains turn the gels photo-responsive, enabling applications in manipulation of cell microenvironment [163]. There are different modes of actions that can be stimulated by light such as photoisomerization, photocleavage, photodimerization, photorearrangement, and photoconjugation [163-165]. For instance, azobenzene [152] group undergoes a reversible cis-trans isomerization upon UV irradiation, while photochromic chromophores like coumarin [166], anthracene [167], and cinnamoyl group [168] undergo reversible dimerization upon UV irradiation. Specifically, polymers containing coumarin, anthracene, and cinnamoyl moieties undergo photodimerization reaction when irradiated with long-wavelength UV light (λ = 300–365 nm), and photoreversible cleavage upon exposure to short-wavelength UV light (λ = 254 nm) [169-171]. Although photoreversible dimerization using these functionalities has been explored in the modulation of hydrogel network, several drawbacks, such as using short-wavelength cytotoxic UV light (λ = 254 nm), long exposure time of UV (0.5 to 1 h typically required to photocleave cinnamylidene acetyl dimer), incomplete network degradation, and undesirable cleavage reactions, limit their use in the manipulation of cell microenvironment [172,173]. In contrast, azobenzene groups absorb light in 350–550 nm wavelength range, enabling isomerization using cytocompatible doses of UV/visible lights [99]. Photoisomerization has been intensively employed for modulation of cell microenvironment. For example, cells seeded on hydrogels containing photo-sensitive spiropyran groups undergo reversible cell detachment/attachment upon exposure to 365/405-nm UV/visible lights due to the rapid transition of spiropyran to hydrophilic/hyrophobic structures [174]. In another study, it has been demonstrated that the storage modulus of PEG-based hydrogel, crosslinked by azobenzene-based crosslinker, decreased upon UV

irradiation, and the hydrogel exhibited a reversible transition from stiff to soft structure due to photoisomerization of azobenzene groups [175].

Besides photoisomerization and photodimerization, hydrogels incorporating photolabile oNB and coumarin groups were intensively investigated for on-demand tuning of biochemical and biophysical cues of the scaffolds [176]. Photocleavage of oNB ester or amide linkages within the hydrogels generates ketone and carboxylic acid, while photocleavage of coumarin ester linkages yields alcohol and carboxylic acid groups [177-179]. Cytocompatible doses of single-photon UV light ($\lambda \geq 365$ nm, ~ 10 mW/cm^2) or pulsed two-photon lights (> 700 nm, ~ 670 μW/μm^2) are typically employed to induce photocleavage reaction [179-181]. The photocleavage profile depends on light wavelength, intensity, and exposure time. Spatiotemporal generation of biochemical and biophysical gradients, and patterning subvolumes within a hydrogel by moving focused two-photon lights ($\lambda > 700$ nm) depend on light intensity, scanning speed, and the number of raster scans. Light intensity varies broadly depending on the exposure time and scanning speed [181]. Significant efforts are currently underway to explore new substituents of oNB and coumarin that exhibit improved degradation rate and possess red-shift absorbance to enable using more cytocompatible doses of light. Temporal and spatial modulation of cell niches has been achieved using coumarin and oNB derivatives as photocages to either block the chemical reactivity of specific functional groups or to mask the bioactivity of biochemical agents [182,183]. For example, photocaged Arg-Gly-Asp (RGD) peptide attached to HA-based hydrogel has been used to modulate the growth direction of cells by selective cleavage of the photosensitive cage in a certain location, to expose the RGD and consequently promote cell attachment. This strategy was employed successfully for patterning several cell types [184].

Furthermore, light-induced rearrangement of allyl sulfide in the presence of thiolated molecules enabled well-tuned reversible tethering and removal of biochemical, as well as modulation of mechanical stiffness using light [185,186]. Formation of thiyl radicals by light initiates the reaction with allyl sulfide, resulting in the generation of new double bond for subsequent reactions. More details about the role of photo-responsive hydrogels in four-dimensional (4D) cell culture will be discussed in later sections.

3.4. Electro-responsive hydrogels

Polyelectrolyte hydrogels display swelling/de-swelling or bending upon applying electric field, due to the generation of opposite potential as a result of the movement of counter ions in solution [152,187,188]. The overall transition from one state to another depends on the pH of the solution, ionic strength, crosslinking density, the strength of the applied field, exposure time to the electrical stimulus, and the direction of hydrogel with respect to the electrodes [189,190]. Moreover, the movement of charged hydrogels from/toward one electrode depends on the charge of the hydrogels. Positively charged hydrogels, such as chitosan/polyaniline, move toward the anode; whereas negatively charged polyelectrolytes, such as HA/PVA, move toward the cathode [191,192]. Other charged polymers, either synthetic or bio-driven, such as PAA [190], poly(2-acrylamido-2-methyl-propane-sulfonic acid) [193] and sodium alginate [194], were also employed in the development of electro-

responsive scaffolds. In addition, conducting polymers, such as polyaniline and poly(3,4-ethylenedioxythiophene), exhibit electro-responsive behavior owing to switching the surface charge from oxidation state to reduction state [195-197].

Furthermore, redox-responsive functionalities, such as O-silyl hydroquinone and ferrocene, undergo reversible electro-mediated oxidation/reduction and change their chemical or physical properties [198,199]. For instance, Peng et al. reported electro-assisted oxidation of hydrophobic ferrocene to hydrophilic ferrocenium, resulting in dissociation of the host-guest complexation with β-CD and hence gel-sol transition of ferrocene-β-CD-based hydrogels [198]. In another study, Xue et al. reported the synthesis of electrochemically active actuator hydrogel that displays a significant change in volume and mechanical properties upon electrochemical stimulation [200]. In their study, redox-sensitive 3,4-dihydroxyphenylalanine (DOPA) was incorporated to 2-naphthalenyl-glycine-phenylalanine-phenylalanine hydrogelator, which self-assembles to form supramolecular peptide hydrogel. Electrochemical oxidation of the hydrogel converted DOPA to dopaquinone and hence switched the hydrogel surface from hydrophilic to hydrophobic, which in turn resulted in up to 50% of volume change and 20-fold increase in the mechanical properties.

Electro-responsive hydrogels have been widely studied to remotely control the release of therapeutic cargo using electric field. For example, the release of safranin from PAA/polypyrrole hydrogels using electric field was investigated by Takahashi et al [201]. Another study by Jensen et al. demonstrated peptide release from chondroitin sulfate hydrogel by electrical stimulation [202]. Cho et al. reported that electrical stimulation of PC12 cells seeded on gelatin/CNTs scaffolds promotes neuronal growth [203]. Alignment of muscle cells on electro-active PAA/fibrin hydrogel has also been achieved by applying electric field [190].

3.5. Mechanically-responsive hydrogels

Native ECMs have heterogeneous compositions that differ depending on the type and location of tissue. It generally comprises of a complex assembly of proteins (such as collagen, fibrin, actin, and laminin), which responds to the mechanical forces applied by cells, therefore enabling the reconstitution of cell microenvironment to guide their functions and fate [204]. In addition, the native tissues are inherently viscoelastic and exhibit time-dependent mechanical properties such as stress-relaxation and strain stiffening behaviors. Mechano-responsive hydrogels are an intriguing class of smart materials that undergo deformation upon subjecting the materials to mechanical force, due to the unique chemical and physical structures of the materials [205-207]. The mechanical force could be internal from cells or applied externally. Hydrogels with stress-relaxation behavior exhibit a decrease in the initial stress that resists the applied strain from cells over time. This is mainly due to the incorporation of week physical forces or covalent dynamic crosslinks within the network, which enables rearrangement and reorganization of the network to adapt to the applied force from the surrounding [147]. Based on hydrogen bonding, ionic interaction, host-guest complexation, several hydrogel systems with stress-relaxation behaviors, which undergo force-dependent reversible unbinding of the crosslinks have been developed [208-210]. Moreover, networks containing adaptable covalent crosslinks

formed by reactions, such as imine formation, Diels Alder reaction, and thioester or disulfide exchange, have also been explored for capturing the viscoelasticity of native tissues [147,211]. Furthermore, ring-sliding hydrogels based on host-guest interaction between PEG and β-CD has enabled the development of tough and elastic networks that can be remodeled by cells through the movement of the mobile crosslinks [212].

Unlike hydrogels displaying stress-relaxation behavior, hydrogels exhibiting strain-stiffening behavior undergo a time-dependent increase of the stiffness with applied strain from cells. Rowan and co-workers reported the development of oligo(ethylene glycol)-functionalized polyisocyanopeptides (PICs) of tunable critical stress values, which represent the minimum strain required to induce stiffening. The PIC polymers incorporating β-helical polyisocyanide backbone stabilized via hydrogen bonding underwent supramolecular bundling to form fibrous hydrogels that could stiffen differently depending on the magnitude of strain applied by cells [208,213].

Besides viscoelasticity, scaffolds with non-linear elasticity have been shown to regulate the differentiation of human mesenchymal stem cells (hMSCs) [208]. Looking to the wide scope beyond hydrogels, incorporation of reversible dynamic bonds into polymeric backbone is the key for the construction of materials with mechano-responsive behavior. Such dynamic bonds can be ruptured by applying mechanical stress and recover its original shape upon stress removal [214]. The most obvious example in nature is titin, a muscle protein that displays an exceptional combination of strength, toughness, and elasticity. It consists of more than 300 protein domains that are connected through unstructured peptides. These domains unfold when the protein is subjected to mechanical force and refold when the tension is removed. The protein displays nonlinear elastic behavior in its folded state, whereas exhibits high tensile strength in its unfolded state. The non-linear elasticity stems from the capacity to absorb the energy, due to the presence of sacrificial non-covalent bonds that can break upon application of mechanical force, while preserving the covalent bonds [215-218].

Guan et al. reported the engineering of biomimetic modular crosslinker, which incorporates hydrogen bonding 4-ureido-2-pyrimidone (UPy) motif in a cyclic manner, for the development of a polymeric network with enhanced mechanical properties [218,219].The resulting polymeric network integrated the high extensibility of soft elastomers and the high stiffness of rigid networks. Reversible decomplexation of the interchain hydrogen bonds between UPy dimers upon stretching promotes energy dissipation capability and enhances the elastomeric stiffness without losing extensibility. This work demonstrated an increase of tensile strength with increasing crosslinker concentration, while maintaining the same level of elongation. Conversely, PEG crosslinker as a blank exhibited an increase of tensile strength at the expense of elongation capacity.

In addition, mechanical stress can be applied directly to hydrogels to induce mechanical deformation of polymer network, which in turn produces a reversible change of volume because of the squeezing/expansion process. Furthermore, mechanical stress could be triggered indirectly by inducing matrix swelling/deswelling through the application of electrical, thermal, or chemical stimulation. For example, multi-stimuli responsive hydrogel

of poly(*N*-acrylamide)-*g*-poly(acrylic acid) has been prepared by Gräfe et al., and it displayed pH and thermo-responsive behavior, providing an easy means of applying a mechanical force by changing the volume of the gel [220].

Furthermore, hydrogels incorporating mechanochemical bonds strengthen with the applied force owing to the formation of additional crosslinks. For example, a hydrogel system based on lipoic acid liberates free thiols upon reduction of the disulfide bond and exhibits increasing stiffness with applied strain because of additional formation of disulfide linkages between polymer chains [221]. Mechanophores are another type of mechanically-responsive materials, which change their color in response to mechanical stress, and could be useful as biosensors in hydrogel scaffolds [222].

4. Modulation of cell microenvironment using stimuli-responsive scaffolds

Thus far, we have provided an overview of chemical and physical strategies employed in hydrogels formation, as well as the chemical toolset of stimuli-responsive functionalities that brings up dynamicity to the scaffold structures. In this section, how stimuli-responsive scaffolds are being utilized to modulate the biophysical and biochemical cell-directing cues in space and time will be elucidated.

4.1. Modulation of biochemical cues using stimuli-responsive scaffolds

Substantial progress has been achieved by using stimuli-responsive scaffolds for modulation of biochemical cues, which dictate the cell function and fate. Early attempts included using the stimuli-responsive scaffolds as passive delivery systems for growth factors and biochemical agents, without in situ control over the biosignals. Four strategies have been employed to incorporate growth factors within stimuli-responsive hydrogels. First, direct loading of growth factors can be made through physical encapsulation within the hydrogel network during hydrogel formation. However, this method usually displays fast release kinetics. Second, growth factors can be loaded on carriers of micro-/nano-particles for entrapment within hydrogels. This method provides prolonged release of growth factors, but the hydrophobic nature of carriers may inactivate them. Third, growth factors can be covalently linked with polymer backbone prior to hydrogel formation. Fourth, growth factors can be loaded via reverse binding, which involves immobilization of growth factors through ECM binding domains, such as heparin and chondroitin sulfate [42,223]. The use of stimuli-responsive scaffolds as passive carriers for the delivery of biochemical cues has been the subject of recent reviews [224-226]. It is important to clarify that stimuli-responsive hydrogels incorporating naturally derived proteins (e.g., Matrigel, laminin, collagen, fibrin) and decellularized ECMs have not been significantly utilized for manipulation of biochemical cues despite their substantial roles in the development of biomimetic scaffolds. The complex bioactive cues exist on these proteins, multiple interactions of decellularized ECMs with cells, and variations of the composition of decellularized ECMs across donors make it challenging to independently manipulate an individual cue to study its effect on cell behavior. Therefore, smart synthetic hydrogels incorporating well-defined bioactive agents are being developed for this purpose. This section provides state-of-art examples of reversible and irreversible on-demand modulation of biochemical signals using stimuli-

responsive scaffolds, which may lead to real-time manipulation of cell microenvironment to mediate cell function.

4.1.1. Modulation of biochemical cues using stimuli-responsive 2D scaffolds

—Cell attachment to native ECMs is orchestrated by a large number of cell-adhesion proteins, such as collagen, Matrigel, laminin, FN, and vitronectin, as well as glycosaminoglycan (e.g., HA), which bind selectively to the integrin receptors on the cell surface [227,228]. Such cell-ECM interaction is important for signal transduction back and forth between cells and ECMs, thus guiding cell proliferation, spreading, and differentiation. Substantial progress has been made using smart 2D interactive scaffolds to study the influence of cell adhesion, morphology, and spreading on the overall cell behavior [13,229]. Stimuli-responsive substrates were at the heart of this progress, enabled reversible and irreversible modulation of cell attachment, as well as provided fruitful insights on cell-material interactions for further development of a new generation of instructive scaffolds with tunable cell response.

pH-responsive substrates have received considerable attention for reversible regulation of cell attachment. For example, Connal and co-workers developed pH and glucose dual-responsive phenyl-boronic acid-containing PEG substrate, via oxime ligation of tri-arm PEG trialdehyde and 3,5-diformylphenyl boronic acid with PEG-diamine, for reversible capture and release of NIH 3T3 fibroblast cells and MCF-7 human breast cancer cells [149]. The phenyl-boronic acid formed boronic ester bond with the carbohydrate on cell surface and enabled cell attachment at pH 6.8 in the absence of glucose, while cells were detached at pH 7.8 in the presence of glucose because of competing of glucose with carbohydrate on cell membrane for the phenylboronic acid sites. Similarly, Jiang and co-workers reported five cycles of capture and release of MCF-7 cells on poly(acrylamidophenylboronic acid)-grafted silicon nanowire, where pH and glucose were employed to trigger the transition between adhesive and repulsive states [230].

Moreover, thermo-responsive surfaces have been extensively employed for reversible manipulation cell adhesion and detachment via thermally-induced switching of surface properties. For example, Desseaux and Klok developed thermo-responsive RGD-containing thin layer via surface-initiated atom transfer radical polymerization (SI-ATRP) of HEMA, PEG methacrylate, and 2-(2-methoxyethoxy)ethyl methacrylate, and demonstrated controlled masking/unmasking of RGD ligand by altering the temperature [231]. Attachment of 3T3 fibroblasts was promoted at 37 °C because of copolymer collapse and presentation of RGD ligand at the surface, while detachment was achieved by cooling to 23 °C. Similarly, Lutz and co-workers reported the modulation of L929 mouse fibroblasts morphology and attachment on gold surface modified with a thermo-responsive copolymer of poly(oligo(ethylene glycol) methacrylate-*co*-2-(2-methoxyethoxy)ethyl methacrylate), by varying the temperature below and above the transition temperature (35 °C) in PBS buffer [232]. The cells exhibited significant cell spreading at 37 °C, while rounded-up at 25 °C. Additionally, thermo-responsive surfaces based on PNIPAM have been intensively explored for reversible capture and release of cells. Interesting work by Jiang and co-workers harnessed topographic and hydrophobic features of PNIPAM-grafted silicon nanopillars to modulate the attachment of MCF-7 cells using temperature [233]. At a temperature higher

than LCST of PNIPAM, MCF-7 cells, decorated with hydrophobic anchors, interacted with hydrophobic PNIPAM chains and the topographic features of the substrate to allow cell attachment. At lower temperature, the wettability change of PNIPAM hindered the interactions with cells, and thus cells were detached.

Furthermore, photo-responsive substrates have demonstrated efficacy in controlling cell adhesion. Maeda and co-workers pursued a strategy that uses the photocleavage approach to modulate cell adhesion [234]. Non-cell-adhesion BSA protein was allowed to adsorb on a glass coverslip treated with silane coupling agent end-capped with photocleavable oNB moiety. Irradiation with UV light selectively released the photolabile oNB motifs along with the adsorbed BSA layer, and then a cell-adhesion protein, FN, was added to the bare area to promote cell attachment (Fig. 3A). It is worth noting that the photocleavage approach is irreversible and the surface functionality cannot be regenerated after irradiation. In another study, Liu et al. harnessed the ability of azobenzene to undergo cis/trans transition upon UV irradiation to reversibly control cell adhesion [235]. Self-assembled monolayer (SAM) of mixed RGD-terminated PEG chains with an azobenzene-based conjugation linkage and hydroxyl-terminated PEG chains was prepared. On trans-configuration of azobenzene, the cell-adhesion RGD ligand was exposed to the surface to support cell adhesion, while after irradiation with UV light (λ = 340–380 nm), the trans-to-cis isomerization masked the RGD ligand within the PEG layer, consequently triggering cell detachment (Fig. 3B). In addition, light-mediated host-guest assembly/disassembly of azobenzene-RGD and CD-modified substrate has been employed to switch the surface bioactivity reversibly between “on” and “off” states, thus allowing dynamic manipulation of cell attachment (Fig. 3C) [236]. Furthermore, another strategy made use of light-induced switching of surface hydrophilicity of substrate to trigger cell attachment/detachment [174,237,238]. For example, Wang et al. demonstrated reversible detachment/attachment of mouse fibroblast L929 cells on spiropyran-containing substrate upon exposure to UV/Vis lights, respectively, due to isomerization of spiropyran and alteration of surface hydrophilicity (Fig. 3D) [174].

In addition, electro-responsive substrates have been also effective for on-demand, dynamic manipulation of cell attachment and migration. Substantial efforts focused on immobilization of electroactive materials such as hydroquinone and conducting polymers on electrodes, therefore they could switch properties (such as surface wettability and charge density) in response to applied electrical potential [239]. Several strategies have been adopted to electrically trigger these changes, thereby enabling on-demand control of cell attachment. These strategies include: 1) electro-cleavage of cell binding ligand; 2) electro-mediated assembly/disassembly of host-guest supramolecular interaction; and 3) electro-mediated conformational change for masking/demasking of cell attachment motifs. Mrksich and co-workers developed a SAM utilizing electroactive O-silyl hydroquinone motif to attach RGD peptide to gold substrate [199]. This system demonstrated electrical modulation of Swiss cells attached to the surface by applying electrical potential, which trigger the oxidation of silyl hydroquinone to benzoquinone, resulting in the release of RGD peptide and hence detachment of cells (Fig. 4A). Moreover, the released benzoquinone functionalities reacted sequentially with cyclopentadiene-decorated RGD peptide to enable reattachment of cells. The same group expanded this strategy to spatially pattern two different populations of Swiss 3T3 cells, where non-cell adhesive hydroquinone-terminated

SAM was used as electroactive mask between a pattern of RGD-terminated SAM, which could be activated electrically to enable immobilization of RGD ligands for further cell attachment [240]. In another approach, Jonkheijm and co-workers developed SAM of a ternary host-guest complex of Cucurbit[8]uril, viologen, and tryptophan-glycine-glycine (WGG)-modified RGDS on a gold substrate, for dynamic manipulation of C2C12 cells attachment [241]. Application of electrical potential induced disassembly of the supramolecular complex, the release of RGD peptide, and detachment of cell (Fig. 4B).

In an alternative approach, since developed by Langer et al., switching the molecular conformation and geometry of surface-bound molecules in response to electric field has been widely explored for the controlled presentation of bioactive cell-binding ligand [242]. Generally, this approach uses multicomponent SAM, wherein one component is static (electro-inactive) and the other component is dynamic (electro-active, with charged terminals). Electrical switching of the conformation of the dynamic layer between extended and collapsed states was used to conceal/expose the bioactive motifs within the static layer (Fig. 4C) [243]. The bioactive functionalities could be attached to either the static or the dynamic layers [243,244]. For example, Mendes and co-workers utilized oligo(ethylene glycol) thiol and cysteine-terminated RGD-oligolysine peptide to develop SAM on a gold substrate, for on-demand regulation of immune macrophage cell attachment. This substrate supported cell attachment in the absence of applied potential, but under applied negative potential the positively charged lysine attracted toward the surface to conceal the RGD motifs within oligo(ethylene glycol) layer, resulting in cell detachment [244]. Expanding the tools for immobilization of bioactive molecules, the same concept with using biotin-oligolysine (Biotin-KKKKC) was employed to electrically-switch the surface bioactivity between “on” and “off” states, thus allowing modulation of biomolecular interaction with neutravidin (Fig. 4D) [245]. Interestingly, Ng et al. reported spatial patterning of silicon electrode with two multicomponent SAMs, one containing RGD ligand and positively charged ammonium terminals and the other one incorporating RGD peptide and negatively charged sulfonate groups [246]. This system enabled spatial manipulation of attachment-detachment of differentiated HL60 cells. Applying positive potential turned off the bioactivity of positively charged regions because of masking of RGD ligand by the extended positive charge, meanwhile exposed the RGD peptides on the negatively charged areas. Lamb and Yousaf combined Huisgen cycloaddition and oxime ligation reactions to develop redox-switchable substrate capable of switching RGD peptide between cyclic and linear structures using non-invasive electrochemical potential (Fig. 4E) [247]. RGD-containing fork-like SAM, incorporating hydroquinone and oxyamine motifs at the fork terminals, was used to form electro-labile oxime linkage upon electro-switching of hydroquinone to benzoquinone. The work demonstrated that RGD peptide could enhance cell spreading on cyclic structure relative to the linear conformation. Another strategy for modulation of cell behavior has also been developed by using conducting polymers as a substrate layer. Biochemical characteristics, such as protein adsorption, cell spreading, attachment, differentiation, could be modulated by electro-switching of polymer between oxidized state and reduced state [248].

4.1.2. Irreversible spatiotemporal modulation of biochemical cuesusing stimuli-responsive 3D scaffolds—

Photo-responsive hydrogels are the most widely explored stimuli-responsive scaffolds for user-defined modulation of biochemical cues, owing to the ability to control where and when light irradiation would occur to trigger desirable biochemical events. Irreversible modulation of biochemical cues involves user-defined presentation or removal of signals. The photochemical strategies employed to modulate the bioactivity of the scaffolds can be generally classified to 1) photo-conjugation, and 2) photocleavage.

4.1.2.1. Photo-conjugation strategy.: It involves the controlled presentation of biochemical cues spatially and temporally via tethering of biomolecules to the photo-reactive functionalities incorporated within the network. Several studies have used photo-conjugation strategy to achieve high-level control of both biochemical and biomechanical cues. For example, Anseth and co-workers used a combination of biorthogonal SPAAC reaction and photochemical thiol-ene reaction to independently tune the mechanical properties of peptide-functionalized hydrogel, and to introduce user-defined biochemical functionality to the network [249]. Biomechanical properties were modulated by varying the reaction stoichiometry between four-arm PEG tetra-azide and dicyclooctyne-terminated allyl-containing peptide, and the molecular weight of PEG-based precursor for SPAAC reaction. Selective tethering of cysteine-containing peptides to the pendant photo-reactive alkene from the network, using different doses of UV light, enabled patterning of multiple peptides spatially and temporally. This system allowed user-defined modulation of biochemical cues in the presence of cells, meanwhile tuning the mechanical properties was predecided by appropriate selections of reaction stoichiometry and molecular weight of precursors. In another study, the same group developed PEG-based hydrogel that allows the biomechanical and biochemical properties to be modulated in real time [250]. Step-growth network was first formed by the SPAAC reaction between four-arm PEG tetra-cyclooctyne and peptide diazide, which contains photo-cleavable oNB ether group and pendent allyl motifs. Precise patterning of bioactive peptides was achieved via thiol-ene photocoupling of cysteine-containing peptides with the pendant allyl motifs, upon irradiation with visible light using photomask. Similarly, mechanical stiffness was modulated via controlled photocleavage of oNB ether groups using either single-photon or two-photon laser. The study demonstrated that 3T3 fibroblast only migrates to the eroded channels that are decorated with RGD adhesive peptide. Because patterning of biomolecules using photoconjugation strategy involves the generation of radicals, potential damage to protein-based biomolecules could occur [251].

4.1.2.2. Photocleavage strategy.: Unlike photo-conjugation of biochemicals to photo-reactive functionalities on the network, photocleavage strategy can enable on-demand removal or presentation of bioactives spatially and temporally. There are three major approaches for irreversible modulation of biomolecules using photocleavage approach: 1) controlled cleavage of the photolabile links that bind the biomolecule to the network; 2) precise cleavage of photolabile cage that blocks the bioactivity of biomolecule; and 3) well-defined cleavage of photolabile cage that masks the chemical reactivity of certain functional group, followed by tethering of biomolecule of interest. As an example for the first

approach, photocleavage of oNB ester linkage that binds RGD motifs to photodegradable PEG-based hydrogel enhanced chondrogenic differentiation of hMSCs relative to the analogue hydrogel with persistent signals [252].

Photolabile cages are involved in the other two photocleavage approaches employed in spatiotemporal modulation of bioactive agents, with oNB and coumarin motifs as the most widely used photocages [43]. Several reactions (such as Michael-type reaction, oxime ligation, enzymatic crosslinking, etc.) could be initiated after photocage removal, to enable well-defined modulation of cell microenvironment. More specifically, agarose hydrogel incorporating coumarin-caged thiols was employed for 3D patterning of sonic hedgehog and ciliary neurotrophic growth factor (CNTF) proteins simultaneously. Sequential irradiation with two-photon light resulted in uncaging of thiol motifs in two different patterns. After each irradiation, the exposed thiol groups further reacted with either barnase-maleimide or streptavidin-maleimide via Michael-type reaction to eventually generate patterns of barnase and streptavidin within the same hydrogel. Subsequently, barstar-SSH and biotin-CNTF were immobilized simultaneously based on barnase–barstar and streptavidin–biotin binding affinity [253]. It is noteworthy that simultaneous patterning maintains high protein bioactivity relative to sequential patterning, in which potential loss of protein bioactivity might occur by excessive washing steps [253]. Similarly, Shoichet and co-workers developed HA-based hydrogel incorporating coumarin-caged thiol via furan-maleimide Diels-Alder reaction, and demonstrated precise patterning of epidermal growth factor (EGF) and CNTF in 3D space [183]. Iodoacetamide-modified EGF was directly conjugated to the multiphoton uncaged thiols, meanwhile streptavidin-maleimide was first conjugated before immobilization of biotin-CNTF (Fig. 5A).

In addition, multi-arm PEG containing photocaged alkoxyamine terminals was designed to crosslink with multi-arm PEG-aldehyde via oxime ligation after photocleavage of 2-(2-nitrophenyl) propyloxycarbonyl (NPPOC) cage (Fig. 5B). Green fluorescence protein (GFP) containing NPPOC-caged alkoxyamine motif was used for in situ modulation of the hydrogel spatially upon irradiation, resulting in higher viability of NIH 3T3 fibroblasts [182]. Moreover, Lutolf and co-workers took benefit of the ability of transglutaminase factor XIII (FXIIIa) to crosslink ε-amine residue of lysine onto γ-carboxamide motifs of glutamine to pattern VEGF 121 ($VEGF_{121}$) within PEG-based hydrogel, using a combination of photocleavage and enzymatic crosslinking reactions (Fig. 5C) [254]. In their work, FXIIIa peptide substrate containing lysine-caged amine was covalently immobilized within PEG hydrogel. Laser-scanning lithography was employed to spatially uncage the amino groups of lysine within the 3D hydrogel, which subsequently reacted with glutaminyl residue of $VEGF_{121}$ via FXIIIa enzyme-mediated crosslinking.

It is worth noting that the potential loss of bioactivity of the incorporated biomolecules (e.g. proteins) is one of the critical concerns for the development of bioactive hydrogels with significant applicability. Change in protein conformation, undesirable protein-hydrogel interaction, multiple washing during sequential immobilization of multiple proteins, and limited stability of fragile biomolecules are the main reasons for protein inactivation [253,255]. In addition, it is difficult to functionalize full-size proteins with photosensitive moieties comparing to functionalization of short-sequence peptides,

because typical bioconjugation reactions are not specific enough and require reaction conditions not sufficiently mild [254]. Appropriate choice of orthogonal chemistry that allows simultaneous, fast and selective immobilization of multiple proteins can provide opportunities to minimize the concerns associated with sequential patterning of different proteins [253].

4.1.3. Reversible spatiotemporal modulation of biochemical cues using stimuli-responsive 3D scaffolds—Native ECMs are inherently heterogeneous, with biochemical cues changing dynamically in space and time [43,256]. Static 3D culture system with time-persistent cell-directing cues are unable to capture the spatiotemporal variation of cues on native cellular niches [257]. Scaffolds with stimuli-responsive functionalities have been demonstrated as a powerful chemical tool for reversible modulation of molecular signals, enabling to a high level of the recapitulation of native ECMs. In addition, owing to the ability to present specific signals spatially and temporally and remove them in a user-directed manner, such reversible manipulation of cell microenvironment can be studied to provide deeper understanding on complex cellular processes, by correlating the changes in cell behavior to user-defined reversible alteration of signals [48,258]. Among all stimuli-responsive materials, photo-responsive scaffolds have attracted the attention for enabling sequential signal presentation and removal spatially and temporally. The major approaches for accomplishing reversible modulation of biochemical cues using light depend on 1) light-mediated attachment and subsequent removal of signals (in which the reactive functionalities get consumed during the photochemical reactions and the number of signal attachment/removal cycles is limited); and 2) living photo-mediated ligand exchange (in which the reactive functionalities are regenerated during the reactions).

A fascinating work by DeForest and Tirrell combined biorthogonal SPAAC, photouncaging-mediated oxime ligation, and photocleavage reactions to engineer photo-responsive platform, which demonstrated reversible patterning of vitronectin and other proteins [181]. In their study, matrix metalloproteinase (MMP)-sensitive PEG hydrogel incorporating NPPOC-caged alkoxyamine moieties was developed by SPAAC between 4-arm PEG tetra-bicyclononyne, N_3-DGPQGIWGQGDK(N_3)-NH_2, and azide-terminated tri(ethylene glycol)-based linker containing NPPOC-caged alkoxyamine (Fig. 6A). Then, the aldehyde-modified protein incorporated with photocleavable oNB moieties was allowed to react with the spatially uncaged-alkoxyamine functionalities via light-assisted oxime-ligation, and thereby protein was confined within subvolumes of the hydrogel with resolution below cell dimensions. Subsequently, controlled removal of protein was achieved by photocleavage of oNB moieties with cytocompatible doses of UV light. Interestingly, hMSCs displayed significant cell attachment and higher expression of osteogenic markers after vitronectin patterning, and reversibly switched to rounded morphology with a lower level of osteogenic markers after vitronectin release. Similarly, with a bioactive agent engineered to contain both a thiol group for photomediated conjugation and a photo-cleavable oNB moiety for subsequent release of biomolecules, Anseth group reported reversible patterning of an engineered peptide within PEG hydrogel containing pendant alkene functionalities. Appropriate control of irradiation conditions enabled signal attachment using visible light, while signal removal was triggered by UV light [48].

In addition, taking advantage of allyl sulfide functionalities to undergo addition-fragmentation chain transfer upon irradiation with light, numerous photo-sensitive scaffolds that enable reversible simultaneous presentation and/or removal of biochemical ligands have been developed [186,259,260]. For example, allyl sulfide hydrogel, developed via Cu-catalyzed click reaction of four-arm PEG tetra-azide and allyl sulfide-based dialkyne crosslinker, undergoes β-scission upon irradiation in the presence of thiolated biomolecule, enabling conjugation of the attacking species as well as the formation of new double bond for further attachment of additional bioactive ligands (Fig. 6B) [186]. Irradiation through photomask confined the exchange reaction to a specific area, therefore allowing spatiotemporal 3D modulation of bioactive molecules. Moreover, owing to the living nature of the alkene functionalities and the reversible exchange ability of allyl sulfide, a recent study has demonstrated the user-defined replacement of attached protein with fresh one [185].

4.2. Modulation of biophysical cues

Tuning the mechanical environment of cells has focused on the engineering of scaffolds with static mechanical properties, however native tissues are dynamic in nature, and undergo time-dependent changes in mechanical stiffness during tissue development, aging, wound healing, and pathological conditions (such as liver fibrosis) [17,36,37,43]. Although softening of biopolymer-based scaffolds via degradation enables changes of mechanical properties over time, such scaffolds could not allow user-defined control over where and when the changes would occur [37]. Stimuli-responsive scaffolds have emerged as powerful systems that enable unidirectional (irreversible) and cyclical (reversible) changes of mechanical cues. This section highlights the state-of-art stimuli-responsive systems employed in the modulation of cellular mechanical environments.

4.2.1. Unidirectional modulation of scaffold stiffness—Scaffolds incorporating stimuli-responsive functionalities capable of undergoing degradation or further crosslinking, by means of external or internal stimuli, have been widely explored for irreversible modulation of mechanical stiffness in the presence of cells. There are two major approaches to alter mechanical stiffness: 1) stimuli-mediated softening, and 2) stimuli-mediated stiffening. Among early attempts to achieve scaffold softening, the development of hydrolytic or proteolytic crosslinkers has been pursued. For example, enzymatically-responsive hydrogels have enabled cell-mediated modulation of local mechanical environment via selective cleavage of a specific peptide sequence incorporated within the hydrogel network by either secreted or exogenous enzymes [261]. In one study, bioactive PEG-based hydrogel incorporating MMP-cleavable peptide sequence was developed by thiol-ene click reaction of 4-armed PEG-tetra-norbornene and cysteine-containing MMP-cleavable (KCGPQG→IWGQCK) sequence (Fig. 7A) [262]. The hydrogel was used to identify synthetic niches with optimal biophysical and biochemical cues required to support motor axon outgrowth. Hydrogels with MMP-cleavable sequence exhibited axonal outgrowth as compared to hydrogels with non-cleavable PEG macromer, which eliminated axon extension. Likewise, aggrecanase- [263], collagenase- [264,265], and plasmin-sensitive [266] hydrogels have been developed. Although hydrolytically and enzymatically-sensitive

hydrogels offer opportunities to remodel cell environment, they could not permit user-directed manipulation of cell-guiding cues [267,268].

In addition, photo-responsive hydrogels have received enormous attention because of their ability to enable user-defined control of degradation using cytocompatible doses of light. Photolabile oNB ether group has been widely explored for precise tuning of crosslinking density of the hydrogel scaffolds [177]. Anseth and co-workers engineered oNB ether-based crosslinker for further development of photodegradable chain-growth hydrogel. On-demand modulation of the physical stiffness of the network in the presence of cells was achieved by moving either single-photon (λ = 365 nm) or two-photon (λ = 750 nm) light in predefined patterns to erode the polymer network, thereby generating 3D features with controlled dimensions. This system enabled elucidation of cell-material interaction in real time upon in situ alterations of the local microenvironment by light [269]. As an alternative to ester-linked oNB crosslinkers of faster degradation rate, the same group developed azide-terminated photolabile crosslinker containing amide-linked oNB motifs, to crosslink with 4-armed PEG-tetra-dibenzocyclooctyne through copper-free click chemistry (Fig. 7B) [178]. The resultant hydrogel underwent degradation to amide- and aldehyde-terminated fragments upon irradiation by either single-photon UV light (λ = 334 and 365 nm) or two-photon visible light (λ = 740 nm). Embryonic stem cell-derived motor neurons (ESMNs) were shown to have extended axons on the channels created via photo-degradation. The major disadvantage of oNB-based systems is light attenuation because of high molar absorptivity of oNB ether motif, and potential toxicity by UV light [177,270]. Besides oNB-based systems, coumarin-based photodegradable hydrogel has been developed by step-growth polymerization of 4-armed PEG-tetra-alkyne and 4-armed PEG-tetra coumarin azide using copper-catalyzed click chemistry (Fig. 7C) [179]. The coumarin moiety was readily cleaved in response to single-photon lights of short wavelengths of 365 nm (UV light), 405 nm (visible light), and two-photon lights of long wavelengths between 720 nm and 860 nm. As compared with oNB systems, which generate protein-reactive aldehyde or ketone during degradation, a critical advantage of coumarin-based platforms is the generation of less reactive alcohol [271,272]. In addition, being degraded at longer wavelengths, these platforms can enable user-directed modulation of mechanical stiffness at more cytompatible conditions [180,271].

Mechanically-responsive hydrogels that exhibit viscoelastic behavior undergo dynamic remodeling by pulling or pushing forces from cells, resulting in stress-relaxation of the network. The relaxation rate of the network has been demonstrated to be a potent regulator of cell fate. For example, 3T3 mouse fibroblast exhibited higher spreading area and more stress fibers on the stress-relaxing substrate as compared to the elastic substrate of the same initial modulus [273]. Mooney and co-workers reported the development of a series of PEG-conjugated alginate-based hydrogels of tunable relaxation time (stress relaxation time constant ($\tau_{1/2}$) ~ 70–3300 s) and similar initial elastic modulus by using different molecular weight of sodium alginate and PEG, as well as controlling the crosslinking density by Ca^{2+} ion [209]. The result of this study demonstrated that hydrogels of faster stress-relaxation (i.e., low molecular weight of PEG-alginate) enhanced hMSCs proliferation and osteogenic differentiation relative to hydrogels of slower stress-relaxation (i.e., high molecular weight of PEG-alginate). In another study, Anseth group developed PEG-based stress-relaxing

hydrogels ($\tau_{1/2}$ ~ 10 s – hours) through Schiff-base coupling of multi-arm PEG-aldehyde with multi-arm PEG-hydrazide [274]. The stress-relaxation was modulated by varying number of arms of aldehyde and hydrazide precursors, as well as using different types of aldehyde (aliphatic and aromatic). C2C12 myoblast exhibited elongated myotube-like morphology on stress-relaxing dynamic hydrogel relative to round morphology on the static hydrogel.

Stimuli-mediated stiffening is an alternative strategy for unidirectional modulation of cell microenvironment. It generally involves the increase of crosslinking density of scaffolds in response to external or internal stimuli. For example, Liu et al. reported tyrosinase-mediated stiffening of PEG-peptide hydrogels [275]. The enzymatically-responsive network was formed by photopolymerization of eight-arm PEG-norbornene with bis-cysteine peptide crosslinker containing two tyrosine groups. Tyrosinase-catalyzed oxidation of the pendant tyrosine residues into DOPA dimer resulted in the formation of additional crosslinks that stiffen the hydrogel (Fig. 8A). Pancreatic stellate cells (PSCs) encapsulated by enzymatically-responsive PEG-peptide hydrogel exhibited less elongation and spreading after tyrosinase-mediated stiffening. Another study by Suggs et al. involved irreversible dynamic tuning of hydrogel stiffness via near-infrared mediated release of calcium spatially and temporally from calcium/gold nanorod-loaded liposome, embedded in 3D alginate-based hydrogel, to increase ionic gelation and hence the stiffness of the hydrogel (Fig. 8B) [37]. Young's modulus increased with increasing the irradiation time, and NIH 3T3 showed more rounded morphology. The same approach was also used to release a chelating agent that competes with alginate chains for Ca^{2+}, and consequently decrease the hydrogel stiffness [37]. Moreover, mechano-responsive hydrogels that exhibit stress-stiffening or strain-stiffening behaviors can increase stiffness in response to the applied stress or strain from the cells [213,276]. Rowan and co-workers reported the synthesis of ultra-mechano-responsive PICs-based hydrogels through polymerization of triethylene glycol-conjugated isocyano-(D)-alanyl-(L)-alanines using different nickel(II) catalyst to monomer molar ratios, to obtain polymers of different chain lengths (Fig. 8C) [208]. PICs undergo sol-gel transition at a temperature range of 19–22°C to form soft gels (~ 0.2–0.4 kPa) of similar bulk stiffness and different lowest critical stress, which indicates minimum external or internal stress required to induce hydrogel stiffening. Encapsulation of hMSCs with PICs hydrogels demonstrated switching of the commitment of cells from adipogenesis in PIC hydrogel of low critical stress (shortest polymer) to osteogenesis in PIC hydrogel of higher critical stress (longest polymer). Recently, inspired by the ability of muscles to strengthen themselves autonomously under repetitive mechanical loading, Gone and co-workers developed mechano-responsive self-growing hydrogel capable of self-stiffening under mechanical loading [277]. Double network hydrogel composed of brittle poly(2-acrylamido-2-methylpropanesulfonic acid) sodium salt network and elastic polyacrylamide network was found to undergo brittle network scission by mechanical force, resulting in the generation of substantial numbers of mechanoradicals. Further polymerization of an embedded monomer/crosslinker by mechanoradicals resulted in the development of new polymer network, which ultimately increased mechanical stiffness. Although this system has not yet been explored in the presence of cells, it expands the chemical toolset toward modulation of mechanical microenvironment in real time.

4.2.2. Cyclical modulation of scaffold stiffness—Several stimuli-responsive scaffolds have been developed to achieve reversible mechanical modulation of cell microenvironment via softening or stiffening. For example, pH-responsive ABA triblock copolymer of poly-(2-(diisopropylamino)ethyl methacrylate)-*block*-poly(2-(methacryloyloxy)ethyl phosphorylcholine)-*block*-poly-(2-(diisopropylamino)ethyl methacrylate), $PDPA_{50}$-*b*-$PMPC_{250}$-*b*-$PDPA_{50}$, was developed to reversibly adjust its stiffness by subtle changes in solution pH at physiologically suitable pH range of 7–8 (Fig. 9A) [278]. At higher pH, the pH-sensitive PDPA block (pKa 6.2) become more deprotonated and hydrophobic, thus inducing stronger interchain hydrophobic interaction and leading to more physically-crosslinked, and hence stiffer, hydrogel. At lower pH, the protonated PDPA blocks result in weaker hydrophobic interaction, leading to softer hydrogel. In another example, dual pH and photo-responsive hydrogel based on thioester exchange has been explored to provide user-defined control on viscoelastic dynamics of the hydrogel. The rate of thioester exchange within the network was modulated using photocaged 4-mercaptophenylacetic acid catalyst or pH, thereby shifting the equilibrium to different mechanical state. Uncaging of 4-mercaptophenylacetic acid exposed thiol group which competes with the thiol of the network for thioester exchange, resulting in stress relaxation of the hydrogel (Fig. 9B) [147]. Anderson and co-workers developed injectable pH-responsive hydrogel in which pH change was employed to reversibly break/reform the dynamic covalent bond between phenylboronic acid-containing multiarm PEG and *cis*-diol of modified PEG, therefore switching mechanical strength of the hydrogel (Fig. 9C) [279]. Furthermore, Heus and co-workers explored DNA-responsive hydrogel that utilizes DNA crosslinkers to bridge the short oligonucleotides conjugated to the polymer network (Fig. 9D) [280,281]. With pH- or ligand-responsive DNA-based crosslinkers that incorporate DNA nanoswitches capable of contracting or relaxing in response to pH or thrombin ligand, reversible tuning of mechanical stiffness was achieved [280,281].

In addition, Sia and co-workers developed ion/salt-responsive hydrogel capable of dynamic switching of mechanical microenvironment [282]. In this study, collagen-alginate hydrogel was first formed via dual crosslinking of collagen and alginate (Fig. 10A). Collagen provided a stable structural network, meanwhile alginate changed its crosslinking state dynamically and reversibly in response to ion/salt. Sodium citrate and Ca^{2+} were employed to induce the transition of alginate between crosslinked and uncrosslinked state, resulting in dynamic softening or stiffening of the hydrogel. Furthermore, a thermo-responsive hydrogel that enables reversible tuning of mechanical elasticity through fine adjustment of temperature was developed by Seiffert and co-workers [283]. In their study, an azide-functionalized copolymer of poly((*N*-(2-hydroxypropyl)-methacrylamide)-*co*-2-hydroxyethyl methacrylate), poly(HPMA-*co*-HEMA), was first synthesized, then reacted with PNIPAM chains end-capped with cyclooctyne moieties to form a comb copolymer. Further crosslinking of the comb copolymer with PEG-bis(cyclooctyne) crosslinker via by SPAAC formed the hydrogel. On raising the temperature above LCST, the dangling PNIPAM side-chains contract to expel water, resulting in collapsed networks with increased mechanical stiffness (Fig. 10B). In another example, Gucht and co-workers reported reversible temperature switching of mechanical stiffness of recombinant protein-based hydrogels, by inducing cyclic assembly/disassembly of triple-helix crosslinks upon cooling

or heating, respectively [284]. Photo-responsive hydrogels have also been employed to induce cyclic changes of mechanical stiffness. For example, the supramolecular hydrogel of HA was developed via host-guest complexation between azobenzene- and β-CD-containing HA chains (Fig. 10C). Irradiation with 365 nm or 400–500 nm light reversibly switched the azobenzene groups between *cis* and *trans* configurations, which consequently altered their binding affinity with β-CD, leading to softening or stiffening of the networks [99]. Similarly, Anseth group developed PEG-based hydrogel incorporating azobenzene crosslinks that can cycle between two different mechanical states upon photoisomerization of azobenzene groups using 365 nm or 420 nm light [175]. Another study by Kong et al. explored redox-responsive protein-based hydrogel capable of switching its conformation between folded and unfolded states upon oxidation/reduction of the incorporated disulfide bonds, which in turn changed mechanical properties of the hydrogel reversibly (Fig. 10D) [151]. Other strategies to trigger reversible changes in mechanical stiffness have also been studied by making use of glucose-responsive networks [279], and magneto-responsive systems [285].

4.3. Modulation of structural properties

Porosity, pore connectivity, geometric alignment and surface topography of hydrogel are essential structural parameters that should be tuned to allow diffusion of nutrients and other biomolecules throughout the scaffolds, and to provide better cell attachment, proliferation and differentiation [286]. In biological systems, cells locate at ~100 μm distance from the capillaries, and diffusion is effective over this distance to maintain tissue viability. So, it is desirable to design scaffolds with a high density of capillaries to ensure cell viability even in the center of the tissue constructs [287,288]. Physical structural parameters of hydrogels, such as crosslinking density, polymer chain length between crosslinking point and volume swelling ratio, define the network mesh size, which in turn influences the diffusion rate throughout the hydrogels [289-292]. Generally, the increase of degree of crosslinking decreases the pore size, and hence restricts diffusion, especially for diffusible species with large molecular weights. In particular, diffusion rates of fibrinogen and albumin through alginate gel decrease with increasing calcium ion concentration or crosslinking time [293]. Surface topography of scaffolds plays a critical role in promoting cell attachment. It has been demonstrated that cell attachment increases with increasing surface roughness, upon the incorporation of biological or electrical fillers, such as conducting polymers. Furthermore, growing of cells on aligned scaffold induces cell alignment and promotes directional tissue growth.

4.3.1. The network structure of the hydrogels—Network structure of hydrogels needs to be thoughtfully designed, in order to control the diffusion of bioactive molecules and essential nutrients throughout the hydrogels, and to significantly alter the migration of cells [41,42]. Benefiting from the ability of stimuli-responsive scaffolds to change their chemical or physical properties with external or internal triggers, the network characteristics could be modulated to alter cell response. Mass swelling ratio (Q_m), volume swelling ratio (Q_v), volume fraction of polymer in swollen state ($v_{2,s}$), number-average molecular weight between crosslinking points (M_c) and network mesh size (ζ) are the major parameters defining the network characteristics (Eqs. (1)-(5)) [42].

$$Q_m = (W_s - W_d) / W_d \quad (1)$$

$$Q_v = V_s / V_d = (Q_m + 1)\rho_1 / \rho_2 \quad (2)$$

$$v_{2,s} = V_d / V_s = Q_v^{-1} \quad (3)$$

$$M_c = M_o / 2X \quad (4)$$

$$\zeta = v_{2,s}^{\frac{-1}{3}}(\gamma_o^2)^{\frac{1}{2}} = Q_v^{\frac{1}{3}}(\gamma_o^2)^{\frac{1}{2}} \quad (5)$$

W_d, W_s, V_d and V_s are the weight and volume of dry polymer and swollen polymer at equilibrium, respectively; ρ_1 and ρ_2 are the solvent and polymer density, respectively; M◦ is the molecular weight of monomer; X is degree of crosslinking; $(\gamma_o^2)^{\frac{1}{2}}$ is the root mean square end-to-end distance between two adjacent crosslinks in swollen state, and can be determined from rubber elasticity theory. Generally, these parameters are largely affected by the crosslinking density, nature of the polymeric chains and fillers. It is well known that the swelling ratio decreases with increasing crosslinking density. On the other hand, hydrogels with ionizable groups exhibit higher swelling ratio due to repulsion between polymer chains [42,294]. Furthermore, polymerization mechanism, either step-growth or chain-growth, affects the network structure. Step-growth copolymerization of monomers with complementary reactive functionalities forms a homogeneous network with superior strength as compared with the analogue chain-growth networks [261].

4.3.2. Porosity—It is essential to open new pores within the scaffolds at specific time points to accommodate the newly developed blood vessels, and to provide a space for the proliferating cells [295]. Unlike most of the current pore-forming strategies (including 3D bioprinting [296], lithography [297], porogen leaching agents [298-301], gas foaming [302], and freeze drying [303]) that generate scaffolds with static porosity, strategies based on stimuli-responsive materials have opened up opportunities for spatiotemporal modulation of scaffolds porosity. Han et al. reported a fascinating approach for dynamic modulation of pore size and pore density over time [295]. In their study, three different stimuli-responsive porogens of gelatin, sodium alginate, and HA were embedded within gelatin-based hydrogel, and then stimulated sequentially at different time points using temperature on day zero, ethylene-diaminetetraacetic acid (EDTA) on day seven, and hyaluronidase after two weeks to enable controlled formation of macropores for facilitating cell proliferation and matrix production (Fig. 11A). This approach resulted in a remarkable production of collagen type II and X by chondrocytes. In addition, stimuli-responsive materials have been employed for the development of scaffolds with dynamic pore geometry. For example, Yang and co-workers utilized stimuli-responsive porogens of alginate fibers to form scaffold having microchannel-like porosity, with porosity changing

over time [304]. Human embryonic kidney cell-loaded alginate fibers were first prepared using the coaxial flow of calcium chloride and a mixture of sodium alginate and cells, and then embedded within gelatin scaffold. Subjecting the scaffold to EDTA solution triggered spatiotemporal dissolution of the alginate fibers and hence releasing of cells, resulting in dynamic formation of inter-connected microchannels with cells growing along luminal surfaces of the channels. In another study, porous scaffolds with dynamic uniaxial tubular pores were developed by Lonov and co-workers [305]. Polymer bilayer composed of hydrophobic poly(methyl methacrylate-*co*-benzophenone acrylate) (poly(MMA-*co*-BA)) layer was deposited on the top of hydrophilic pH-responsive poly(*N*-isopropylacrylamide-*co*-acrylic acid-*co*-benzophenone acrylate) (poly(NIPAM-*co*-AA-*co*-BA)) layer using dip coating, and then irradiated with UV through photomask, followed by washing to remove the uncrosslinked regions, to eventually generate crosslinked rectangular strips. The resultant polymer films underwent reversible pH-responsive self-rolling to generate 3D structure with aligned pores, and the rolling rate can be modulated by tuning pH, temperature, and ionic strength (Fig. 11B). This strategy enables uniform seeding of cells on the polymer film before folding to the tubular structure.

4.3.3. Alignment topography—Stimuli-responsive scaffolds capable of programmed deformation with external or internal stimuli to change their configurations have received increasing attention for dynamic tuning of the topographical microenvironment [306,307]. Zhao et al. prepared a bilayer consisting of a layer of shape memory poly(lactide-*co*-trimethylene carbonate) copolymer and a layer of electrospun PCL/GelMA for endothelial cell attachment [308]. The bilayer scaffold exhibited temporary 2D planar structure at room temperature, while self-rolled into 3D tubular structure at physiological temperature, resulting in a closed-tubular scaffold of the confluent endothelial monolayer (Fig. 11C). In addition, dynamic modulation of topographical cues in real time, as well as capturing the changes in cell morphology upon sequential alteration of subcellular microtopographies, has been explored by Anseth and co-workers. In their study, photodegradable hydrogel was synthesized by radical copolymerization of PEG monoacrylate and oNB-based PEG diacrylate crosslinker. Subsequently, the smooth surface of hydrogel was seeded with hMSCs, and then exposed to controlled UV irradiation after 24 h and 48 h to create anisotropic channels and isotropic squares patterns, respectively. The hMSCs dynamically changed its morphology from rounded feature on the smooth surface to elongated and back to more rounded morphology on channels and squares topographies, respectively (Fig. 11D) [309]. Unlike scaffolds with stimuli-responsive shape memory that display dynamic topographies predesigned based on substrate materials and very often require changes of cell culture temperature or pH, photo-degradable hydrogels have enabled multiple dynamic alterations of surface topography that is independent of substrate [309,310]. Furthermore, electro-responsive scaffolds have also been employed for dynamic modulation of cell alignments. For example, Post and co-workers reported alignment of porcine smooth muscle cells on electro-responsive semi-interpenetrating PAA/fibrin network after electrical stimulation using direct electric field and switching the polarization voltage. Electro-mediated swelling/deswelling of PAA/fibrin hydrogel engendered dynamic mechanical forces that guided cell alignment relative to static scaffolds [190].

5. Integration of stimuli-responsive scaffolds with biofabrication technologies

Native ECMs composed of highly organized multi-cellular structures over multiscale sizes, spanning from nanoscale and mesoscale to macroscale dimensions [311]. Thus, engineering of cell microenvironment necessitates not only endowing dynamicity to the scaffolds, but also emulating the structure organization of native tissues. Unlike the random distribution of cells within scaffolds that lack structural arrangement, coupling the structural organization capacity of biofabrication technology with the dynamicity of stimuli-responsive materials enables the development of biologically-relevant scaffolds with higher-order arrangement of cells over multiple length scales. This section highlights the integration of stimuli-responsive scaffolds with recent biofabrication strategies including lithography, micromolding, microcontact printing, microfluidics-assisted biofabrication and bioprinting modalities, with the aim to develop in vitro dynamic scaffolds with structural and organizational complexity similar to native tissues for manipulation of structural cues.

5.1. Photolithography

Photolithography is a widely used technique in microelectronics for patterning hard substrates with a material of interest [312]. UV light, photoresist, and photo-mask are the major components used to generate a patterned surface. Nonetheless, mask-based photolithography involves irradiation of photoactive materials with light, typically UV light, through 2D photomask to confine photochemical reactions within the irradiated area [313]. Early work toward understanding the cell-cell contact, cell-ECM interaction and biochemical cross-talk focused on the development of biochemical 2D patterns on static hard substrates [314-316]. In recent years, significant progress has been made using mask-based photolithography to develop 3D scaffolds that capture the heterogeneity of in vivo microenvironment. As discussed in the previous section, integration of photo-responsive materials with photolithographic technique has enabled the fabrication of dynamic hydrogel micropatterns with specific shapes and dimensions, as well as the generation of spatiotemporal biochemical and biophysical patterns/gradients on soft hydrogel scaffolds for many studies such as interpretation of cell-matrices interaction, elucidation of cell-directing cues, regulation of cell morphogenesis [317-319]. For example, photodegradable GelMA hydrogel based on photocleavable oNB ester bonds was patterned using UV light into different shapes to enhance spreading, alignment, and beating profile of neonatal rat cardiomyocytes (Fig. 12A) [320]. A variety of photochemical reactions can occur upon irradiation with light such as crosslinking of photocurable monomers/macromers, degradation of photodegradable scaffolds, removal of photolabile cages to induce further reactions, photo-release of biochemical signals, or photoconjugation of biomolecules. Appropriate control over irradiation time, light intensity, and photoinitiator concentration is required to maintain pattern fidelity and avoid undesired reactions from non-irradiated regions, as well as eliminating potential cytotoxicity from photoinitiator [321]. Importantly, mask-based lithography is a high throughput technique that enables microfabrication of precise X–Y patterns of varying features spanning from micron to submicron. However, it fails to achieve 3D control, because of the propagation of photochemical reactions in the whole irradiated regions within the hydrogel [172]. Therefore, this technique is

effective for the modulation of bulk biochemical and biophysical cues of 3D scaffolds, but the inability of on-demand 3D control of local microenvironment of cells is a major limitation of this approach. Recently, other light-based strategies such as single-photon laser scanning lithography and multiphoton laser scanning lithography have emerged as excellent alternatives to photolithography, enabling precise 3D spatiotemporal patterning of the decisive biochemical and biophysical cues within subvolumes of the hydrogel scaffolds. The former approach depends on using single-photon light to confine photochemical reactions near the focal point to somewhat achieve 3D controlled patterning, while the latter approach uses multiphoton light to provide the energy required for initiation exactly at the focal point. Numerous examples depicting spatial and temporal patterning of growth factors, peptides, and proteins within hydrogels incorporating oNB and coumarin functionalities for manipulating cell spreading and fate have been discussed in previous sections.

Furthermore, photolithography has a prominent role in 4D biofabrication of smart scaffolds with shape-morphing effect, enabling shape transformation into geometrical structures that are not attainable by classical biofabrication techniques [322,323]. For instance, Gracias et al. developed PEG bilayers of different swelling, via sequential crosslinking of PEG diacrylate of different molecular weights using photopatterned mask (Fig. 12B). Owing to the differential swelling of the bilayers, the planar PEG bilayer self-folded in water into cylindrical, spherical capsules, and helices-shaped 3D hydrogels, depending on the mask pattern. Insulin-secreting β-TC-6 cells encapsulated within self-folded cylindrical hydrogels showed significant insulin release upon stimulation with glucose, as compared with those cultured within planar hydrogels. Also, multi-cellular cylindrical hydrogel was developed by self-folding of PEG bilayers, each containing a different population of L929 cells [324]. Interestingly, this strategy allowed the fabrication of responsive bilayer from non-responsive PEG layers. In another study, micropatterned bilayers composed of thermo-responsive PNIPAM and non-responsive PLA-*b*-PEG-*b*-PLA triblock copolymer was developed by photolithography, and showed reversible rolling/unrolling at a temperature below/above LCST of PNIPAM. The rolled bilayer encapsulating cardiomyocytes at 25 °C unfolded at physiological temperature to release the cardiac microtissues to the diseased tissues [323]. In another example, trilayers consisting of hydrophilic poly(*N*-isopropylacrylamide-*co*-acrylic acid) (poly(NIPAM-*co*-AA)) copolymer as bottom layer, hydrophobic poly(stearyl methacrylate-*co*-benzophenone acrylate) (poly(SMA-*co*-BA); melting point: 34 °C) as middle layer, and patterned PEG as top layer was developed via sequential deposition of poly(NIPAM-*co*-AA) and poly(SMA-*co*-BA) on silicon wafer to form bilayer, followed by photolithography patterning of PEG macromer (Fig. 12C) [325]. At physiological temperature, the swelling gradient between poly(NIPAM-*co*-AA) layer and softened poly(SMA-*co*-BA) layer engendered stress, which triggers the folding of trilayers into a tubular structure. The PEG-patterned trilayer was successfully used to develop spatially patterned cell-wrap of cells of F3T3 cells at 37 °C.

5.2. Microcontact printing

Microcontact printing (μCP) is a soft lithographic technique commonly used to pattern cells, proteins and other biological compounds by transferring the pattern from soft elastomeric stamp, usually made from PDMS, to a substrate surface (Fig. 13A(a)) [326,327]. Integration

of stimuli-responsive materials with μCP has enabled the development of smart cell culture substrates that could be stimulated to trigger desirable structural, chemical, and biological events.

Thermo-responsive PNIPAM has been widely used as a sacrificial layer in μCP, to enable functionalization of cells, spatial control of cell attachment/detachment, and the formation of aligned and easily harvested cell sheets [328-330]. For instance, patterns of polyelectrolyte microparticles and poly(lactic-*co*-glycolic acid) nanoparticles were created by bringing the inked PDMS stamps in contact with a sacrificial layer of PNIPAM-coated glass at 37 °C, and then used for seeding K562 cells, mouse embryonic stem cells (mESCs) and hMSCs (Fig. 13B). At a temperature lower than LCST, the single cell-particles complexes were released from PNIPAM layer to form a complex assembly of cells [329]. The polyelectrolyte microparticle decorating cells could be used for delivery of growth factors or for modulation of stem cell differentiation [329,331]. In another study, μCP of cell-adhesive FN on the surface of PNIPAM-grafted substrate was used to develop aligned cell sheet of vascular smooth muscle cells (VSMCs). Lowering the temperature enabled the transformation of the organized cell sheet to gelatin stamp without destroying cell alignment because of cell contraction. Cells displayed well-aligned and elongated morphology on FN-PNIPAM pattern as compared to non-patterned FN-NIPAM substrate [328]. Similarly, Okano et al. developed a pattern of rhodamine-FN on thermo-responsive cell culture plate for the generation of cell-sheet micropattern after co-culture of normal human dermal fibroblast and bovine artery endothelial cells. This system enabled defining the appropriate stamping force required in μCP to generate high-quality cell sheet micropattern. The thermo-responsive dish facilitated the harvesting of cell sheet by lowering temperature and increasing hydrophilicity [330].

Besides PNIPAM, other thermo-responsive materials, such as tetronic tyramine and elastin-like polypeptides, have also been employed for formation of geometrically aligned microtissues [332,333]. For example, Shin et al. reported patterning of the surface of thermally expandable Tetronic-tyramine hydrogel with polydopamine lanes of different widths, for the spatially controlled culture of human dermal fibroblasts (HDFBs) (Fig. 13C). The strip-like microtissues were translocated to FN-coated glass by thermal expansion of the contacted hydrogel at 4 °C [332]. Interestingly, the cell strips started to migrate to fill the bar areas on the glass with structurally aligned tissues, suggesting that the aligned cell strips by itself provide topographical guidance to the migrating cells. In another example, a pattern of thermo-responsive lysine-containing elastin-like polypeptides (K-ELP) on aldehyde-modified glass was developed by μCP of a removable polymer template, which masked the aldehyde moieties within specific regions, thus allowing conjugation K-ELP to the bare areas [333]. After coating the pattern with FN, the resultant dynamic 2D pattern reversibly enabled the attachment/detachment of fibroblast cells upon changing temperature above/below the transition temperature of K-ELP (30 °C), because of hydrophilicity-hydrophobicity change. Although μCP of biomolecules on hydrogel surfaces has encountered some difficulties such as deformation of patterns upon pressing on PDMS stamp and inability of soft hydrogels to withstand pressure, more efforts are given to integration of μCP with other biofabrication technologies such as microfluidics [334]. Moreover, integration of μCP and photolithography has also been studied to develop a

unique pattern of electro-responsive hydroquinone-terminated SAM on a hard substrate for dynamic manipulation of cell attachment/detachment [335].

5.3. Micromolding patterning

Micromolding is also a soft lithographic technique enabling fabrication of hydrogel scaffolds with controlled sizes, shapes, and topographies, through casting hydrogel-forming polymers into micromolds with predefined patterns, and subsequently gelling of the polymers to form 3D constructs (Fig. 13A(b)) [336-338]. PDMS micromold with controllable features can be easily fabricated using silicon wafer with the desired pattern generated by photolithography, and therefore allow the development of micro- and nanoscale patterns. Unlike conventional micromolding strategy that uses non-stimuli-responsive polymers like PEG to form static microgels, integration of stimuli-responsive materials with micromolding approach allows the development of dynamic micromolds. For example, Khademhosseini et al. developed multicompartment hydrogel microstructure composed of two or more spatially patterned gels using stimuli-responsive micromolds of different shapes (Fig. 14A) [49]. In their study, thermo-responsive PNIPAM micromolds of microgrooves, circular, and square shapes were first developed, and then the first gel was crosslinked inside the microwells at 4 °C. After that, the temperature of micromold was raised to 37 °C to create empty spaces upon collapsing of PNIPAM, wherein sequential patterning of the second gel was performed. The first and second agarose gels were loaded with microparticles of a different color, and efficient patterning was revealed. This approach also demonstrated successful patterning of 3T3 fibroblasts, HepG2 cells, and HUVECs cells. Similarly, the same group reported conformal coating of the microgroove pattern of PDMS micromold with PNIPAM layer using initiated chemical vapor deposition. PNIPAM-coated micromold was used to align NIH 3T3 cells, and enable harvesting of the longitudinal tissue construct by changing the temperature below LCST to increase the swelling and hydrophilicity of PNIPAM, thus leading to detachment of cells [339].

In addition, Navaei et al. utilized the micromolding approach to create a pattern of GelMA/gold nanorod (GelMA-GNR) composite hydrogel. Cardiomyocytes seeded on this pattern displayed significant cell alignment, and upregulated expression of sacromeric α-actinin and connexin 43 was noticed as compared to the blank GelMA hydrogel (Fig. 14B) [340]. Furthermore, hydrogel scaffolds with microchannels or porous structures have been developed using sacrificial micromolds, which can be dissolved after solidification of polymer around the sacrificial template. A sacrificial micromold of thermo-dissolvable gelatin has been used to produce hydrogels with microfluidic channels [341].

5.4. Microfluidic-assisted patterning

Microfluidics relies on the manipulation of small volumes of liquids at microliter to picoliter scale through capillaries (Fig. 15A) [342]. Substantial progress has been made to prepare hydrogel scaffolds using microfluidic devices, allowing the development of biomimetic environments relative to conventional culture systems by promoting cell-ECM interaction. This technique has several appreciable advantages. First, it allows precise control over the distribution of biochemical and biophysical cues spatially and temporally. Second, it enables well-tuned geometric patterning of cells and biomolecules by laminar flow of multiple

streams of fluids in a microfluidic capillary with small dimensions, as well as patterning of cell culture media itself [343]. The streams flow parallel to each other without mixing, and only diffusion across liquid-liquid interfaces occurs [344]. Third, it facilitates the study of subcellular processes by allowing two different streams to flow over a single cell placed at the interface between the two streams [345]. Fourth, it permits assessment of cell differentiation using a fewer number of cells and minimum quantities of reagents. Fifth, it enables precise control of cell microenvironment by using small volumes of liquids. Sixth, it allows co-culture and hierarchical growth of different cell types in 3D system using laminar flow through multiple microchannels. In addition, by using automated microfluidic devices with mechanical valves or osmotic pumps, on-demand delivery of biofactors and generation of a gradient of growth factors can be achieved [346]. Moreover, microfluidic devices allow manipulation of shear stress, oxygen tension, pH/temperature gradients, and diffusion of bio-essentials, which are decisive biophysical cues for determination of cell phenotypes [347]. The setup for the laminar flow experiment includes the fabrication of pattern of multiple capillaries, with different inlets which are combined in one main capillary on PDMS. Subsequently, contact the patterned PDMS to a glass surface generates the channels [344].

Significant progress in biomaterials fabrication has been achieved via the integration of stimuli-responsive materials with microfluidics, enabling the development of smart microgels, microfibers, and scaffolds with controlled porosity and alignment [348-352]. For example, Yoon and co-workers developed multi-stimuli responsive hydrogel microfibers and microtubes for potentially capturing the dynamics and geometrical alignment of native tissues [47]. Crosslinked hydrogel microfibers were generated by the coaxial flow of NIPAM, sodium acrylate or allylamine, *N,N′*-methylenebis(acrylamide) crosslinker, and alginate in the inner capillaries and $CaCl_2$ in the outer capillaries of a microfluidic device, along with irradiating the emerging fibers with UV light (Fig. 15A). Likewise, a tubular hydrogel was created by using $CaCl_2$ as inner fluid, and the rest of components as an outer fluid. Alginate template was removed using EDTA solution after the fabrication of fibers and microtubes. Both microfibers and microtubes exhibited reversible phase transition and changes of the microtube diameter and wall thickness with pH and temperature. The hydrogel microfibers also supported attachment and proliferation of Hep G2 cells. The same group also developed magneto- and photo-responsive PNIPAM-based microfibers, wherein the magnetic nanoparticles generate heat upon irradiation with visible light to induce volume change of PNIPAM microfibers [353]. Precise control over the physicochemical features of the particles could be achieved by controlling the concentrations of materials precursors in solvents, the flow rate of the inner and outer fluids, and total flow rate.

In another study, Haag and co-workers reported the fabrication of pH-responsive cell-laden microgel for encapsulation and release of NIH 3T3 cells [348]. In their study, azide-terminated dendritic polyglycerol incorporating pH-sensitive benzacetal functionalities, PEG-dicyclooctyne, and NIH 3T3 cells were injected through microfluidic channels, and thus crosslinked via SPAAC to form monodispersed microgel (Fig. 15B). The cell-loaded microgels exhibited pH-sensitive release of cells at pH of 6 owing to the cleavage of benzaacetal functionalities. Furthermore, photo- and thermo-responsive materials play an

integral role in the development of microfluidic devices, as smart microvalves, pumps, and actuators [354,355].

5.5. 3D bioprinting modalities

Bioprinting combines 3D printing technology, cell biology and biomaterial sciences to construct 3D structures of geometrical and organizational features similar to native tissues by layer-by-layer positioning of printable bioink [356]. The major bioprinting technologies include inkjet bioprinting [357], microextrusion [358], laser-assisted printing [359], and stereolithography [360]. Unlike conventional 3D bioprinting which generally creates static 3D scaffolds, integration of stimuli-responsive materials with 3D bioprinting technology results in 3D objects capable of the programmable transformation of their shapes or functions upon stimulation with external or intrinsic stimuli [361,362]. Owing to its' time-dependent transformation of the printed 3D object, 4D bioprinting is a commonly used term to specifically indicate 3D printing of stimuli-responsive materials. Substantial progress in 4D bioprinting has been achieved using stimuli-responsive hydrogels as smart bioinks. Precise patterning of multi-materials of gradient properties enables programmable on-demand transformation into pre-designed shapes. Temperature, humidity, and ions are among the most favorable stimuli because they can be applied in broad ranges (e.g., 4–40 °C) without altering cell viability [363,364]. Conversely, other stimuli, such as pH and UV irradiation, have narrow application range to maintain considerable viability of cells. Liu et al. developed bioinspired thermo-responsive tubular implants capable of a variety of temperature-triggered shape transformation, such as radial expansion, bending, gripping, and uniaxial elongation (Fig. 16A). In their study, segmental patterning of acrylamide-laponite and NIPAM-laponite bioinks into tube-like structure was achieved using direct ink writing and photocuring. The spatial arrangement of thermo-responsive PNIPAM, amenable to undergo swelling/shrinking transition with temperature, and non-responsive polyacrylamide induced shape changing because of differential swelling [46]. In addition, 4D bioprinting using thermo-responsive gelatin or agarose as fugitive bioinks provides promising solutions toward the development of vascularized scaffolds [365,366]. For instance, Forgacs and co-workers developed scaffold-free vascular constructs by concomitant layer-by-layer deposition of agarose rods (which act as sacrificial templates), and multicellular cylinders or spheroids (Fig. 16B) [366]. The hollow tubular construct of pig smooth muscle cells was generated after the thermal dissolution of the inner agarose rod. Likewise, double-layered tubes of smooth muscle cells (HUVSMCs) and human skin fibroblasts (HSFs) were created, wherein the cells self-adhere to each other to integrate the construct.

Besides external stimuli, intrinsic stimuli were also used to trigger programmable self-folding of the printed scaffolds. This relies on the generation of gradients of swelling, osmolarity, and wettability, thereby internal stresses could be generated to trigger well-defined shape changing. Lewis and co-workers reported biomimetic 4D printing of plant-inspired shape-morphing structures such as flowers and leaves [367]. Direct ink writing of smart bioink composed of NIPAM, nanofibrillated cellulose (NFC), hectorite nanoclay, photoinitiator, glucose, and glucose oxidase resulted in a shear-induced alignment of NFC, which in turn generated anisotropic stiffness, leading to preferential swelling on the longitudinal direction as compared to transverse direction (Fig. 17A). Precise control

over the positioning of the anisotropic swelling within a bilayer structure resulted in the programmable folding/unfolding of the printed pattern (e.g. flower-shaped structure) upon swelling. In another study, Lonov and co-workers reported the development of hollow self-folding tubes with tunable diameters via extrusion-based printing of self-morphing methacrylated alginate (AA-MA) and HA-MA on glass or polystyrene (PS) substrates (Fig. 17B) [368]. Crosslinking of the printed AA-MA or HA-MA using visible light generated crosslinking gradient within the polymer film because of excessive exposure of top layer to light relative to the bottom layer, thereby tubular structures by irreversible folding were created. The diameter and thickness of tubes were tuned by appropriate control of printing speed, polymer concentration, light exposure, and substrate. The reversible folding/unfolding of AA-MA tubes was achieved using Ca^{2+} ions and EDTA to trigger crosslinking/de-crosslinking processes, respectively. 4D bioprinting of hollow tubes encapsulating human bone marrow stromal cells demonstrated higher cell viability after 7 days of culture. Additionally, Bayley et al. developed 3D droplet networks capable of spontaneous deformation into pre-defined geometries using heterogeneous lipid-coated microdroplets of different osmolarities (Fig. 17C) [369]. A strip and flower-shaped bilayer of droplets of different KCl concentration folded spontaneously to form closed ring and hollow sphere structures, respectively. The integrity of the droplet network was maintained by the cohesive interactions between the lipid layers, and the osmolarity difference between the droplets induced shrinking/swelling of the network and thus deformation into the final structure. This strategy could be promising for the printing of soft tissues over multiple length scales, and the droplet networks could be modified with specific proteins to enable cross-talk between cells over pre-defined paths.

6. Conclusions and future perspectives

Hydrogel-based scaffolds with stimuli-responsive behavior have attracted significant interest in the development of dynamic 3D constructs, which allow spatiotemporal modulation of physical and biological cues, as well as real-time monitoring of cell behavior. This review highlights the intriguing role of stimuli-responsive hydrogels in on-demand manipulation of cell-directing cues reversibly and irreversibly. It also emphasizes the integration of stimuli-responsive biomaterials with advanced biofabrication technologies (such as microfluidics, lithography, 3D bioprinting, and patterning-based techniques etc.), which provides opportunities to develop sophisticated 3D constructs with organizational features similar to native tissues over multiple length scales and capable of undergoing programmable shape change in response to external stimuli. Studies using such 3D constructs can prompt understanding on complex cellular processes.

Although significant progress has been achieved, there are still substantial challenges. From a chemistry perspective, the limited degradability of synthetic scaffolds under physiological conditions and the inevitable utilization of certain concentrations of toxic chemicals (such as photo-initiators) remain as concerns. Although this review summarizes the toolbox of chemistry that can be employed to tackle the degradability issue, and presents the current strategies to modulate the biological features of the scaffolds, it is critical to explore new biologically benign chemistries with optimized reaction parameters. Moreover, the current library of stimuli-responsive scaffolds mostly is smart in one aspect, and the current

experimental approaches typically explore separately the influence of individual property on cellular behavior. However, a cascade of inter-independent changes commonly happens in vivo. Thus, it is a pressing demand to develop multi-stimuli-responsive scaffolds with tunable responses and specific selectivity for spatiotemporal dynamic control of multiple cell-guiding signals simultaneously. Furthermore, pH- and thermally-sensitive structures have revealed promising results in vitro for the delivery of biological cues and the development of smart cell-laden injectable hydrogels; however, rigorous optimization of the molecular structure should be performed to ensure maintaining the responsive nature under physiological conditions of the targeted tissues. Additionally, considering the grand goal of TE, which is the development of functional tissue replacements with clinically relevant sizes, generally the reported stimuli-responsive hydrogels are mechanically weak. The TE scaffolds for tissue replacements are supposed to undergo dynamic changes, meanwhile incorporating hierarchically branched vascular networks to enable diffusion of bio-essentials. Interpenetrating double network hydrogels and hydrogel composites have been extensively studied to improve the mechanical stability of scaffolds, but rigorous optimization of their mechanical characteristics to maintain their stimuli-responsive features and sustain the function of the embedded vascular networks remains a challenge. Added to that, despite the significant progress in the development of smart 3D scaffolds that enable the spatiotemporal presentation of physical and biological cues, continuous discovery of new biorthogonal chemistries and stimuli-sensitive groups for reversible modulation of cell-directing cues, with time-dependent appearance/disappearance of signals, is needed. Besides, considering the integration of smart materials with the advanced biofabrication technologies (such as 3D printing), the exploration of new bioinks with optimal physical characteristics, which fit the prerequisites dictated by biofabrication process without interfering with the required physical and biological characteristics of the scaffolds, is also critical.

In cell biology and TE landscape, the development of intelligent 3D scaffolds enabling spatiotemporal presentation of biological and physical cues to triggers specific cellular events (such as cell attachment, proliferation, and differentiation) is still in its infancy; mimicking the exact sequential expression of biological signals from native ECMs, in time-dependent manner, is still a challenge. Noteworthily, despite the significant progress devoted to modulation of degradability of the dynamic 3D scaffolds via introducing labile bonds to the scaffolds, the differences between the scaffolds and native ECMs on the spatial distribution and reactivity of cleavable bonds result in a mismatch between the degradation rate of the biomaterials and the regeneration rate of new tissues. More efforts need to be invested to comprehensively understand the distribution pattern and reactivity of degradable moieties within native ECMs. Moreover, controlling topographical features and molecular orientation of amorphous hydrogel-based scaffolds requires further studies in order to mimic the fibrillar alignment of ECMs. Furthermore, new analytical approaches need to be explored for real-time monitoring cell-matrix interactions upon spatiotemporal modulation of the scaffolds. In addition, because so far most stimuli-responsive scaffolds are rationally designed to grow single cell population, research efforts should be greatly extended to develop smart bioactive scaffolds for co-culture of multiple types of cells for better mimicking the organizational complexity of tissues. The generation of gradients

of multiple biological and physical triggers and the development of gradient-forming approaches may critically prompt the studies to interpret the inter-independent cellular events, and subsequently provide the essential inputs for a feedback loop for the rational design of smart 3D scaffolds with optimal physical and biological characteristics.

Besides engineering and manipulation of cell microenvironment of healthy tissues, there are also ongoing attempts for the development of smart 3D scaffolds that closely resemble the biological and physiological microenvironment of tumor tissues. These studies would boost the understanding on cancer biology and help to develop appropriate cancer-combating strategies. Moreover, the advances in micro-/nanotechnologies pave the way toward the generation of miniaturized organ model for testing and screening therapeutically active anticancer drugs. On the other hand, more endeavors are needed to explore more sophisticated smart scaffolds that mimic to a greater extent the complexity of different types of cancer tissues.

Taken together, we envision that the development of smart 3D scaffolds with complexity similar to native tissues and allowing the dynamic manipulation of multiple cues spatially and temporally requires the integration of multidisciplinary approaches, guided by the advances in chemistry, material science, bioengineering, and biology. It is obvious that the remarkable complexity of tissues cannot be resembled by only one simple type of materials, and multicomponent materials as the combination of multiple types of smart materials are needed to recapitulate essential features of ECMs. Such multicomponent materials should be integrated with the advances of biofabrication technologies to generate smart 3D constructs with organizational features over multiple size scales; whereby sophisticated in vitro models can be built up for comprehensive studies to interpret complex cellular processes by monitoring the real-time response of cells upon spatiotemporal changes of the cell microenvironment. The resulting insightful understanding on complex cellular processes, especially about cell-cell and cell-material interactions, will critically prompt the development of 3D scaffolds with optimal physical and biological characteristics, as a key step towards the generation of functional tissue equivalents. Moreover, based on the future progress in interpreting the interactions of decellularized ECMs with cells and biomaterials, the development of hybrid 3D scaffolds by the combination of stimuli-responsive hydrogels with decellularized ECMs may eventually lead to the formation of tissue mimetic structures with all the complexity and essential functions of native tissues.

Acknowledgements

Mohamed Alaa Mohamed acknowledges the Egyptian Ministry of Higher Education and Scientific Research for supporting him during his PhD study in University at Buffalo.

Abbreviations:

μCP
microcontact printing

$\tau_{1/2}$
stress relaxation time constant

2D
two-dimensional

3D
three-dimensional

4D
four-dimensional

AA-MA
methacrylated alginate

BA
benzophenone acrylate

BMP
bone morphogenetic protein

CDs
cyclodextrins

CNTF
ciliary neurotrophic factor

DMAEMA
2-(dimethylamino)ethyl methacrylate

DOPA
3,4-dihydroxyphenylalanine

ECM
extracellular matrix

EDTA
ethylenediaminetetraacetic acid

EGF
epidermal growth factor

ELP
elastin-like polypeptides

ESMNs
embryonic stem cell-derived motor neurons

FGF2
fibroblast growth factor basic

FGFs
fibroblast growth factors

Fmoc
fluoren-9-ylmethoxy)carbonyl

FN
fibronectin

FXIIIa
transglutaminase factor XIII enzyme

GAGs
glycosaminoglycans

GelMA
methacrylated gelatin

GNR
gold nanorod

HA
hyaluronic acid

HA-MA
methacrylated hyaluronic acid

HDFBs
human dermal fibroblasts

HEMA
2-hydroxyethyl methacrylate

hMSCs
human mesenchymal stem cells

HRP
horseradish peroxidase

HSFs
human skin fibroblasts

HUVSMCs
human umbilical vein smooth muscle cells

K-ELP
lysine-containing elastin-like polypeptides

LCST
lower critical solution temperature

mESCs
mouse embryonic stem cells

MMP
matrix metalloproteinase

NFC
nanofibrillated cellulose

NGF
neural growth factor

NIPAM
N-isopropylacrylamide

NPPOC
2-(2-nitrophenyl) propyloxycarbonyl

oNB
o-nitrobenzyl

PAA
poly(acrylic acid)

PMMA
poly(methyl methacrylate)

PNIPAM
poly(*N*-isopropylacrylamide)

poly(HPMA-*co*-HEMA)
poly((*N*-(2-hydroxypropyl)-methacrylamide)-*co*-2-hydroxyethyl methacrylate)

poly(MMA-*co*-BA)
poly(methyl methacrylate-*co*-benzophenone acrylate)

poly(NIPAM-*co*-AA)
poly(*N*-isopropylacrylamide-*co*-acrylic acid)

poly(NIPAM-*co*-AA-*co*-BA)
poly(*N*-isopropylacrylamide-*co*-acrylic acid-*co*-benzophenone acrylate)

poly(PEGDMA-*co*-DMAEMA)
poly(PEG dimethacrylate-*co*-2-(dimethylamino)ethyl methacrylate)

poly(SMA-*co*-BA)
poly(stearyl methacrylate-*co*-benzophenone acrylate)

PSCs
pancreatic stellate cells

PVA

poly(vinyl alcohol)

RGD
Arg-Gly-Asp

RGDS
Arg-Gly-Asp-Ser

RGES
Arg-Gly-Glu-Ser

SAM
self-assembled monolayer

SMPs
shape memory polymers

TE
tissue engineering

TGF-β
transforming growth factor-β

TGFβ1
transforming growth factor β1

UCST
upper critical solution temperature

UPy
4-ureido-2-pyrimidone

VEGF
vascular endothelial growth factor

VSMCs
vascular smooth muscle cells

References

[1]. Wang H, Heilshorn SC. Adaptable hydrogel networks with reversible linkages for tissue engineering. Adv Mater 2015;27:3717–36. [PubMed: 25989348]

[2]. Cai L, Heilshorn SC. Designing ECM-mimetic materials using protein engineering. Acta Biomater 2014;10:1751–60. [PubMed: 24365704]

[3]. Chan G, Mooney DJ. New materials for tissue engineering: towards greater control over the biological response. Trends Biotechnol 2008;26:382–92. [PubMed: 18501452]

[4]. Engler AJ, Sen S, Sweeney HL, Discher DE. Matrix elasticity directs stem cell lineage specification. Cell 2006;126:677–89. [PubMed: 16923388]

[5]. Hoffman BD, Grashoff C, Schwartz MA. Dynamic molecular processes mediate cellular mechanotransduction. Nature 2011;475:316–23. [PubMed: 21776077]

[6]. Pek YS, Wan ACA, Ying JY. The effect of matrix stiffness on mesenchymal stem cell differentiation in a 3D thixotropic gel. Biomaterials 2010;31:385–91. [PubMed: 19811817]

[7]. Rice JJ, Martino MM, De Laporte L, Tortelli F, Briquez PS, Hubbell JA. Engineering the regenerative microenvironment with biomaterials. Adv Healthc Mater 2013;2:57–71. [PubMed: 23184739]

[8]. Daley WP, Peters SB, Larsen M. Extracellular matrix dynamics in development and regenerative medicine. J Cell Sci 2008;121:255–64. [PubMed: 18216330]

[9]. Ellis V, Murphy G. Cellular strategies for proteolytic targeting during migration and invasion. FEBS Lett 2001;506:1–5. [PubMed: 11591360]

[10]. Murphy G, Gavrilovic J. Proteolysis and cell migration: creating a path? Curr Opin Cell Biol 1999;11:614–21. [PubMed: 10508651]

[11]. Hynes RO. Stretching the boundaries of extracellular matrix research. Nat Rev Mol Cell Biol 2014;15:761–3. [PubMed: 25574535]

[12]. Berry MF, Engler AJ, Woo YJ, Pirolli TJ, Bish LT, Jayasankar V, et al. Mesenchymal stem cell injection after myocardial infarction improves myocardial compliance. Am J Physiol Heart Circ Physiol 2006;290:H2196–203. [PubMed: 16473959]

[13]. Huang G, Li F, Zhao X, Ma Y, Li Y, Lin M, et al. Functional and biomimetic materials for engineering of the three-dimensional cell microenvironment. Chem Rev 2017;117:12764–850. [PubMed: 28991456]

[14]. Jansen K, Bacabac R, Piechocka I, Koenderink G. Cells actively stiffen fibrin networks by generating contractile stress. Biophys J 2013;105:2240–51. [PubMed: 24268136]

[15]. Liu F, Mih JD, Shea BS, Kho AT, Sharif AS, Tager AM, et al. Feedback amplification of fibrosis through matrix stiffening and COX-2 suppression. J Cell Biol 2010;190:693–706. [PubMed: 20733059]

[16]. Acerbi I, Cassereau L, Dean I, Shi Q, Au A, Park C, et al. Human breast cancer invasion and aggression correlates with ECM stiffening and immune cell infiltration. Integr Biol 2015;7:1120–34.

[17]. Levental KR, Yu H, Kass L, Lakins JN, Egeblad M, Erler JT, et al. Matrix crosslinking forces tumor progression by enhancing integrin signaling. Cell 2009;139:891–906. [PubMed: 19931152]

[18]. Sunyer R, Conte V, Escribano J, Elosegui-Artola A, Labernadie A, Valon L, et al. Collective cell durotaxis emerges from long-range intercellular force transmission. Science 2016;353:1157–61. [PubMed: 27609894]

[19]. Sant S, Hancock MJ, Donnelly JP, Iyer D, Khademhosseini A. Biomimetic gradient hydrogels for tissue engineering. Can J Chem Eng 2010;88:899–911. [PubMed: 21874065]

[20]. Russo TA, Stoll D, Nader HB, Dreyfuss JL. Mechanical stretch implications for vascular endothelial cells: altered extracellular matrix synthesis and remodeling in pathological conditions. Life Sci 2018;213:214–25. [PubMed: 30343127]

[21]. Moretti M, Prina-Mello A, Reid AJ. Endothelial cell alignment on cyclically-stretched silicone surfaces. J Mater Sci Mater Med 2004;15:1159–64. [PubMed: 15516879]

[22]. Ando J, Yamamoto K. Effects of shear stress and stretch on endothelial function. Antioxid Redox Signal 2010;15:1389–403.

[23]. Ao M, Brewer BM, Yang L, Franco Coronel OE, Hayward SW, Webb DJ, et al. Stretching fibroblasts remodels fibronectin and alters cancer cell migration. Sci Rep 2015;5, 8334/1–9. [PubMed: 25660754]

[24]. Otis JS, Burkholder TJ, Pavlath GK. Stretch-induced myoblast proliferation is dependent on the COX2 pathway. Exp Cell Res 2005;310:417–25. [PubMed: 16168411]

[25]. Bansai S, Morikura T, Onoe H, Miyata S. Effect of cyclic stretch on tissue maturation in myoblast-laden hydrogel fibers. Micromachines 2019;10, 339/1–9. [PubMed: 31121955]

[26]. Mihic A, Li J, Miyagi Y, Gagliardi M, Li S-H, Zu J, et al. .The effect of cyclic stretch on maturation and 3D tissue formation of human embryonic stem cell-derived cardiomyocytes. Biomaterials 2014;35:2798–808. [PubMed: 24424206]

[27]. Dan P, Velot É, Decot V, Menu P. The role of mechanical stimuli in the vascular differentiation of mesenchymal stem cells. J Cell Sci 2015;128:2415–22. [PubMed: 26116570]

[28]. Guo T, Yu L, Lim CG, Goodley AS, Xiao X, Placone JK, et al. Effect of dynamic culture and periodic compression on human mesenchymal stem cell proliferation and chondrogenesis. Ann Biomed Eng 2016;44:2103–13. [PubMed: 26577256]

[29]. Sekiya I, Vuoristo JT, Larson BL, Prockop DJ. In vitro cartilage formation by human adult stem cells from bone marrow stroma defines the sequence of cellular and molecular events during chondrogenesis. Proc Natl Acad Sci U S A 2002;99:4397–402. [PubMed: 11917104]

[30]. Ramirez F, Rifkin DB. Cell signaling events: a view from the matrix. Matrix Biol 2003;22:101–7. [PubMed: 12782137]

[31]. Briquez PS, Clegg LE, Martino MM, Gabhann FM, Hubbell JA. Design principles for therapeutic angiogenic materials. Nat Rev Mater 2016;1, 15006/1–15.

[32]. Makarenkova HP, Hoffman MP, Beenken A, Eliseenkova AV, Meech R, Tsau C, et al. Differential interactions of FGFs with heparan sulfate control gradient formation and branching Morphogenesis. Sci Signal 2009;2(ra55):1–21.

[33]. Swartz MA. Signaling in morphogenesis: transport cues in morphogenesis. Curr Opin Biotechnol 2003;14:547–50. [PubMed: 14580587]

[34]. Mai J, Fok L, Gao H, Zhang X, Po M-m. Axon initiation and growth cone turning on bound protein gradients. J Neurosci 2009;29:7450–8. [PubMed: 19515913]

[35]. Wang F The signaling mechanisms underlying cell polarity and chemotaxis. Cold Spring Harb Perspect Biol 2009;1:1–17, a002980.

[36]. Wells RG. The role of matrix stiffness in regulating cell behavior. Hepatology 2008;47:1394–400. [PubMed: 18307210]

[37]. Stowers RS, Allen SC, Suggs LJ. Dynamic phototuning of 3D hydrogel stiffness. Proc Natl Acad Sci U S A 2015;112:1953–8. [PubMed: 25646417]

[38]. Larsen M, Artym VV, Green JA, Yamada KM. The matrix reorganized: extracellular matrix remodeling and integrin signaling. Curr Opin Cell Biol 2006;18:463–71. [PubMed: 16919434]

[39]. Hunt NC, Grover LM. Cell encapsulation using biopolymer gels for regenerative medicine. Biotechnol Lett 2010;32:733–42. [PubMed: 20155383]

[40]. Liu SQ, Tay R, Khan M, Ee PLR, Hedrick JL, Yang YY. Synthetic hydrogels for controlled stem cell differentiation. Soft Matter 2010;6:67–81.

[41]. Slaughter BV, Khurshid SS, Fisher OZ, Khademhosseini A, Peppas NA. Hydrogels in regenerative medicine. Adv Mater 2009;21:3307–29. [PubMed: 20882499]

[42]. Zhu J, Marchant RE. Design properties of hydrogel tissue-engineering scaffolds. Expert Rev Med Devices 2011;8:607–26. [PubMed: 22026626]

[43]. Brown TE, Anseth KS. Spatiotemporal hydrogel biomaterials for regenerative medicine. Chem Soc Rev 2017;46:6532–52. [PubMed: 28820527]

[44]. Ahadian S, Sadeghian RB, Salehi S, Ostrovidov S, Bae H, Ramalingam M, et al. Bioconjugated hydrogels for tissue engineering and regenerative medicine. Bioconjugate Chem 2015;26:1984–2001.

[45]. Kai D, Prabhakaran MP, Stahl B, Eblenkamp M, Wintermantel E, Ramakrishna S. Mechanical properties and in vitro behavior of nanofiber-hydrogel composites for tissue engineering applications. Nanotechnology 2012;23(095705):1–10.

[46]. Liu J, Erol O, Pantula A, Liu W, Jiang Z, Kobayashi K, et al. Dual-gel 4D printing of bioinspired Tubes. ACS Appl Mater Interfaces 2019;11:8492–8. [PubMed: 30694051]

[47]. Kim D, Jo A, Imani KBC, Kim D, Chung JW, Yoon J. Microfluidic fabrication of multistimuli-responsive tubular hydrogels for cellular scaffolds. Langmuir 2018;34:4351–9. [PubMed: 29553747]

[48]. DeForest CA, Anseth KS. Photoreversible patterning of biomolecules within Click-based hydrogels. Angew Chem Int Ed 2012;51:1816–9.

[49]. Tekin H, Tsinman T, Sanchez JG, Jones BJ, Camci-Unal G, Nichol JW, et al. Responsive micromolds for sequential patterning of hydrogel microstructures. J Am Chem Soc 2011;133:12944–7. [PubMed: 21766872]

[50]. Guillemot F, Mironov V, Nakamura M. Bioprinting is coming of age: report from the international Conference on Bioprinting and Biofabrication in Bordeaux (3B'09). Biofabrication 2010;2(010201):1–7.

[51]. Pedde RD, Mirani B, Navaei A, Styan T, Wong S, Mehrali M, et al. Emerging biofabrication strategies for engineering complex tissue constructs. Adv Mater 2017;29(1606061):1–27.

[52]. Malda J, Visser J, Melchels FP, Juengst T, Hennink WE, Dhert WJA, et al. 25th Anniversary article: engineering hydrogels for biofabrication. Adv Mater 2013;25:5011–28. [PubMed: 24038336]

[53]. Theocharis AD, Skandalis SS, Gialeli C, Karamanos NK. Extracellular matrix structure. Adv Drug Deliv Rev 2016;97:4–27. [PubMed: 26562801]

[54]. Freudenberg U, Liang Y, Kiick KL, Werner C. Glycosaminoglycan-based biohybrid hydrogels: a sweet and smart choice for multifunctional biomaterials. Adv Mater 2016;28:8861–91. [PubMed: 27461855]

[55]. Geiger B, Spatz JP, Bershadsky AD. Environmental sensing through focal adhesions. Nat Rev Mol Cell Biol 2009;10:21–33. [PubMed: 19197329]

[56]. Wang N, Butler JP, Ingber DE. Mechanotransduction across the cell surface and through the cytoskeleton. Science 1993;260:1124–7. [PubMed: 7684161]

[57]. Ooi HW, Hafeez S, van Blitterswijk CA, Moroni L, Baker MB. Hydrogels that listen to cells: a review of cell-responsive strategies in biomaterial design for tissue regeneration. Mater Horiz 2017;4:1020–40.

[58]. Gaharwar AK, Peppas NA, Khademhosseini A. Nanocomposite hydrogels for biomedical applications. Biotechnol Bioeng 2014;111:441–53. [PubMed: 24264728]

[59]. Tan H, Marra KG. Injectable, biodegradable hydrogels for tissue engineering applications. Materials 2010;3:1746–67.

[60]. Durst CA, Cuchiara MP, Mansfield EG, West JL, Grande-Allen KJ. Flexural characterization of cell encapsulated PEGDA hydrogels with applications for tissue engineered heart valves. Acta Biomater 2011;7:2467–76. [PubMed: 21329770]

[61]. Hutson CB, Nichol JW, Aubin H, Bae H, Yamanlar S, Al-Haque S, et al. Synthesis and characterization of tunable poly(ethylene glycol): gelatin methacrylate composite hydrogels. Tissue Eng Part A 2011;17:1713–23. [PubMed: 21306293]

[62]. Lee KY, Mooney DJ. Hydrogels for tissue engineering. Chem Rev 2001;101:1869–79. [PubMed: 11710233]

[63]. Anderson SB, Lin CC, Kuntzler DV, Anseth KS. The performance of human mesenchymal stem cells encapsulated in cell-degradable polymer-peptide hydrogels. Biomaterials 2011;32:3564–74. [PubMed: 21334063]

[64]. Williams CG, Malik AN, Kim TK, Manson PN, Elisseeff JH. Variable cytocompatibility of six cell lines with photoinitiators used for polymerizing hydrogels and cell encapsulation. Biomaterials 2005;26:1211–8. [PubMed: 15475050]

[65]. Jenkins AD, Loening KL. Nomenclature. In: Allen G, Bevington JC, editors. Comprehensive polymer science and supplements, Vol 1. Amsterdam: Pergamon; 1989. p. 13–54.

[66]. Luo Y, Kobler JB, Heaton JT, Jia X, Zeitels SM, Langer R. Injectable hyaluronic acid-dextran hydrogels and effects of implantation in ferret vocal fold. J Biomed Mater Res B 2010;93:386–93.

[67]. Hunt JA, Chen R, van Veen T, Bryan N. Hydrogels for tissue engineering and regenerative medicine. J Mater Chem B 2014;2:5319–38. [PubMed: 32261753]

[68]. Grover GN, Braden RL, Christman KL. Oxime cross-linked injectable hydrogels for catheter delivery. Adv Mater 2013;25:2937–42. [PubMed: 23495015]

[69]. Hennink WE, van Nostrum CF. Novel crosslinking methods to design hydrogels. Adv Drug Deliv Rev 2002;54:13–36. [PubMed: 11755704]

[70]. Malkoch M, Vestberg R, Gupta N, Mespouille L, Dubois P, Mason AF, et al. Synthesis of well-defined hydrogel networks using click chemistry. Chem Commun 2006:2774–6.

[71]. Liu SQ, Ee RPL, Ke CY, Hedrick JL, Yang YY. Biodegradable poly(ethylene glycol)-peptide hydrogels with well-defined structure and properties for cell delivery. Biomaterials 2009;30:1453–61. [PubMed: 19097642]

[72]. Nimmo CM, Shoichet MS. Regenerative biomaterials that click: simple, aqueous-based protocols for hydrogel synthesis, surface immobilization, and 3D patterning. Bioconjugate Chem 2011;22:2199–209.

[73]. van Dijk M, van Nostrum CF, Hennink WE, Rijkers DTS, Liskamp RMJ. Synthesis and characterization of enzymatically biodegradable PEG and peptide-based hydrogels prepared by click chemistry. Biomacromolecules 2010;11:1608–14. [PubMed: 20496905]

[74]. Agard NJ, Prescher JA, Bertozzi CR. A strain-promoted [3+2] azide-alkyne cycloaddition for covalent modification of biomolecules in living systems. J Am Chem Soc 2004;126:15046–7. [PubMed: 15547999]

[75]. Kolb HC, Finn MG, Sharpless KB. Click chemistry: diverse chemical function from a few good reactions. Angew Chem Int Ed 2001;40:2004–21.

[76]. Sanyal A Diels-Alder cycloaddition-cycloreversion: a powerful combo in materials design. Macromol Chem Phys 2010;211:1417–25.

[77]. Blackman ML, Royzen M, Fox JM. Tetrazine ligation: fast bioconjugation based on inverse-electron-demand Diels-Alder reactivity. J Am Chem Soc 2008;130:13518–9. [PubMed: 18798613]

[78]. Lowe AB, Hoyle CE, Bowman CN. Thiol-yne click chemistry: a powerful and versatile methodology for materials synthesis. J Mater Chem 2010;20:4745–50.

[79]. Hu BH, Su J, Messersmith PB. Hydrogels cross-linked by native chemical ligation. Biomacromolecules 2009;10:2194–200. [PubMed: 19601644]

[80]. Gohil SV, Brittain SB, Kan HM, Drissi H, Rowe DW, Nair LS. Evaluation of enzymatically crosslinked injectable glycol chitosan hydrogel. J Mater Chem B 2015;3:5511–22. [PubMed: 32262522]

[81]. Ren K, He C, Cheng Y, Li G, Chen X. Injectable enzymatically crosslinked hydrogels based on a poly(L-glutamic acid) graft copolymer. Polym Chem 2014;5:5069–76.

[82]. Hoffman AS. Hydrogels for biomedical applications. Adv Drug Deliv Rev 2012;64(Suppl):18–23.

[83]. Garbern JC, Minami E, Stayton PS, Murry CE. Delivery of basic fibroblast growth factor with a pH-responsive, injectable hydrogel to improve angiogenesis in infarcted myocardium. Biomaterials 2011;32:2407–16. [PubMed: 21186056]

[84]. Krische MJ, Lehn JM. The utilization of persistent H-bonding motifs in the self-assembly of supramolecular architectures. In: Fuiita M, editor. Molecular self-assembly: organic versus inorganic approaches. Structure & bonding, Vol 96. Berlin: Springer-Verlag; 2000. p. 3–29.

[85]. Voorhaar L, Hoogenboom R. Supramolecular polymer networks: hydrogels and bulk materials. Chem Soc Rev 2016;45:4013–31. [PubMed: 27206244]

[86]. Appel EA, del Barrio J, Loh XJ, Scherman OA. Supramolecular polymeric hydrogels. Chem Soc Rev 2012;41:6195–214. [PubMed: 22890548]

[87]. Lange RFM, Van Gurp M, Meijer EW. Hydrogen-bonded supramolecular polymer networks. J Polym Sci Part A Polym Chem 1999;37:3657–70.

[88]. Su T, Liu Y, He H, Li J, Lv Y, Zhang L, et al. Strong bioinspired polymer hydrogel with tunable stiffness and toughness for mimicking the extracellular matrix. ACS Macro Lett 2016;5:1217–21. [PubMed: 35614748]

[89]. Koenigs MME, Pal A, Mortazavi H, Pawar GM, Storm C, Sijbesma RP. Tuning cross-link density in a physical hydrogel by supramolecular self-sorting. Macromolecules 2014;47:2712–7.

[90]. Ghoussoub A, Lehn JM. Dynamic sol-gel interconversion by reversible cation binding and release in G-quartet-based supramolecular polymers. Chem Commun 2005:5763–5.

[91]. Webber MJ, Appel EA, Meijer EW, Langer R. Supramolecular biomaterials. Nat Mater 2016;15:13–26. [PubMed: 26681596]

[92]. Peng F, Li G, Liu X, Wu S, Tong Z. Redox-responsive gel-sol/sol-gel transition in poly(acrylic acid) aqueous solution containing Fe(III) ions switched by light. J Am Chem Soc 2008;130:16166–7. [PubMed: 18998675]

[93]. Guo M, Jiang M, Pispas S, Yu W, Zhou C. Supramolecular hydrogels made of end-functionalized low-molecular-weight PEG and α-cyclodextrin and their hybridization with SiO_2 nanoparticles through host-guest interaction. Macromolecules 2008;41:9744–9.

[94]. Harries D, Rau DC, Parsegian VA. Solutes probe hydration in specific association of cyclodextrin and adamantane. J Am Chem Soc 2005;127:2184–90. [PubMed: 15713096]

[95]. Bin Imran A, Esaki K, Gotoh H, Seki T, Ito K, Sakai Y, et al. Extremely stretchable thermosensitive hydrogels by introducing slide-ring polyrotaxane cross-linkers and ionic groups into the polymer network. Nat Commun 2014;5, 5124/1–8. [PubMed: 25296246]

[96]. Hernández R, Rusa M, Rusa CC, López D, Mijangos C, Tonelli AE. Controlling PVA hydrogels with γ-cyclodextrin. Macromolecules 2004;37:9620–5.

[97]. Ren L, He L, Sun T, Dong X, Chen Y, Huang J, et al. Dual-responsive supramolecular hydrogels from water-soluble PEG-grafted copolymers and cyclodextrin. Macromol Biosci 2009;9:902–10. [PubMed: 19544291]

[98]. Harada A, Li J, Kamachi M. Double-stranded inclusion complexes of cyclodextrin threaded on poly(ethylene glycol). Nature 1994;370:126–8.

[99]. Rosales AM, Rodell CB, Chen MH, Morrow MG, Anseth KS, Burdick JA. Reversible control of network properties in azobenzene-containing hyaluronic acid-based hydrogels. Bioconjugate Chem 2018;29:905–13.

[100]. Ouyang L, Highley C, Rodell C, Sun W, Burdick JA. 3D Printing of shear-thinning hyaluronic acid hydrogels with secondary cross-linking. ACS Biomater Sci Eng 2016;2:1743–51. [PubMed: 33440472]

[101]. Jung H, Park JS, Yeom J, Selvapalam N, Park KM, Oh K, et al. 3D Tissue engineered supramolecular hydrogels for controlled chondrogenesis of human mesenchymal stem cells. Biomacromolecules 2014;15:707–14. [PubMed: 24605794]

[102]. Cross D, Jiang X, Ji W, Han W, Wang C. Injectable hybrid hydrogels of hyaluronic acid crosslinked by well-defined synthetic polycations: preparation and characterization in vitro and in vivo. Macromol Biosci 2015;15:668–81. [PubMed: 25630277]

[103]. Wang Q, Mynar JL, Yoshida M, Lee E, Lee M, Okuro K, et al. High-water-content moldable hydrogels by mixing clay and a dendritic molecular binder. Nature 2010;463:339–43. [PubMed: 20090750]

[104]. Sun TL, Kurokawa T, Kuroda S, Ihsan AB, Akasaki T, Sato K, et al. Physical hydrogels composed of polyampholytes demonstrate high toughness and viscoelasticity. Nat Mater 2013;12:932–7. [PubMed: 23892784]

[105]. Agarwal T, Kabiraj P, Narayana GH, Kulanthaivel S, Kasiviswanathan U, Pal K, et al. Alginate bead based hexagonal close packed 3D implant for bone tissue engineering. ACS Appl Mater Interfaces 2016;8:32132–45. [PubMed: 27933834]

[106]. Leena RS, Vairamani M, Selvamurugan N. Alginate/gelatin scaffolds incorporated with silibinin-loaded chitosan nanoparticles for bone formation in vitro. Colloids Surf B 2017;158:308–18.

[107]. Salehi M, Naseri-Nosar M, Azami M, Nodooshan SJ, Arish J. Comparative study of poly(L-lactic acid) scaffolds coated with chitosan nanoparticles prepared via ultrasonication and ionic gelation techniques. Tissue Eng Regener Med 2016;13:498–506.

[108]. Compaan AM, Christensen K, Huang Y. Inkjet bioprinting of 3D silk fibroin cellular constructs using sacrificial alginate. ACS Biomater Sci Eng 2017;3:1519–26. [PubMed: 33429638]

[109]. Brus J, Urbanova M, Czernek J, Pavelkova M, Kubova K, Vyslouzil J, et al. Structure and dynamics of alginate gels cross-linked by polyvalent ions probed via solid state NMR spectroscopy. Biomacromolecules 2017;18:2478–88. [PubMed: 28636347]

[110]. Raz M, Moztarzadeh F, Kordestani SS. Synthesis, characterization and in-vitro study of chitosan/gelatin/calcium phosphate hybrid scaffolds fabricated via ion diffusion mechanism for bone tissue engineering. Silicon 2018;10:277–86.

[111]. Yang JA, Yeom J, Hwang BW, Hoffman AS, Hahn SK. In situ-forming injectable hydrogels for regenerative medicine. Prog Polym Sci 2014;39:1973–86.

[112]. Zhao F, Yao D, Guo R, Deng L, Dong A, Zhang J Composites of polymer hydrogels and nanoparticulate systems for biomedical and pharmaceutical applications. Nanomaterials 2015;5:2054–130. [PubMed: 28347111]

[113]. de Jong SJ, De Smedt SC, Wahls MWC, Demeester J, Kettenes-van den Bosch JJ, Hennink WE. Novel self-assembled hydrogels by stereocomplex formation in aqueous solution of enantiomeric lactic acid oligomers grafted to dextran. Macromolecules 2000;33:3680–6.

[114]. Chung HJ, Lee Y, Park TG. Thermo-sensitive and biodegradable hydrogels based on stereocomplexed Pluronic multi-block copolymers for controlled protein delivery. J Control Release 2008;127:22–30. [PubMed: 18234389]

[115]. Hassan CM, Peppas NA. Structure and applications of poly(vinyl alcohol) hydrogels produced by conventional crosslinking or by freezing/thawing methods. In: Biopolymers · PVA hydrogels, anionic polymerisation nanocomposites. Berlin: Springer-Verlag; 2000. p. 37–65.

[116]. Sanabria-DeLong N, Crosby AJ, Tew GN. Photo-cross-linked PLA-PEO-PLA hydrogels from self-assembled physical networks: mechanical properties and influence of assumed constitutive relationships. Biomacromolecules 2008;9:2784–91. [PubMed: 18817440]

[117]. Zhao SP, Zhang LM, Ma D. Supramolecular hydrogels induced rapidly by inclusion complexation of poly(*ε*-caprolactone)-poly(ethylene glycol)-poly(*ε*-caprolactone) block copolymers with α-cyclodextrin in aqueous solutions. J Phys Chem B 2006;110:12225–9. [PubMed: 16800542]

[118]. Lau HK, Kiick KL. Opportunities for multicomponent hybrid hydrogels in biomedical applications. Biomacromolecules 2015;16:28–42. [PubMed: 25426888]

[119]. Luo T, Kiick KL. Collagen-like peptides and peptide-polymer conjugates in the design of assembled materials. Eur Polym J 2013;49:2998–3009. [PubMed: 24039275]

[120]. Xia XX, Xu Q, Hu X, Qin G, Kaplan DL. Tunable self-assembly of genetically engineered silk-elastin-like potein polymers. Biomacromolecules 2011;12:3844–50. [PubMed: 21955178]

[121]. Luo T, Kiick KL. Noncovalent modulation of the inverse temperature transition and self-assembly of elastin-*b*-collagen-like peptide bioconjugates. J Am Chem Soc 2015;137:15362–5. [PubMed: 26633746]

[122]. Grieshaber SE, Farran AJE, Bai S, Kiick KL, Jia X. Tuning the properties of elastin mimetic hybrid copolymers via a modular polymerization method. Biomacromolecules 2012;13:1774–86. [PubMed: 22533503]

[123]. Du X, Zhou J, Shi J, Xu B. Supramolecular hydrogelators and hydrogels: from soft matter to molecular biomaterials. Chem Rev 2015;115:13165–307. [PubMed: 26646318]

[124]. Wang H, Yang Z. Short-peptide-based molecular hydrogels: novel gelation strategies and applications for tissue engineering and drug delivery. Nanoscale 2012;4:5259–67. [PubMed: 22814874]

[125]. Kleinsmann AJ, Weckenmann NM, Nachtsheim BJ. Phosphate-triggered self-assembly of *N*-[(uracil-5-yl)methyl]urea: a minimalistic urea-derived hydrogelator. Chem Eur J 2014;20:9753–61. [PubMed: 25042699]

[126]. Thompson CB, Korley LTJ. Harnessing supramolecular and peptidic self-assembly for the construction of reinforced polymeric tissue scaffolds. Bioconjugate Chem 2017;28:1325–39.

[127]. Tam AYY, Wong KMC, Yam VWW. Unusual luminescence enhancement of metallogels of alkynylplatinum(II) 2,6-bis(*N*-alkylbenzimidazol-2′-yl)pyridine complexes upon a gel-to-sol Phase transition at elevated temperatures J Am Chem Soc 2009;131:6253–60. [PubMed: 19354251]

[128]. Ogawa Y, Yoshiyama C, Kitaoka T. Helical assembly of azobenzene-conjugated carbohydrate hydrogelators with specific affinity for lectins. Langmuir 2012;28:4404–12. [PubMed: 22339091]

[129]. Moreau L, Barthelemy P, El Maataoui M, Grinstaff MW. Supramolecular assemblies of nucleoside phosphocholine amphiphiles. J Am Chem Soc 2004;126:7533–9. [PubMed: 15198600]

[130]. Wu EC, Zhang S, Hauser CAE. Self-assembling peptides as cell-interactive scaffolds. Adv Funct Mater 2012;22:456–68.

[131]. Dou XQ, Feng CL. Amino acids and peptide-based supramolecular hydrogels for three-dimensional cell culture. Adv Mater 2017;29, 1604062/1–21.

[132]. Tang C, Smith AM, Collins RF, Ulijn RV, Saiani A. Fmoc-diphenylalanine self-assembly mechanism induces apparent pKa shifts. Langmuir 2009;25:9447–53. [PubMed: 19537819]

[133]. Zhang Y, Gu H, Yang Z, Xu B. Supramolecular hydrogels respond to ligand-receptor interaction. J Am Chem Soc 2003;125:13680–1. [PubMed: 14599204]

[134]. Cao CH, Cao MW, Fan HM, Xia DH, Xu H, Lu JR. Redox modulated hydrogelation of a self-assembling short peptide amphiphile. Chin Sci Bull 2012;57:4296–303.

[135]. Muraoka T, Koh CY, Cui H, Stupp SI. Light-triggered bioactivity in three dimensions. Angew Chem Int Ed 2009;48:5946–9.

[136]. Yang Z, Gu H, Fu D, Gao P, Lam JK, Xu B. Enzymatic formation of supramolecular hydrogels. Adv Mater 2004;16:1440–4.

[137]. Chen G, Chen J, Liu Q, Ou C, Gao J. Enzymatic formation of a meta-stable supramolecular hydrogel for 3D cell culture. RSC Adv 2015;5:30675–8.

[138]. Chronopoulou L, Togna AR, Guarguaglini G, Masci G, Giammaruco F, Togna GI, et al. Self-assembling peptide hydrogels promote microglial cells proliferation and NGF production. Soft Matter 2012;8:5784–90.

[139]. Gil ES, Hudson SM. Stimuli-responsive polymers and their bioconjugates. Prog Polym Sci 2004;29:1173–222.

[140]. Lu Y, Aimetti AA, Langer R, Gu Z. Bioresponsive materials. Nat Rev Mater 2017;2, 16075/1–17.

[141]. Philippova OE, Hourdet D, Audebert R, Khokhlov AR. pH-Responsive gels of hydrophobically modified poly(acrylic acid). Macromolecules 1997;30:8278–85.

[142]. Torres-Lugo M, Peppas NA. Molecular design and in vitro studies of novel pH-sensitive hydrogels for the oral delivery of calcitonin. Macromolecules 1999;32:6646–51.

[143]. Lee AS, Buetuen V, Vamvakaki M, Armes SP, Pople JA, Gast AP. Structure of pH-dependent block copolymer micelles: charge and ionic strength dependence. Macromolecules 2002;35:8540–51.

[144]. Siegel RA. Hydrophobic weak polyelectrolyte gels: studies of swelling equilibria and kinetics. Adv Polym Sci 1993;109:233–67.

[145]. Halacheva SS, Freemont TJ, Saunders BR. pH-Responsive physical gels from poly(meth)acrylic acid-containing crosslinked particles: the relationship between structure and mechanical properties. J Mater Chem B 2013;1:4065–78. [PubMed: 32260959]

[146]. Yu F, Cao X, Du J, Wang G, Chen X. Multifunctional hydrogel with good structure integrity self-healing, and tissue-adhesive property formed by combining Diels–Alder click reaction and acylhydrazone bond. ACS Appl Mater Interfaces 2015;7:24023–31. [PubMed: 26466997]

[147]. Brown TE, Carberry BJ, Worrell BT, Dudaryeva OY, McBride MK, Bowman CN, et al. Photopolymerize dynamic hydrogel with tunable viscoelastic properties through thioester exchange. Biomaterials 2018;178:496–503. [PubMed: 29653871]

[148]. Deng CC, Brooks WLA, Abboud KA, Sumerlin BS. Boronic acid-bealing at neutral and acidic pH. ACS Macro Lett 2015;4:220–4. [PubMed: 35596411]

[149]. Karimi F, Collins J, Heath DE, Connal LA. Dynamic covalent hydrogels for triggered cell capture and release. Bioconjugate Chem 2017;28:2235–40.

[150]. Zhang S, Bellinger AM, Glettig DL, Barman R, Lee YAL, Zhu J, et al. A pH-responsive supramolecular polymergel as an enteric elastomer for use in gastric devices. Nat Mater 2015;14:1065–71. [PubMed: 26213897]

[151]. Kong N, Peng Q, Li H. Rationally designed dynamic protein hydrogels with reversibly tunable mechanical properties. Adv Funct Mater 2014;24:7310–7.

[152]. Lim HL, Hwang Y, Kar M, Varghese S. Smart hydrogels as functional biomimetic systems. Biomater Sci 2014;2:603–18. [PubMed: 32481841]

[153]. Klouda L, Mikos AG. Thermoresponsive hydrogels in biomedical applications. Eur J Pharm Biopharm 2008;68:34–45. [PubMed: 17881200]

[154]. Prabaharan M, Mano JF. Stimuli-responsive hydrogels based on polysaccharides incorporated with thermo-responsive polymers as novel biomaterials. Macromol Biosci 2006;6:991–1008. [PubMed: 17128423]

[155]. Sun T, Wang G, Feng L, Liu B, Ma Y, Jiang L, et al. Reversible switching between superhydrophilicity and superhydrophobicity. Angew Chem Int Ed 2004;43:357–60.

[156]. Liu XM, Wang LS, Wang L, Huang J, He C. The effect of salt and pH on the phase-transition behaviors of temperature-sensitive copolymers based on *N*-isopropylacrylamide. Biomaterials 2004;25:5659–66. [PubMed: 15159082]

[157]. Dadoo N, Gramlich WM. Spatiotemporal modification of stimuli-responsive hyaluronic acid/poly(*N*-isopropylacrylamide) hydrogels. ACS Biomater Sci Eng 2016;2:1341–50. [PubMed: 33434987]

[158]. Lai PL, Hong DW, Ku KL, Lai ZT, Chu IM. Novel thermosensitive hydrogels based on methoxy polyethylene glycol-*co*-poly(lactic acid-*co*-aromatic anhydride) for cefazolin delivery. Nanomedicine 2014;10:553–60. [PubMed: 24096031]

[159]. Mostafalu P, Kiaee G, Giatsidis G, Khalilpour A, Nabavinia M, Dokmeci MR, et al. A textile dressing for temporal and dosage controlled drug delivery. Adv Funct Mater 2017;27, 1702399/1–10.

[160]. Chenite A, Chaput C, Wang D, Combes C, Buschmann MD, Hoemann CD, et al. Novel injectable neutral solutions of chitosan form biodegradable gels in situ. Biomaterials 2000;21:2155–61. [PubMed: 10985488]

[161]. Joly-Duhamel C, Hellio D, Djabourov M. All gelatin networks: 1. Biodiversity and physical chemistry. Langmuir 2002;18:7208–17.

[162]. Balakrishnan B, Banerjee R. Biopolymer-based hydrogels for cartilage tissue engineering. Chem Rev 2011;111:4453–74. [PubMed: 21417222]

[163]. Tomatsu I, Peng K, Kros A. Photoresponsive hydrogels for biomedical applications. Adv Drug Deliv Rev 2011;63:1257–66. [PubMed: 21745509]

[164]. Habault D, Zhang H, Zhao Y. Light-triggered self-healing and shape-memory polymers. Chem Soc Rev 2013;42:7244–56. [PubMed: 23440057]

[165]. Peng K, Tomatsu I, Kros A. Light controlled protein release from a supramolecular hydrogel. Chem Commun 2010;46:4094–6.

[166]. Chujo Y, Sada K, Saegusa T. Polyoxazoline having a coumarin moiety as a pendant group. Synthesis and photogelation. Macromolecules 1990;23:2693–7.

[167]. Froimowicz P, Frey H, Landfester K. Towards the generation of self-healing materials by means of a reversible photo-induced approach. Macromol Rapid Commun 2011;32:468–73. [PubMed: 21433201]

[168]. Chung CM, Roh YS, Cho SY, Kim JG. Crack healing in polymeric materials via photochemical [2+2] cycloaddition. Chem Mater 2004;16:3982–4.

[169]. Zheng Y, Andreopoulos FM, Micic M, Huo Q, Pham SM, Leblanc RM. A novel photoscissile poly(ethylene glycol)-based hydrogel. Adv Funct Mater 2001;11:37–40.

[170]. Zheng Y, Micic M, Mello SV, Mabrouki M, Andreopoulos FM, Konka V, et al. PEG-based hydrogel synthesis via the photodimerization of anthracene groups. Macromolecules 2002;35:5228–34.

[171]. Maddipatla MVSN, Wehrung D, Tang C, Fan W, Oyewumi MO, Miyoshi T, et al. Photoresponsive coumarin polyesters that exhibit cross-linking and chain scission properties. Macromolecules 2013;46:5133–40.

[172]. Ruskowitz ER, DeForest CA. Photoresponsive biomaterials for targeted drug delivery and 4D cell culture. Nat Rev Mater 2018;3, 17087/1–17.

[173]. DeForest CA, Anseth KS. Advances in bioactive hydrogels to probe and direct cell fate. Annu Rev Chem Biomol Eng 2012;3:421–44. [PubMed: 22524507]

[174]. Wang N, Li Y, Zhang Y, Liao Y, Liu W. High-strength photoresponsive hydrogels enable surface-mediated gene delivery and light-induced reversible cell adhesion/detachment. Langmuir 2014;30:11823–32. [PubMed: 25201559]

[175]. Rosales AM, Mabry KM, Nehls EM, Anseth KS. Photoresponsive eastic properties of azobenzene-containing poly(ethylene glycol)-based hydrogels. Biomacromolecules 2015;16:798–806. [PubMed: 25629423]

[176]. Hilderbrand AM, Ovadia EM, Rehmann MS, Kharkar PM, Guo C, Kloxin AM. Biomaterials for 4D stem cell culture. Curr Opin Solid State Mater Sci 2016;20:212–24. [PubMed: 28717344]

[177]. Griffin DR, Kasko AM. Photodegradable macromers and hydrogels for live cell encapsulation and release. J Am Chem Soc 2012;134:13103–7. [PubMed: 22765384]

[178]. McKinnon DD, Brown TE, Kyburz KA, Kiyotake E, Anseth KS. Design and characterization of a synthetically accessible, photodegradable hydrogel for user-directed formation of neural networks. Biomacromolecules 2014;15:2808–16. [PubMed: 24932668]

[179]. Azagarsamy MA, McKinnon DD, Alge DL, Anseth KS. Coumarin-based photodegradable hydrogel: design, synthesis, gelation, and degradation kinetics. ACS Macro Lett 2014;3:515–9. [PubMed: 35590721]

[180]. Azagarsamy MA, Anseth KS. Wavelength-controlled photocleavage for the orthogonal and sequential release of multiple proteins. Angew Chem Int Ed 2013;52:13803–7.

[181]. DeForest CA, Tirrell DA. A photoreversible protein-patterning approach for guiding stem cell fate in three-dimensional gels. Nat Mater 2015;14:523–31. [PubMed: 25707020]

[182]. Farahani PE, Adelmund SM, Shadish JA, DeForest CA. Photomediated oxime ligation as a bioorthogonal tool for spatiotemporally-controlled hydrogel formation and modification. J Mater Chem B 2017;5:4435–42. [PubMed: 32263971]

[183]. Tam RY, Fisher SA, Baker AEG, Shoichet MS. Transparent porous polysaccharide cryogels provide biochemically defined, biomimetic matrices for tunable 3D cell culture. Chem Mater 2016;28:3762–70.

[184]. Goubko CA, Basak A, Majumdar S, Cao X. Dynamic cell patterning of photoresponsive hyaluronic acid hydrogels. J Biomed Mater Res A 2014;102:381–91. [PubMed: 23520029]

[185]. Grim JC, Brown TE, Aguado BA, Chapnick DA, Viert AL, Liu X, et al. A reversible and repeatable thiol–ene bioconjugation for dynamic patterning of signaling proteins in hydrogels. ACS Central Sci 2018;4:909–16.

[186]. Gandavarapu NR, Azagarsamy MA, Anseth KS. Photo-click living strategy for controlled, reversible exchange of biochemical ligands. Adv Mater 2014;26:2521–6. [PubMed: 24523204]

[187]. Murdan S Electro-responsive drug delivery from hydrogels. J Control Release 2003;92:1–17. [PubMed: 14499181]

[188]. Shang J, Shao Z, Chen X. Electrical behavior of a natural polyelectrolyte hydrogel: chitosan/carboxymethylcellulose hydrogel. Biomacromolecules 2008;9:1208–13. [PubMed: 18311921]

[189]. Lim HL, Chuang JC, Tran T, Aung A, Arya G, Varghese S. Dynamic electromechanical hydrogel matrices for stem cell culture. Adv Funct Mater 2011;21:55–63.

[190]. Rahimi N, Molin DG, Cleij TJ, van Zandvoort MA, Post MJ. Electrosensitive polyacrylic acid/fibrin hydrogel facilitates cell seeding and alignment. Biomacromolecules 2012;13:1448–57. [PubMed: 22515272]

[191]. Kim SJ, Shin SR, Lee JH, Lee SH, Kim SI. Electrical response characterization of chitosan/polyacrylonitrile hydrogel in NaCl solutions. J Appl Polym Sci 2003;90:91–6.

[192]. Kim SJ, Yoon SG, Lee YM, Kim HC, Kim SI. Electrical behavior of polymer hydrogel composed of poly(vinyl alcohol)-hyaluronic acid in solution. Biosens Bioelectron 2004;19:531–6. [PubMed: 14683636]

[193]. Lin X, Tang D, Cui W, Cheng Y. Controllable drug release of electrospun thermoresponsive poly(*N*-isopropylacrylamide)/poly(2-acrylamido-2-methylpropanesulfonic acid) nanofibers. J Biomed Mater Res A 2012;100:1839–45. [PubMed: 22488676]

[194]. Peng L, Liu Y, Huang J, Li J, Gong J, Ma J. Microfluidic fabrication of highly stretchable and fast electro-responsive graphene oxide/polyacrylamide/alginate hydrogel fibers. Eur Polym J 2018;103:335–41.

[195]. Wang S, Guan S, Li W, Ge D, Xu J, Sun C, et al. .3D culture of neural stem cells within conductive PEDOT layer-assembled chitosan/gelatin scaffolds for neural tissue engineering. Mater Sci Eng C 2018;93:890–901.

[196]. Thomas CA, Zong K, Schottland P, Reynolds JR. Poly(3,4-alkylenedioxypyrrole)s as highly stable aqueous-compatible conducting polymers with biomedical implications. Adv Mater 2000;12:222–5.

[197]. Ghasemi-Mobarakeh L, Prabhakaran MP, Morshed M, Nasr-Esfahani MH, Ramakrishna S. Electrical stimulation of nerve cells using conductive nanofibrous scaffolds for nerve tissue engineering. Tissue Eng Part A 2009;15:3605–19. [PubMed: 19496678]

[198]. Peng L, Zhang H, Feng A, Huo M, Wang Z, Hu J, et al. Electrochemical redox responsive supramolecular self-healing hydrogels based on host-guest interaction. Polym Chem 2015;6:3652–9.

[199]. Yeo WS, Yousaf MN, Mrksich M. Dynamic interfaces between cells and surfaces: electroactive substrates that sequentially release and attach cells. J Am Chem Soc 2003;125:14994–5. [PubMed: 14653727]

[200]. Xue B, Qin M, Wang T, Wu J, Luo D, Jiang Q, et al. Electrically controllable actuators based on supramolecular peptide hydrogels. Adv Funct Mater 2016;26:9053–62.

[201]. Takahashi SH, Lira LM, Cordoba de Torresi SI. Zero-order release profiles from a multistimuli responsive electro-conductive hydrogel. J Biomater Nanobiotechnol 2012;3:262–8.

[202]. Jensen M, Birch Hansen P, Murdan S, Frokjaer S, Florence AT. Loading into and electro-stimulated release of peptides and proteins from chondroitin 4-sulphate hydrogels. Eur J Pharm Sci 2002;15:139–48. [PubMed: 11849910]

[203]. Cho Y, Ben Borgens R. Electrically controlled release of the nerve growth factor from a collagen-carbon nanotube composite for supporting neuronal growth. J Mater Chem B 2013;1:4166–70. [PubMed: 32260970]

[204]. Nam S, Hu KH, Butte MJ, Chaudhuri O. Strain-enhanced stress relaxation impacts nonlinear elasticity in collagen gels. Natl Acad Sci U S A 2016;113:5492–7.

[205]. Sagara Y, Kato T. Mechanically induced luminescence changes in molecular assemblies. Nat Chem 2009;1:605–10. [PubMed: 21378953]

[206]. Yang QZ, Huang Z, Kucharski TJ, Khvostichenko D, Chen J, Boulatov R. A molecular force probe. Nat Nanotechnol 2009;4:302–6. [PubMed: 19421215]

[207]. Eslahi N, Abdorahim M, Simchi A. Smart polymeric hydrogels for cartilage tissue engineering: a review on the chemistry and biological functions. Biomacromolecules 2016;17:3441–63. [PubMed: 27775329]

[208]. Das RK, Gocheva V, Hammink R, Zouani OF, Rowan AE. Stress-stiffening-mediated stem-cell commitment switch in soft responsive hydrogels. Nat Mater 2016;15:318–25. [PubMed: 26618883]

[209]. Chaudhuri O, Gu L, Klumpers D, Darnell M, Bencherif SA, Weaver JC, et al. Hydrogels with tunable stress relaxation regulate stem cell fate and activity. Nat Mater 2016;15:326–34. [PubMed: 26618884]

[210]. Highley CB, Rodell CB, Burdick JA. Direct 3D printing of shear-thinning hydrogels into self-healing hydrogels. Adv Mater 2015;27:5075–9. [PubMed: 26177925]

[211]. Kloxin CJ, Scott TF, Adzima BJ, Bowman CN. Covalent adaptable networks (CANs): a unique paradigm in cross-linked polymers. Macromolecules 2010;43:2643–53. [PubMed: 20305795]

[212]. Tong X, Yang F. Sliding hydrogels with mobile molecular ligands and crosslinks as 3D stem cell niche. Adv Mater 2016;28:7257–63. [PubMed: 27305637]

[213]. Kouwer PHJ, Koepf M, Le Sage VAA, Jaspers M, van Buul AM, Eksteen-Akeroyd ZH, et al. Responsive biomimetic networks from polyisocyanopeptide hydrogels. Nature 2013;493:651–5. [PubMed: 23354048]

[214]. Fang L, Hmadeh M, Wu J, Olson MA, Spruell JM, Trabolsi A, et al. . Acid-base actuation of [c2]daisy chains. J Am Chem Soc 2009;131:7126–34. [PubMed: 19419175]

[215]. Wojtecki RJ, Meador MA, Rowan SJ. Using the dynamic bond to access macroscopically responsive structurally dynamic polymers. Nat Mater 2011;10:14–27. [PubMed: 21157495]

[216]. Tskhovrebova L, Trinick J. Titin: properties and family relationships. Nat Rev Mol Cell Biol 2003;4:679–89. [PubMed: 14506471]

[217]. Smith BL, Schaffer TE, Viani M, Thompson JB, Frederick NA, Kind J, et al. Molecular mechanistic origin of the toughness of natural adhesives, fibers and composites. Nature 1999;399:761–3.

[218]. Kushner AM, Vossler JD, Williams GA, Guan Z. A biomimetic modular polymer with tough and adaptive properties. J Am Chem Soc 2009;131:8766–8. [PubMed: 19505144]

[219]. Kushner AM, Gabuchian V, Johnson EG, Guan Z. Biomimetic design of reversibly unfolding cross-linker to enhance mechanical properties of 3D network polymers. J Am Chem Soc 2007;129:14110–1. [PubMed: 17973379]

[220]. Gräfe D, Frank P, Erdmann T, Richter A, Appelhans D, Voit B. Tetra-sensitive graft copolymer gels as active material of chemomechanical valves. ACS Appl Mater Interfaces 2017;9:7565–76. [PubMed: 28249364]

[221]. Tran YH, Rasmuson MJ, Emrick T, Klier J, Peyton SR. Strain-stiffening gels based on latent crosslinking. Soft Matter 2017;13:9007–14. [PubMed: 29164222]

[222]. Lowe C, Weder C. Oligo(*p*-phenylene vinylene) excimers as molecular probes: deformation-induced colo changes in photoluminescent polymer blends. Adv Mater 2002;14:1625–9.

[223]. Prokoph S, Chavakis E, Levental KR, Zieris A, Freudenberg U, Dimmeler S, et al. Sustained delivery of SDF-1α from heparin-based hydrogels to attract circulating pro-angiogenic cells. Biomaterials 2012;33:4792–800. [PubMed: 22483246]

[224]. Seidi F, Jenjob R, Crespy D. Designing smart polymer conjugates for controlled release of payloads. Chem Rev 2018;118:3965–4036. [PubMed: 29533067]

[225]. Morey M, Pandit A. Responsive triggering systems for delivery in chronic wound healing. Adv Drug Deliv Rev 2018;129:169–93. [PubMed: 29501700]

[226]. Lavrador P, Gaspar VM, Mano JF. Stimuli-responsive nanocarriers for delivery of bone therapeutics - barriers and progresses. J Control Release 2018;273:51–67. [PubMed: 29407678]

[227]. Zheng W, Zhang W, Jiang X. Precise control of cell adhesion by combination of surface chemistry and soft lithography. Adv Healthc Mater 2013;2:95–108. [PubMed: 23184447]

[228]. Chen N, Zhang Z, Soontornworajit B, Zhou J, Wang Y. Cell adhesion on an artificial extracellular matrix using aptamer-functionalized PEG hydrogels. Biomaterials 2012;33:1353–62. [PubMed: 22079002]

[229]. Zhang Z, Chen N, Li S, Battig MR, Wang Y. Programmable hydrogels for controlled cell catch and release using hybridized aptamers and complementary sequences. J Am Chem Soc 2012;134:15716–9. [PubMed: 22970862]

[230]. Liu H, Li Y, Sun K, Fan J, Zhang P, Meng J, et al. Dual-responsive surfaces modified with phenylboronic acid-containing polymer brush to reversibly capture and release cancer cells. J Am Chem Soc 2013;135:7603–9. [PubMed: 23601154]

[231]. Desseaux S, Klok HA. Temperature-controlled masking/unmasking of cell-adhesive cues with poly(ethylene glycol) methacrylate based brushes. Biomacromolecules 2014;15:3859–65. [PubMed: 25208302]

[232]. Wischerhoff E, Uhlig K, Lankenau A, Börner HG, Laschewsky A, Duschl C, et al. Controlled cell adhesion on PEG-based switchable surfaces. Angew Chem Int Ed 2008;47:5666–8.

[233]. Liu H, Liu X, Meng J, Zhang P, Yang G, Su B, et al. Hydrophobic interaction-mediated capture and release of cancer cells on thermoresponsive nanostructured surfaces. Adv Mater 2013;25:922–7. [PubMed: 23161781]

[234]. Nakanishi J, Kikuchi Y, Takarada T, Nakayama H, Yamaguchi K, Maeda M. Photoactivation of a substrate for cell adhesion under standard fluorescence microscopes. J Am Chem Soc 2004;126:16314–5. [PubMed: 15600320]

[235]. Liu D, Xie Y, Shao H, Jiang X. Using azobenzene-embedded self-assembled monolayers to photochemically control cell adhesion reversibly. Angew Chem Int Ed 2009;48:4406–8.

[236]. Gong YH, Li C, Yang J, Wang HY, Zhuo RX, Zhang XZ. Photoresponsive “smart template” via host–guest interaction for reversible cell adhesion. Macromolecules 2011;44:7499–502.

[237]. Edahiro JI, Sumaru K, Tada Y, Ohi K, Takagi T, Kameda M, et al. In situ control of cell adhesion using photoresponsive culture surface. Biomacromolecules 2005;6:970–4. [PubMed: 15762667]

[238]. Ming Z, Hua X, Xue Y, Lin Q, Bao C, Zhu L. Visible light controls cell adhesion on a photoswitchable biointerface. Colloids Surf B 2018;169:41–8.

[239]. Uto K, Tsui JH, DeForest CA, Kim DH. Dynamically tunable cell culture platforms for tissue engineering and mechanobiology. Prog Polym Sci 2017;65:53–82. [PubMed: 28522885]

[240]. Yousaf MN, Houseman BT, Mrksich M. Using electroactive substrates to pattern the attachment of two different cell populations. Natl Acad Sci U S A 2001;98:5992–6.

[241]. An Q, Brinkmann J, Huskens J, Krabbenborg S, de Boer J, Jonkheijm P. A supramolecular system for the electrochemically controlled release of cells. Angew Chem Int Ed 2012;51:12233–7.

[242]. Lahann J, Mitragotri S, Tran TN, Kaido H, Sundaram J, Choi IS, et al. A reversibly switching surface. Science 2003;299:371–4. [PubMed: 12532011]

[243]. Ng CCA, Magenau A, Ngalim SH, Ciampi S, Chockalingham M, Harper JB, et al. Using an electrical potential to reversibly switch surfaces between two states for dynamically controlling cell adhesion. Angew Chem Int Ed 2012;51:7706–10.

[244]. Lashkor M, Rawson FJ, Stephenson-Brown A, Preece JA, Mendes PM. Electrically-driven modulation of surface-grafted RGD peptides for manipulation of cell adhesion. Chem Commun 2014;50:15589–92.

[245]. Yeung CL, Iqbal P, Allan M, Lashkor M, Preece JA, Mendes PM. Tuning specific biomolecular interactions using electro-switchable oligopeptide surfaces. Adv Funct Mater 2010;20:2657–63.

[246]. Battig MR, Soontornworajit B, Wang Y. Programmable release of multiple protein drugs from aptamer-functionalized hydrogels via nucleic acid hybridization. J Am Chem Soc 2012;134:12410–3. [PubMed: 22816442]

[247]. Lamb BM, Yousaf MN. Redox-switchable surface for controlling peptide structure. J Am Chem Soc 2011;133:8870–3. [PubMed: 21595476]

[248]. Faxälv L, Bolin MH, Jager EWH, Lindahl TL, Berggren M. Electronic control of platelet adhesion using conducting polymer microarrays. Lab Chip 2014;14:3043–9. [PubMed: 24960122]

[249]. DeForest CA, Sims EA, Anseth KS. Peptide-functionalized click hydrogels with independently tunable mechanics and chemical functionality for 3D cell culture. Chem Mater 2010;22:4783–90. [PubMed: 20842213]

[250]. DeForest CA, Anseth KS. Cytocompatible click-based hydrogels with dynamically tunable properties through orthogonal photoconjugation and photocleavage reactions. Nat Chem 2011;3:925–31. [PubMed: 22109271]

[251]. Grim JC, Marozas IA, Anseth KS. Thiol-ene and photo-cleavage chemistry for controlled presentation of biomolecules in hydrogels. J Control Release 2015;219:95–106. [PubMed: 26315818]

[252]. Kloxin AM, Tibbitt MW, Anseth KS. Synthesis of photodegradable hydrogels as dynamically tunable cell culture platforms. Nat Protoc 2010;5:1867–87. [PubMed: 21127482]

[253]. Wylie RG, Ahsan S, Aizawa Y, Maxwell KL, Morshead CM, Shoichet MS. Spatially controlled simultaneous patterning of multiple growth factors in three-dimensional hydrogels. Nat Mater 2011;10:799–806. [PubMed: 21874004]

[254]. Mosiewicz KA, Kolb L, van der Vlies AJ, Martino MM, Lienemann PS, Hubbell JA, et al. In situ cell manipulation through enzymatic hydrogel photopatterning. Nat Mater 2013;12:1072–8. [PubMed: 24121990]

[255]. Ji W, Sun Y, Yang F, van den Beucken JJJP, Fan M, Chen Z, et al. Bioactive electrospun scaffolds delivering growth factors and genes for tissue engineering applications. Pharm Res 2011;28:1259–72. [PubMed: 21088985]

[256]. Lutolf MP. Spotlight on hydrogels. Nat Mater 2009;8:451–3. [PubMed: 19458644]

[257]. Burdick JA, Murphy WL. Moving from static to dynamic complexity in hydrogel design. Nat Commun 2012;3, 1269/1–8. [PubMed: 23232399]

[258]. Lutolf MP. Cell environments programmed with light. Nature 2012;482:477–8. [PubMed: 22358833]

[259]. Kloxin CJ, Scott TF, Park HY, Bowman CN. Mechanophotopatterning on a photoresponsive elastomer. Adv Mater 2011;23:1977–81. [PubMed: 21360784]

[260]. Kloxin CJ, Scott TF, Bowman CN. Stress relaxation via addition–fragmentation chain transfer in a thiol-ene photopolymerization. Macromolecules 2009;42:2551–6. [PubMed: 20160931]

[261]. Fairbanks BD, Schwartz MP, Halevi AE, Nuttelman CR, Bowman CN, Anseth KS. A versatile synthetic extracellular matrix mimic via thiol-norbornene photopolymerization. Adv Mater 2009;21:5005–10. [PubMed: 25377720]

[262]. McKinnon DD, Kloxin AM, Anseth KS. Synthetic hydrogel platform for three-dimensional culture of embryonic stem cell-derived motor neurons. Biomater Sci 2013;1:460–9. [PubMed: 32482009]

[263]. Skaalure SC, Chu S, Bryant SJ. An enzyme-sensitive PEG hydrogel based on aggrecan catabolism for cartilage tissue engineering. Adv Healthc Mater 2015;4:420–31. [PubMed: 25296398]

[264]. Sokic S, Papavasiliou G. FGF-1 and proteolytically mediated cleavage site presentation influence three-dimensional fibroblast invasion in biomimetic PEGDA hydrogels. Acta Biomater 2012;8:2213–22. [PubMed: 22426138]

[265]. Barati D, Kader S, Pajoum Shariati SR, Moeinzadeh S, Sawyer RH, Jabbari E. Synthesis and characterization of photo-cross-linkable keratin hydrogels for stem cell encapsulation. Biomacromolecules 2017;18:398–412. [PubMed: 28000441]

[266]. Patterson J, Hubbell JA. SPARC-derived protease substrates to enhance the plasmin sensitivity of molecularly engineered PEG hydrogels. Biomaterials 2011;32:1301–10. [PubMed: 21040970]

[267]. Leijten J, Seo J, Yue K, Trujillo-de Santiago G, Tamayol A, Ruiz-Esparza GU, et al. Spatially and temporally controlled hydrogels for tissue engineering. Mater Sci Eng R Rep 2017;119:1–35. [PubMed: 29200661]

[268]. LeValley PJ, Kloxin AM. Chemical approaches to dynamically modulate the properties of synthetic matrices. ACS Macro Lett 2019;8:7–16. [PubMed: 32405440]

[269]. Kloxin AM, Kasko AM, Salinas CN, Anseth KS. Photodegradable hydrogels for dynamic tuning of physical and chemical properties. Science 2009;324:59–63. [PubMed: 19342581]

[270]. Forman J, Dietrich M, Todd Monroe W. Photobiological and thermal effects of photoactivating UVA light doses on cell cultures. Photochem Photobiol Sci 2007;6:649–58. [PubMed: 17549267]

[271]. Babin J, Pelletier M, Lepage M, Allard JF, Morris D, Zhao Y. A new two-photon-sensitive block copolymer nanocarrier. Angew Chem Int Ed 2009;48:3329–32.

[272]. Givens RS, Rubina M, Wirz J. Applications of *p*-hydroxyphenacyl (pHP) and coumarin-4-ylmethyl photoremovable protecting groups. Photochem Photobiol Sci 2012;11:472–88. [PubMed: 22344608]

[273]. Chaudhuri O, Gu L, Darnell M, Klumpers D, Bencherif SA, Weaver JC, et al. Substrate stress relaxation regulates cell spreading. Nat Commun 2015;6, 6365/1–7.

[274]. McKinnon DD, Domaille DW, Cha JN, Anseth KS. Biophysically defined and cytocompatible covalently adaptable networks as viscoelastic 3D cell culture systems Adv Mater 2014;26:865–72. [PubMed: 24127293]

[275]. Liu HY, Greene T, Lin TY, Dawes CS, Korc M, Lin CC. Enzyme-mediated stiffening hydrogels for probing activation of pancreatic stellate cells. Acta Biomater 2017;48:258–69. [PubMed: 27769941]

[276]. Jaspers M, Dennison M, Mabesoone MFJ, MacKintosh FC, Rowan AE, Kouwer PHJ. Ultra-responsive soft matter from strain-stiffening hydrogels. Nat Commun 2014;5, 5808/1–8. [PubMed: 25510333]

[277]. Matsuda T, Kawakami R, Namb R, Nakajima T, Gong JP. Mechanoresponsive self-growing hydrogels inspired by muscle training. Science 2019;363:504–8. [PubMed: 30705187]

[278]. Yoshikawa HY, Rossetti FF, Kaufmann S, Kaindl T, Madsen J, Engel U, et al. Quantitative evaluation of mechanosensing of cells on dynamically tunable hydrogels. J Am Chem Soc 2011;133:1367–74. [PubMed: 21218794]

[279]. Yesilyurt V, Webber MJ, Appel EA, Godwin C, Langer R, Anderson DG. Injectable self-healing glucose-responsive hydrogels with pH-regulated mechanical properties. Adv Mater 2016;28:86–91. [PubMed: 26540021]

[280]. Deshpande SR, Hammink R, Nelissen FHT, Rowan AE, Heus HA. Biomimetic stress sensitive hydrogel controlled by DNA nanoswitches. Biomacromolecules 2017;18:3310–7. [PubMed: 28930451]

[281]. Zhou X, Li C, Shao Y, Chen C, Yang Z, Liu D. Reversibly tuning the mechanical properties of a DNA hydrogel by a DNA nanomotor. Chem Commun 2016;52:10668–71.

[282]. Gillette BM, Jensen JA, Wang M, Tchao J, Sia SK. Dynamic hydrogels: switching of 3D microenvironments using two-component naturally derived extracellular matrices. Adv Mater 2010;22:686–91. [PubMed: 20217770]

[283]. Hackelbusch S, Rossow T, Steinhilber D, Weitz DA, Seiffert S. Hybrid microgels with thermo-tunable elasticity for controllable cell confinement. Adv Healthc Mater 2015;4:1841–8. [PubMed: 26088728]

[284]. Rombouts WH, de Kort DW, Pham TTH, van Mierlo CPM, Werten MWT, de Wolf FA, et al. Reversible temperature-switching of hydrogel stiffness of coassembled, silk-collagen-like hydrogels. Biomacromolecules 2015;16:2506–13. [PubMed: 26175077]

[285]. Abdeen AA, Lee J, Bharadwaj NA, Ewoldt RH, Kilian KA. Temporal modulation of stem cell activity using magnetoactive hydrogels. Adv Healthc Mater 2016;5:2536–44. [PubMed: 27276521]

[286]. Ahadian S, Yamada S, Ramon-Azcon J, Estili M, Liang X, Nakajima K, et al. Hybrid hydrogel-aligned carbon nanotube scaffolds to enhance cardiac differentiation of embryoid bodies. Acta Biomater 2016;31:134–43. [PubMed: 26621696]

[287]. Drury JL, Mooney DJ. Hydrogels for tissue engineering: scaffold design variables and applications. Biomaterials 2003;24:4337–51. [PubMed: 12922147]

[288]. Vander AJ, James HS, Luciano DS. Human physiology: the mechanisms of body function. 2nd ed. New York: McGraw-Hill; 1975. p. 614.

[289]. Bell CL, Peppas NA. Water, solute and protein diffusion in physiologically responsive hydrogels of poly(methacrylic acid-*g*-ethylene glycol). Biomaterials 1996;17:1203–18. [PubMed: 8799505]

[290]. Amsden B Solute diffusion within hydrogels. Mechanisms and models. Macromolecules 1998;31:8382–95.

[291]. Cruise GM, Scharp DS, Hubbell JA. Characterization of permeability and network structure of interfacially photopolymerized poly(ethylene glycol) diacrylate hydrogels. Biomaterials 1998;19:1287–94. [PubMed: 9720892]

[292]. Lu S, Anseth KS. Release behavior of high molecular weight solutes from poly(ethylene glycol)-based degradable networks. Macromolecules 2000;33:2509–15.

[293]. Li RH, Altreuter DH, Gentile FT. Transport characterization of hydrogel matrices for cell encapsulation. Biotechnol Bioeng 1996;50:365–73. [PubMed: 18626985]

[294]. Deiber JA, Ottone ML, Piaggio MV, Peirotti MB. Characterization of cross-linked polyampholytic gelatin hydrogels through the rubber elasticity and thermodynamic swelling theories. Polymer 2009;50:6065–75.

[295]. Han LH, Lai JH, Yu S, Yang F. Dynamic tissue engineering scaffolds with stimuli-responsive macroporosity formation. Biomaterials 2013;34:4251–8. [PubMed: 23489920]

[296]. Kankala RK, Xu XM, Liu CG, Chen AZ, Wang SB. 3D-printing of microfibrous porous scaffolds based on hybrid approaches for bone tissue engineering. Polymers 2018;10, 807/1–17. [PubMed: 30960731]

[297]. Wray LS, Tsioris K, Gil ES, Omenetto FG, Kaplan DL. Microfabricated porous silk scaffolds for vascularizing engineered tissues. Adv Funct Mater 2013;23:3404–12. [PubMed: 24058328]

[298]. Xiao L, Liu S, Yao D, Ding Z, Fan Z, Lu Q, et al. Fabrication of silk scaffolds with nanomicroscaled structures and tunable stiffness. Biomacromolecules 2017;18:2073–9. [PubMed: 28574695]

[299]. Zhang W, Zhu C, Ye D, Xu L, Zhang X, Wu Q, et al. Porous silk scaffolds for delivery of growth factors and stem cells to enhance bone regeneration. PLoS One 2014;9, e102371/1–9. [PubMed: 25050556]

[300]. Abbott RD, Kimmerling EP, Cairns DM, Kaplan DL. Silk as a biomaterial to support long-term three-dimensional tissue cultures. ACS Appl Mater Interfaces 2016;8:21861–8. [PubMed: 26849288]

[301]. Lu G, Liu S, Lin S, Kaplan DL, Lu Q. Silk porous scaffolds with nanofibrous microstructures and tunable properties. Colloids Surf B 2014;120:28–37.

[302]. Manavitehrani I, Le TYL, Daly S, Wang Y, Maitz PK, Schindeler A, et al. Formation of porous biodegradable scaffolds based on poly(propylene carbonate) using gas foaming technology. Mater Sci Eng C 2019;96:824–30.

[303]. Rasoulianboroujeni M, Kiaie N, Tabatabaei FS, Yadegari A, Fahimipour F, Khoshroo K, et al. Dual porosity protein-based scaffolds with enhanced cell infiltration and proliferation. Sci Rep 2018;8, 14889/1–10. [PubMed: 30291271]

[304]. Hammer J, Han LH, Tong X, Yang F. A facile method to fabricate hydrogels with microchannel-like porosity for tissue engineering. Tissue Eng Part C 2013;20:169–76.

[305]. Zakharchenko S, Puretskiy N, Stoychev G, Waurisch C, Hickey SG, Eychmüller A, et al. Stimuli-responsive hierarchically self-assembled 3D porous polymer-based structures with aligned pores. J Mater Chem B 2013;1:1786–93. [PubMed: 32261143]

[306]. Zhang B, Filion TM, Kutikov AB, Song J. Facile stem cell delivery to bone grafts enabled by smart shape recovery and stiffening of degradable synthetic periosteal membranes. Adv Funct Mater 2017;27, 1604784/1–8.

[307]. Gong T, Zhao K, Liu X, Lu L, Liu D, Zhou S. A dynamically tunable, bioinspired micropatterned surface regulates vascular endothelial and smooth muscle cells growth at vascularization. Small 2016;12:5769–78. [PubMed: 27595865]

[308]. Zhao Q, Wang J, Cui H, Chen H, Wang Y, Du X. Programmed shape-morphing scaffolds enabling facile 3D endothelialization. Adv Funct Mater 2018;28, 1801027/1–11.

[309]. Kirschner CM, Anseth KS. In situ control of cell substrate microtopographies using photolabile hydrogels. Small 2013;9:578–84. [PubMed: 23074095]

[310]. Le DM, Kulangara K, Adler AF, Leong KW, Ashby VS. Dynamic topographical control of mesenchymal stem cells by culture on responsive poly(ε-caprolactone) surfaces. Adv Mater 2011;23:3278–83. [PubMed: 21626577]

[311]. Tibbitt MW, Rodell CB, Burdick JA, Anseth KS. Progress in material design for biomedical applications. Natl Acad Sci U S A 2015;112:14444–51.

[312]. Fan H, Lu Y, Stump A, Reed ST, Baer T, Schunk R, et al. Rapid prototyping of patterned functional nanostructures. Nature 2000;405:56–60. [PubMed: 10811215]

[313]. Khan F, Tanaka M, Ahmad SR. Fabrication of polymeric biomaterials: a strategy for tissue engineering and medical devices. J Mater Chem B 2015;3:8224–49. [PubMed: 32262880]

[314]. Bhatia SN, Yarmush ML, Toner M. Controlling cell interactions by micropatterning in co-cultures: hepatocytes and 3T3 fibroblasts. J Biomed Mater Res 1997;34:189–99. [PubMed: 9029299]

[315]. Healy KE, Thomas CH, Rezania A, Kim JE, McKeown PJ, Lom B, et al. Kinetics of bone cell organization and mineralization on materials with patterned surface chemistry. Biomaterials 1996;17:195–208. [PubMed: 8624396]

[316]. Park TH, Shuler ML. Integration of cell culture and microfabrication technology. Biotechnol Prog 2003;19:243–53. [PubMed: 12675556]

[317]. Wirkner M, Alonso JM, Maus V, Salierno M, Lee TT, García AJ, et al. Triggered cell release from materials using bioadhesive photocleavable linkers. Adv Mater 2011;23:3907–10. [PubMed: 21618293]

[318]. Khetan S, Burdick JA. Patterning network structure to spatially control cellular remodeling and stem cell fate within 3-dimensional hydrogels. Biomaterials 2010;31:8228–34. [PubMed: 20674004]

[319]. Weis S, Lee TT, del Campo A, García AJ. Dynamic cell-adhesive microenvironments and their effect on myogenic differentiation. Acta Biomater 2013;9:8059–66. [PubMed: 23791677]

[320]. Tsan KMC, Annabi N, Ercole F, Zhou K, Karst DJ, Li F, et al. Facile one-step micropatterning using photodegradable gelatin hydrogels for improved cardiomyocyte organization and alignment. Adv Funct Mater 2015;25:977–86. [PubMed: 26327819]

[321]. Zorlutuna P, Annabi N, Camci-Unal G, Nikkhah M, Cha JM, Nichol JW, et al. Microfabricated biomaterials for engineering 3D tissues. Adv Mater 2012;24:1782–804. [PubMed: 22410857]

[322]. Vasiev I, Greer AIM, Khokhar AZ, Stormonth-Darling J, Tanner KE, Gadegaard N. Self-folding nano- and micropatterned hydrogel tissue engineering scaffolds by single step photolithographic process. Microelectron Eng 2013;108:76–81.

[323]. Pedron S, van Lierop S, Horstman P, Penterman R, Broer DJ, Peeters E. Stimuli responsive delivery vehicles for cardiac microtissue transplantation. Adv Funct Mater 2011;21:1624–30.

[324]. Jamal M, Kadam SS, Xiao R, Jivan F, Onn TM, Fernandes R, et al. Bio-origami hydrogel scaffolds composed of photocrosslinked PEG bilayers. Adv Healthc Mater 2013;2:1142–50. [PubMed: 23386382]

[325]. Stroganov V, Pant J, Stoychev G, Janke A, Jehnichen D, Fery A, et al. 4D biofabrication: 3D cell patterning using shape-changing films. Adv Funct Mater 2018;28, 1706248/1–8.

[326]. Jackman RJ, Wilbur JL, Whitesides GM. Fabrication of submicron features on curved substrates by microcontact printing. Science 1995;269:664–6. [PubMed: 7624795]

[327]. Weibel DB, DiLuzio WR, Whitesides GM. Microfabrication meets microbiology. Nat Rev Microbiol 2007;5:209–18. [PubMed: 17304250]

[328]. Williams C, Tsuda Y, Isenberg BC, Yamato M, Shimizu T, Okano T, et al. Aligned cell sheets grown on thermo-responsive substrates with microcontact printed protein patterns. Adv Mater 2009;21:2161–4.

[329]. Wang Z, Xia J, Yan Y, Tsai AC, Li Y, Ma T, et al. Facile functionalization and assembly of live cells with microcontact-printed polymeric biomaterials. Acta Biomater 2015;11:80–7. [PubMed: 25305514]

[330]. Tanaka N, Ota H, Fukumori K, Miyake J, Yamato M, Okano T. Micro-patterned cell-sheets fabricated with stamping-force-controlled micro-contact printing. Biomaterials 2014;35:9802–10. [PubMed: 25239040]

[331]. Shah NJ, Macdonal ML, Beben YM, Pader RF, Samuel RE, Hammond PT. Tunable dual growth factor delivery from polyelectrolyte multilayer films. Biomaterials 2011;32:6183–93. [PubMed: 21645919]

[332]. Lee YB, Kim SJ, Kim EM, Byun H, Chang Hk, Park J, et al. Microcontact printing of polydopamine on thermally expandable hydrogels for controlled cell adhesion and delivery of geometrically defined microtissues. Acta Biomater 2017;61:75–87. [PubMed: 28760620]

[333]. Na K, Jung J, Kim O, Lee J, Lee TG, Park YH, et al. “Smart” biopolymer for a reversible stimuli-responsive platform in cell-based biochips. Langmuir 2008;24:4917–23. [PubMed: 18348578]

[334]. Zhang H, Hanson Shepherd JN, Nuzzo RG. Microfluidic contact printing: a versatile printing platform for patterning biomolecules on hydrogel substrates. Soft Matter 2010;6:2238–45.

[335]. Chan EWL, Park S, Yousaf MN. An electroactive catalytic dynamic substrate that immobilizes and releases patterned ligands, proteins, and cells. Angew Chem Int Ed 2008;47:6267–71.

[336]. Khademhosseini A, Langer R. Microengineered hydrogels for tissue engineering. Biomaterials 2007;28:5087–92. [PubMed: 17707502]

[337]. Fukuda J, Khademhosseini A, Yeo Y, Yang X, Yeh J, Eng G, et al. Micromolding of photocrosslinkable chitosan hydrogel for spheroid microarray and co-cultures. Biomaterials 2006;27:5259–67. [PubMed: 16814859]

[338]. Yeh J, Ling Y, Karp JM, Gantz J, Chandawarkar A, Eng G, et al. Micromolding of shape-controlled, harvestable cell-laden hydrogels. Biomaterials 2006;27:5391–8. [PubMed: 16828863]

[339]. Tekin H, Ozaydin-Ince G, Tsinman T, Gleason KK, Langer R, Khademhosseini A, et al. Responsive microgrooves for the formation of harvestable tissue constructs. Langmuir 2011;27:5671–9. [PubMed: 21449596]

[340]. Navaei A, Moore N, Sullivan RT, Truong D, Migrino RQ, Nikkhah M. Electrically conductive hydrogel-based micro-topographies for the development of organized cardiac tissues. RSC Adv 2017;7:3302–12.

[341]. Golden AP, Tien J. Fabrication of microfluidic hydrogels using molded gelatin as a sacrificial element. Lab Chip 2007;7:720–5. [PubMed: 17538713]

[342]. Liu D, Zhang H, Fontana F, Hirvonen JT, Santos HA. Current developments and applications of microfluidic technology toward clinical translation of nanomedicines. Adv Drug Deliv Rev 2018;128:54–83. [PubMed: 28801093]

[343]. Sackmann EK, Fulton AL, Beebe DJ. The present and future role of microfluidics in biomedical research. Nature 2014;507:181–9. [PubMed: 24622198]

[344]. Kane RS, Takayama S, Ostuni E, Ingber DE, Whitesides GM. Patterning proteins and cells using soft lithography. Biomaterials 1999;20:2363–76. [PubMed: 10614942]

[345]. Takayama S, Ostuni E, LeDuc P, Whitesides GM. Laminar flows: subcellular positioning of small molecules. Nature 2001;411, 1016–6. [PubMed: 11429594]

[346]. Chung BG, Flanagan LA, Rhee SW, Schwartz PH, Lee AP, Monuki ES, et al. Human neural stem cell growth and differentiation in a gradient-generating microfluidic device. Lab Chip 2005;5:401–6. [PubMed: 15791337]

[347]. Karimi M, Bahrami S, Mirshekari H, Basri SMM, Nik AB, Aref AR, et al. Microfluidic systems for stem cell-based neural tissue engineering Lab Chip 2016;16:2551–71. [PubMed: 27296463]

[348]. Steinhilber D, Rossow T, Wedepohl S, Paulus F, Seiffert S, Haag R. A microgel construction kit for bioorthogonal encapsulation and pH-controlled release of living cells. Angew Chem Int Ed 2013;52:13538–43.

[349]. Tamayol A, Akbari M, Zilberman Y, Comotto M, Lesha E, Serex L, et al. Flexible pH-sensing hydrogel fibers for epidermal applications. Adv Healthc Mater 2016;5:711–9. [PubMed: 26799457]

[350]. Nakajima S, Kawano R, Onoe H. Stimuli-responsive hydrogel microfibers with controlled anisotropic shrinkage and cross-sectional geometries. Soft Matter 2017;13:3710–9. [PubMed: 28436503]

[351]. Venancio-Marques A, Barbaud F, Baigl D. Microfluidic mixing triggered by an external LED illumination. J Am Chem Soc 2013;135:3218–23. [PubMed: 23350581]

[352]. Bischel LL, Young EWK, Mader BR, Beebe DJ. Tubeless microfluidic angiogenesis assay with three-dimensional endothelial-lined microvessels. Biomaterials 2013;34:1471–7. [PubMed: 23191982]

[353]. Lim D, Lee E, Kim H, Park S, Baek S, Yoon J. Multi stimuli-responsive hydrogel microfibers containing magnetite nanoparticles prepared using microcapillary devices. Soft Matter 2015;11:1606–13. [PubMed: 25594916]

[354]. ter Schiphorst J, Saez J, Diamond D, Benito-Lopez F, APHJ Schenning. Light-responsive polymers for microfluidic applications. Lab Chip 2018;18:699–709. [PubMed: 29431804]

[355]. Jadhav AD, Yan B, Luo RC, Wei L, Zhen X, Chen CH, et al. Photoresponsive microvalve for remote actuation and flow control in microfluidic devices. Biomicrofluidics 2015;9, 034114/1–12. [PubMed: 26180571]

[356]. Murphy SV, Atala A. 3D bioprinting of tissues and organs. Nat Biotechnol 2014;32:773–85. [PubMed: 25093879]

[357]. Cui X, Boland T, D'Lima DD, Lotz MK. Thermal inkjet printing in tissue engineering and regenerative medicine. Recent Pat Drug Deliv Formul 2012;6:149–55. [PubMed: 22436025]

[358]. Iwami K, Noda T, Ishida K, Morishima K, Nakamura M, Umeda N. Bio rapid prototyping by extruding/aspirating/refilling thermoreversible hydrogel. Biofabrication 2010;2, 014108/1–5. [PubMed: 20811123]

[359]. Guillotin B, Souquet A, Catros S, Duocastella M, Pippenger B, Bellance S, et al. Laser assisted bioprinting of engineered tissue with high cell density and microscale organization. Biomaterials 2010;31:7250–6. [PubMed: 20580082]

[360]. Wang Z, Abdulla R, Parker B, Samanipour R, Ghosh S, Kim K. A simple and high-resolution stereolithography-based 3D bioprinting system using visible light crosslinkable bioinks. Biofabrication 2015;7, 045009/1–10. [PubMed: 26696527]

[361]. Miao S, Castro N, Nowicki M, Xia L, Cui H, Zhou X, et al. 4D printing of polymeric materials for tissue and organ regeneration. Mater Today 2017;20:577–91.

[362]. Yang GH, Yeo M, Koo YW, Kim GH. 4D Bioprinting: technological advances in biofabrication. Macromol Biosci 2019;0, 1800441/1–10.

[363]. Ionov L 4D Biofabrication: materials, methods, and applications. Adv Healthc Mater 2018;7, 1800412/1–14.

[364]. Momeni F, Mehdi M, Hassani NS, Liu X, Ni J. A review of 4D printing. Mater Design 2017;122:42–79.

[365]. Kolesky DB, Truby RL, Gladman AS, Busbee TA, Homan KA, Lewis JA. 3D Bioprinting of vascularized, heterogeneous cell-laden tissue constructs. Adv Mater 2014;26:3124–30. [PubMed: 24550124]

[366]. Norotte C, Marga FS, Niklason LE, Forgacs G. Scaffold-free vascular tissue engineering using bioprinting. Biomaterials 2009;30:5910–7. [PubMed: 19664819]

[367]. Sydney Gladman A, Matsumoto EA, Nuzzo RG, Mahadevan L, Lewis JA. Biomimetic 4D printing. Nat Mater 2016;15:413–8. [PubMed: 26808461]

[368]. Kirillova A, Maxson R, Stoychev G, Gomillion CT, Ionov L. 4D Biofabrication using shape-morphing hydrogels. Adv Mater 2017;29, 1703443/1–8.

[369]. Villar G, Graham AD, Bayley H. A tissue-like printed material. Science 2013;340:48–52. [PubMed: 23559243]

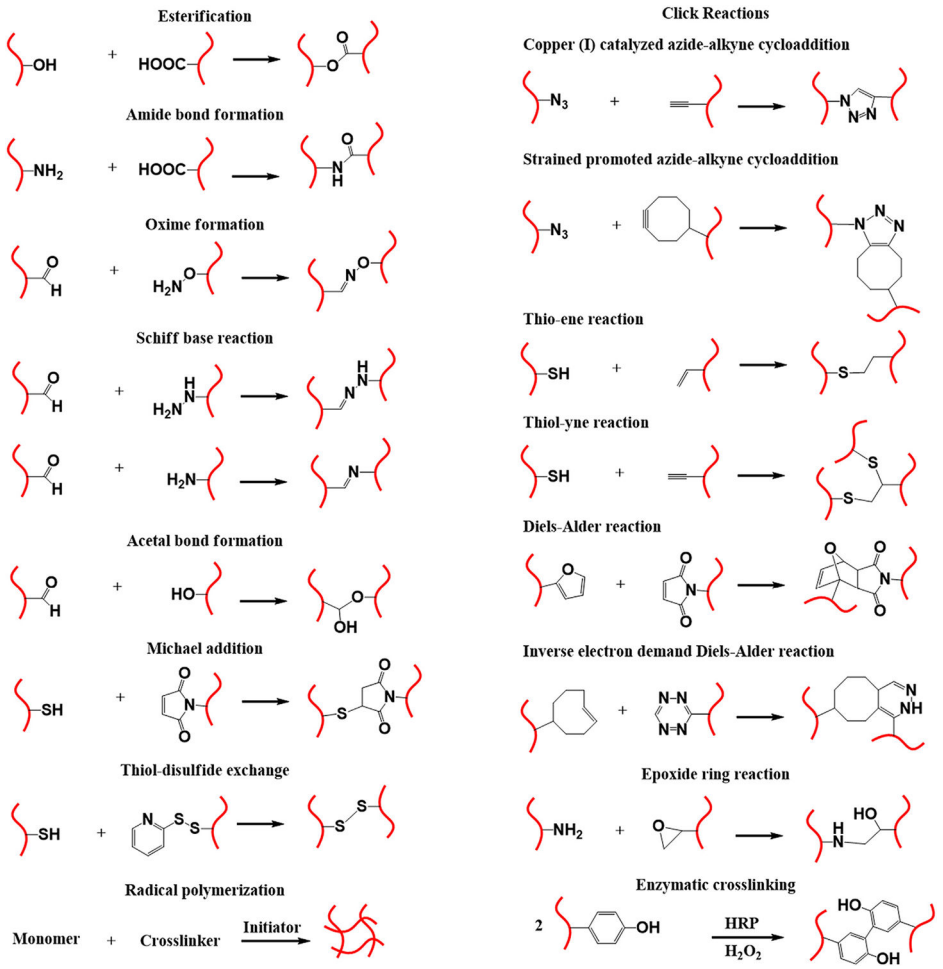

Fig. 1.

Schematic representation of chemical crosslinking strategies employed in the construction of 3D hydrogel scaffolds, and the chemistries implicated in functionalization/conjugation of biomolecules.

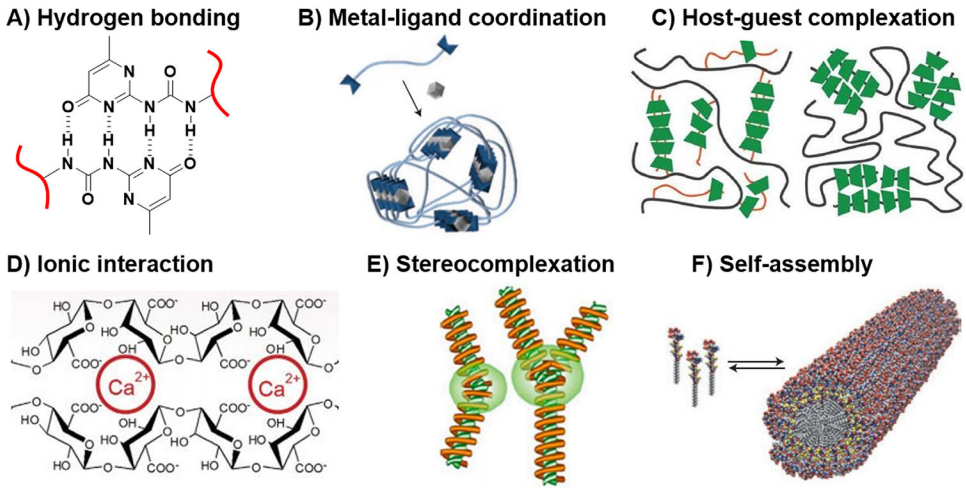

Fig. 2.

Schematic illustration of physical crosslinking strategies of hydrogels: (A) hydrogen bonding, (B) metal-ligand coordination, (C) host-guest complexation, (D) ionic interaction, (E) stereocomplexation, and (F) self-assembly. B, F: [91], Copyright 2015. Reproduced with permission from Nature publishing group. C: [86], Copyright 2012. Reproduced with permission from the Royal Society of Chemistry. D: [111], Copyright 2014. Reproduced with permission from Elsevier Inc. E: [112], Copyright 2015. Reproduced with permission from MDPI.

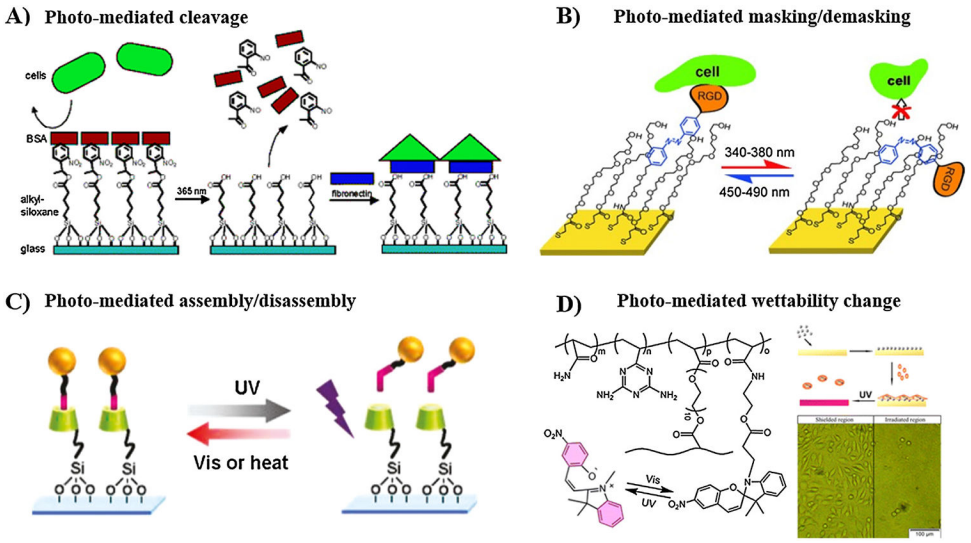

Fig. 3.

Manipulation of cell adhesion using photo-responsive substrates. (A) Photocleavage to induce the release of non-adhesive BSA protein to enable subsequent immobilization of cell-adhesive FN. (B) Photoisomerization of azobenzene-containing SAMs for masking/demasking of cell adhesion RGD ligand within the PEG layer. (C) Photoreversible assembly/disassembly of β-CD-azobenzene host-guest complex, where the guest azobenzene is modified with cell adhesive peptide. (D) Photo-mediated isomerization of spiropyran, and thus switching the surface wettability to reversibly attach and release fibroblast L929 cells. A: [234], Copyright 2004. Reproduced with permission from American Chemical Society. B: [235], Copyright 2017. Reproduced with permission from John Wiley and Sons Inc. C: [236], Copyright 2011. Reproduced with permission from American Chemical Society. D: [174], Copyright 2014. Reproduced with permission from American Chemical Society.

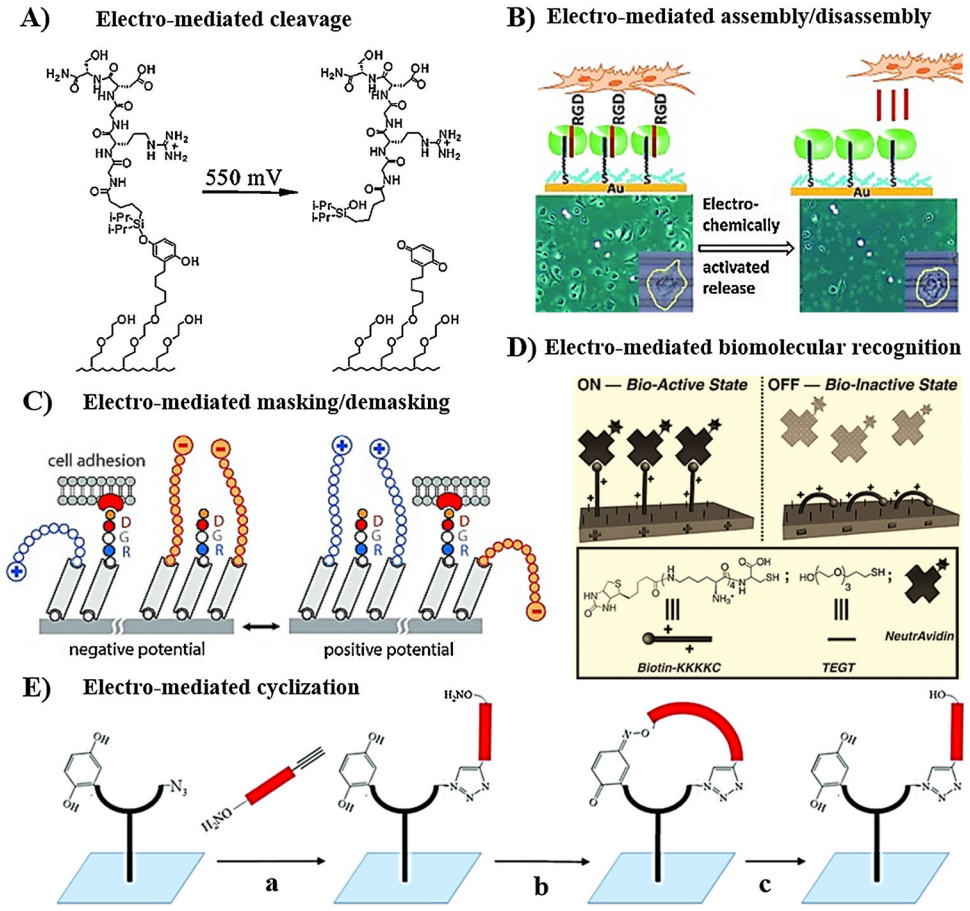

Fig. 4.

Modulation of cell adhesion using electro-responsive substrates. (A) Electro-cleavage of cell adhesion peptide upon oxidation of silyl hydroquinone to benzoquinone. (B) Electro-mediated assembly/disassembly of WGG-modified RGD (guest) to Cucurbit [8]uril (host) immobilized on a gold substrate. (C) Electro-mediated masking/demasking of RGD ligand spatially. (D) Electro-mediated “On” and “OFF” switching of biomolecular recognition between positively charged Biotin-KKKKC peptide and Avidin. (E) Electro-switchable cell adhesion: (a) functionalization of the substrate with alkoxyamine-RGD-alkyne via Huisgen cycloaddition; (b) electro-mediated oxidation of hydroquinone to benzoquinone induced oxime ligation between alkoxyamine and benzoquinone to form a cyclic structure that enhances cell spreading; (c) electro-reduction induced opening of the cyclic structure. A: [199], Copyright 2003. Reproduced with permission from American Chemical Society. B: [241], Copyright 2012. Reproduced with permission from John Wiley and Sons Inc. C: [243], Copyright 2012. Reproduced with permission from John Wiley and Sons Inc. D: [245], Copyright 2010. Reproduced with permission from John Wiley and Sons Inc. E: [247], Copyright 2011. Reproduced with permission from American Chemical Society.

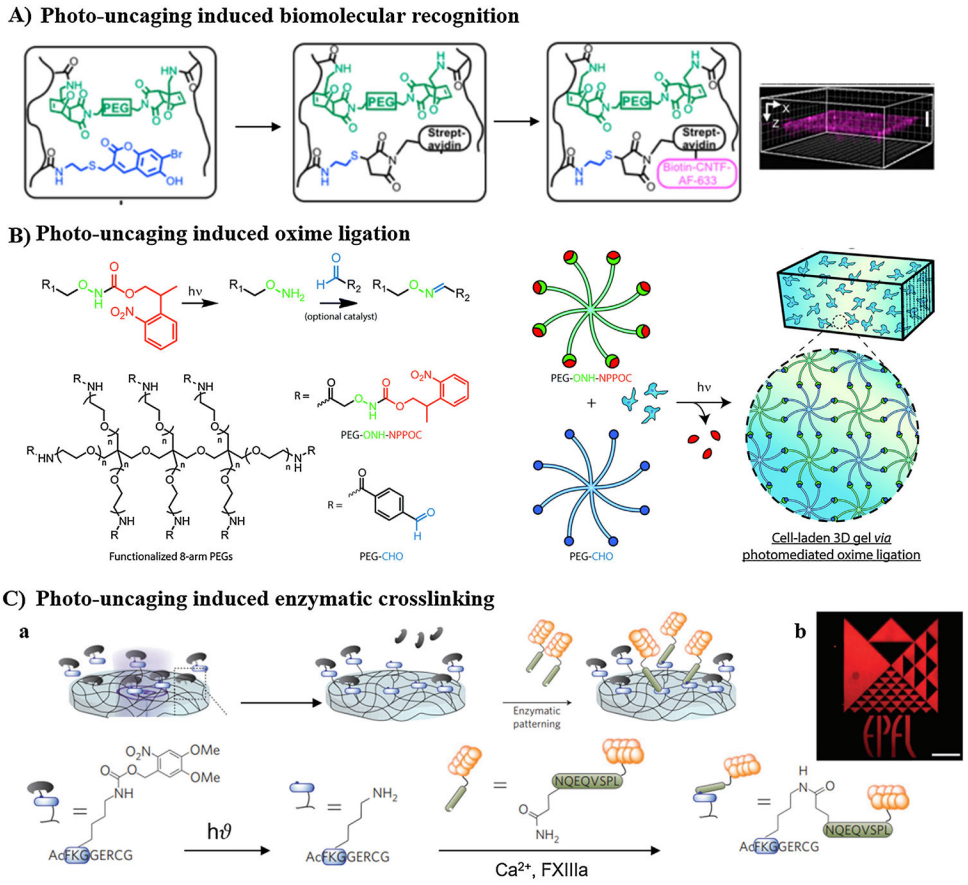

Fig. 5.

Irreversible modulation of biochemical cues involving photocleavage of caged functionalities. (A) Photo-induced biomolecular recognition: photocleavage of coumarin-caged thiol induced immobilization of streptavidin-maleimide via Michael addition reaction, and then enabled on-demand 3D patterning of biotin-modified protein within HA-based cryogel. (B) Photo-induced oxime ligation: photocleavage of NPPOC-protected alkoxyamine terminals of multi-arm PEG crosslinker induced oxime ligation with multiarm PEG-aldehyde. (C) Photo-induced enzymatic crosslinking: (a) photodeprotection of lysine-amine of FXIIIa substrate induced enzymatic crosslinking with glutamine-carboxamide of $VEGF_{121}$ protein; (b) representative image of well-tuned 3D patterning using photolithography. A: [183], Copyright 2016. Reproduced with permission from American Chemical Society. B: [182], Copyright 2016. Reproduced with permission from Royal Society of Chemistry. C: [254], Copyright 2013. Reproduced with permission from Nature publishing group.

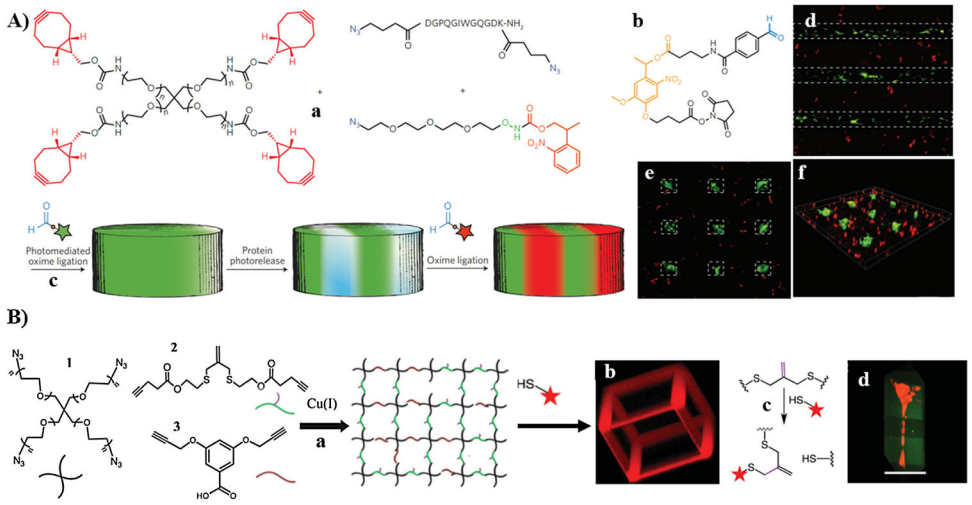

Fig. 6.

Reversible modulation of biochemical cues. (A) photoreversible patterning of proteins: (a) development of enzymatically cleavable PEG-based hydrogel via SPAAC in the presence of NPPOC-photocaged alkoxyamine functionalities; (b) reaction of protein with CHO-oNB-NHS enabled photo-patternability via on-demand photocleavable oNB moieties; (c) schematic representation of dual-protein patterning; (d) hMSC differentiation on vitronectin-patterned hydrogels showing positive osteocalcein staining on the patterned area only; (e and f) after photo-removal of vitronectin, the confinement of osteocalein staining to the patterned islands. (B) Reversible manipulation of biochemical environments via ligand exchange using allyl sulfide functionalities: (a) PEG hydrogel formation via Cu catalyzed click reaction; (b) cage pattern formed by irradiation with 720 nm two-photon light; (c) bioactive ligand exchange mechanism; (d) hMSC stained with tracker red encapsulated on green rectangular fluorescent RGD-modified hydrogel, in which the fluorescent RGD in the middle part was replaced with non-fluorescent RGD. A: [181], Copyright 2015. Reproduced with permission from Nature publishing group. B: [186], Copyright 2014. Reproduced with permission from John Wiley and Sons Inc.

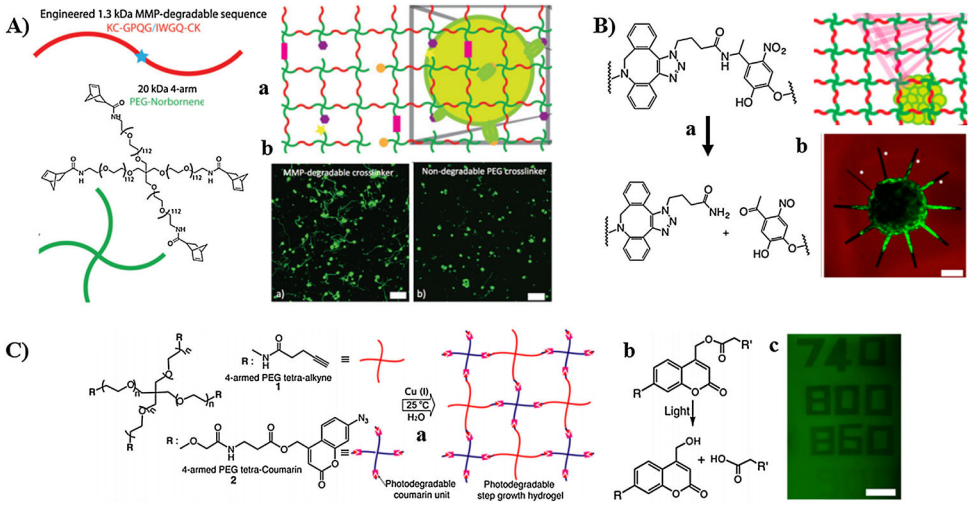

Fig. 7.

Irreversible modulation of mechanical stiffness via stimuli-induced softening of the hydrogel scaffolds. (A) Softening via enzymatic degradation: (a) development of MMP-cleavable PEG hydrogel via thiol-ene reaction; (b) stem cell-derived motor neurons on MMP-degradable PEG hydrogels showed high axon outgrowth, while those encapsulated on non-degradable PEG hydrogel failed to extend axons. (B) Softening of oNB-containing PEG hydrogel via photocleavage of oNB amide linkages using 365 nm light (a); motor neurons extended axons on the fully eroded channels, while failed to migrate through the non-fully degradable channels (b). (C) Photodegradable PEG hydrogel based on coumarin group was developed via Cu catalyzed click reaction (a); softening of PEG-based hydrogel via photocleavage of coumarin ester linkages (b); spatiotemporal degradation using two-photon lights of 740, 800, 860 nm eliminated the inherent fluorescence of coumarin from the degraded pattern (c). A: [262], Copyright 2013. Reproduced with permission from Royal Society of Chemistry. B: [178], Copyright 2014. Reproduced with permission from American Chemical Society. C: [179], Copyright 2014. Reproduced with permission from American Chemical Society.

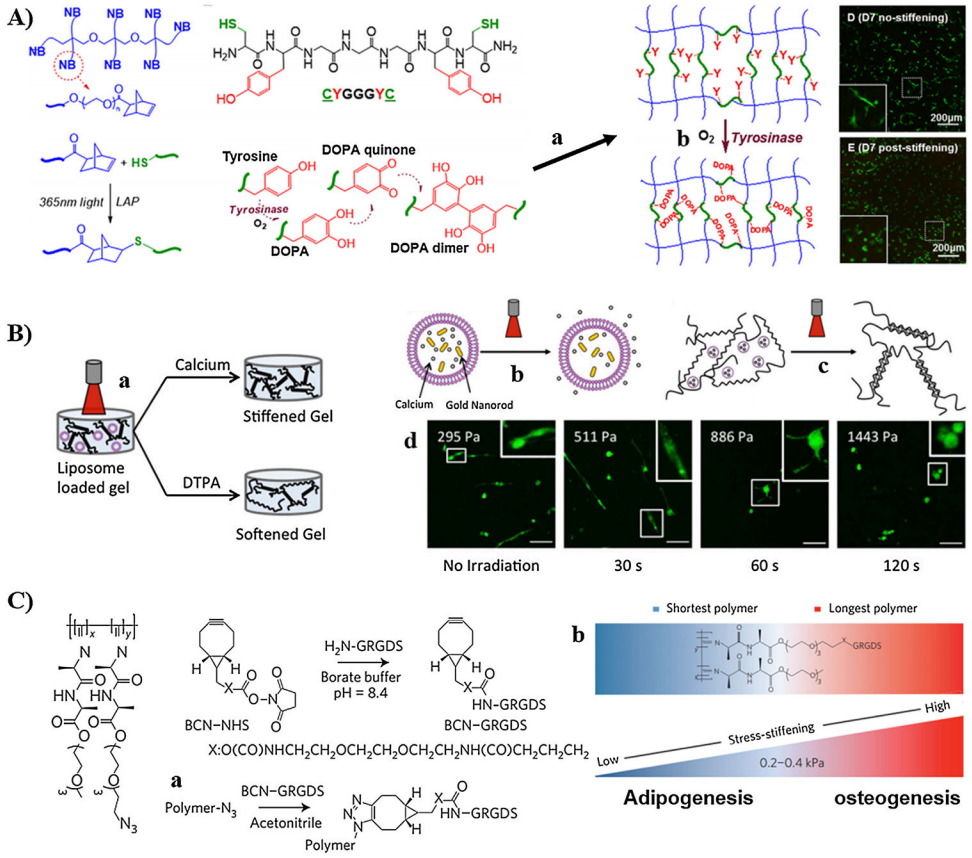

Fig. 8.

Irreversible modulation of mechanical stiffness via stimuli-induced stiffening of the hydrogel scaffolds. (A) Tyrosinase-mediated stiffening: (a) the hydrogel developed via thiol-ene reaction of multiarm PEG-norbornene and bis-cysteine-bis-tyrosine peptide (CYGGGYC); (b) oxidation of tyrosine to DOPA dimer by tyrosinase; (c) live-dead staining of PSCs encapsulated on PEG-peptide hydrogel, before (top image) and after (below image) stiffening, showed more spreading of cells before stiffening. (B) Matrix stiffening modulated via photothermal release of Ca^{2+}: (a) liposome loaded with gold and Ca^{2+} was encapsulated within Alginate gel; (b) liposome releases Ca^{2+} upon UV irradiation; (c) the released Ca^{2+} induced further crosslinking of alginate gel; (d) mechanical stiffness increased with increasing irradiation time, and NIH 3T3 cell spreading was hindered. (C) Mechanical modulation via stress stiffening: (a) functionalization of azide-terminated PICs of different chain lengths with cell-adhesive peptides via SPAAC; (b) influence of stress stiffening of functionalized PICs on hMSCs' fate. A: [275], Copyright 2016. Reproduced with permission from Elsevier Inc. B: [37], Copyright 2015. Reproduced with permission from the National Academy of Science. C: [208], Copyright 2016. Reproduced with permission from Nature publishing group.

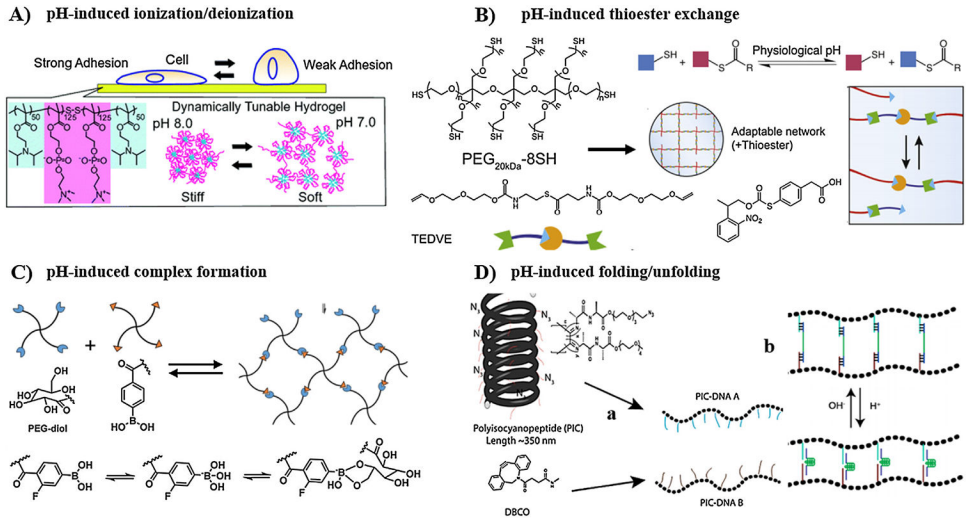

Fig. 9.

Reversible modulation of mechanical stiffness using different types of pH-responsive hydrogels. (A) Mechanical modulation via pH-responsive $PDPA_{50}$-*b*-$PMPC_{250}$-*b*-$PDPA_{50}$ triblock copolymer based on ionizable functionalities. (B) Mechanical modulation via pH-induced thioester exchange. (C) pH-induced reversible binding between phenylboronic acid- and *cis*-diol-containing PEG macromers. (D) Mechanical modulation via pH-dependent folding/unfolding of DNA-incorporating hydrogels: (a) development of two different DNA-conjugated PIC via SPAAC; (b) hydrogel formation using DNA crosslinker incorporating the complementary sequence of the other DNAs. A: [278], Copyright 2011. Reproduced with permission from American Chemical Society. B: [147], Copyright 2018. Reproduced with permission from Elsevier Inc. C: [279], Copyright 2015. Reproduced with permission from John Wiley and Sons Inc. D: [280], Copyright 2017. Reproduced with permission from American Chemical Society.

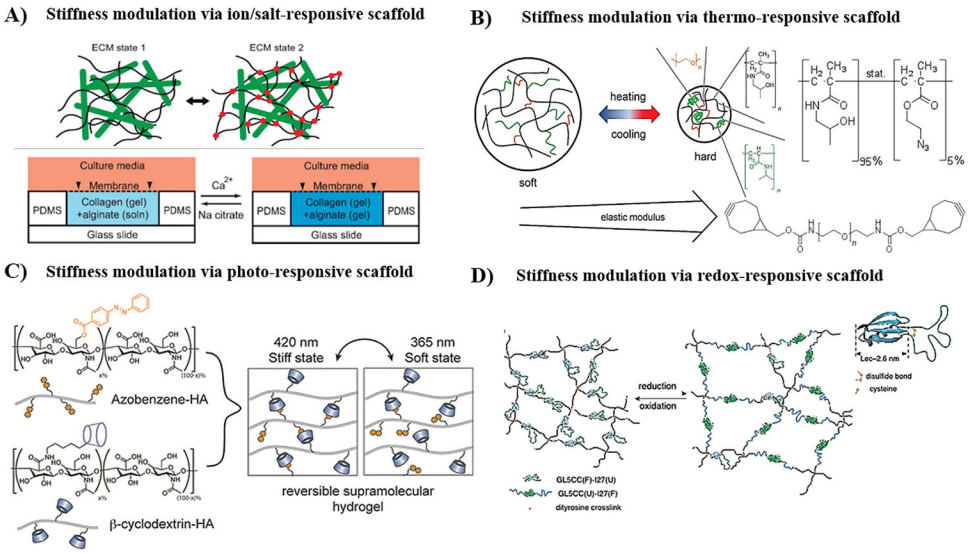

Fig. 10.

Reversible modulation of mechanical microenvironment using stimuli-responsive scaffolds. (A) Modulation of matrix mechanics using ion/salt-responsive scaffold, in which Ca^{2+} and sodium citrate were used to reversibly crosslink/de-crosslink alginate-collagen gel. (B) Thermo-responsive hybrid microgel developed via SPAAC between azide-containing poly(HPMA-*co*-HEMA) copolymer, cyclooctyne-terminated PNIPAM, and PEG-bis(cyclooctyne) reversibly switches the mechanical stiffness with temperature. (C) Photoreversible modulation of matrix mechanics based on the host-guest pairing of azobenzene and β-CD-containing HA. (D) Redox-responsive hydrogel switches between two mechanical states upon reduction of the disulfide bond, which induces the transition of folded protein domains to unfolded states. A: [282], Copyright 2010. Reproduced with permission from John Wiley and Sons Inc B: [283], Copyright 2015. Reproduced with permission from John Wiley and Sons Inc C: [99], Copyright 2018. Reproduced with permission from the American Chemical Society D: [151], Copyright 2014. Reproduced with permission from John Wiley and Sons Inc.

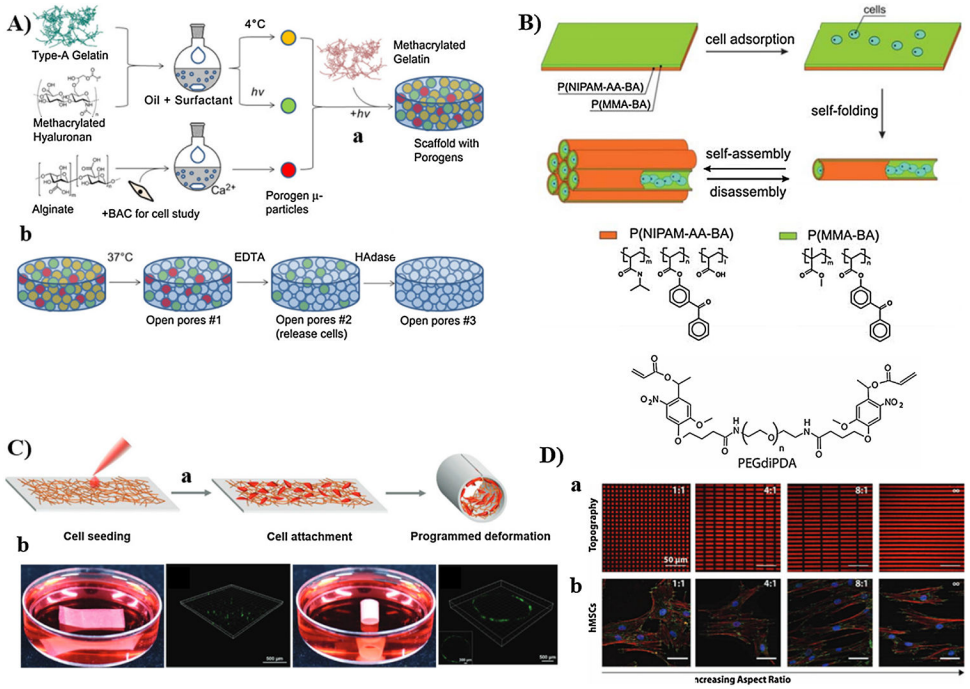

Fig. 11.

(A) Scheme depicting dynamic modulation of scaffold porosity using stimuli-responsive porogens: (a) encapsulation of three stimuli-responsive porogens (gelatin, methacrylated hyaluronan, and alginate) within crosslinked gelatin; (b) dynamic macropore formation using temperature, EDTA, and Hyaluronidase stimuli for temporal sequential removal of porogens. (B) Dynamic manipulation of pore geometry using thermo-responsive hydrophilic PNIPAM-based copolymer and hydrophobic PMMA-based copolymer, to induce self-assembly of 3D structure with tubular aligned pores. (C) Illustration of topography manipulation using shape-morphing scaffolds: (a) the temporary planar scaffold cultured with HUVECs self-rolled at physiological temperature to form permeant 3D tubular structure; (b) calcein staining of HUVECs shows the tubular organization of cells on the 3D tubular scaffold as compared to the 2D planar scaffold. (D) Influence substrate topography on hMSCs migration: (a) substrates of different aspect ratio developed by photolithography using photodegradable PEG hydrogel; (b) immunostaining for cytoskeleton components to show the increasing alignment of hMSCs with increasing the aspect ratio. A: [295], Copyright 2013. Reproduced with permission from Elsevier Inc. B: [305], Copyright 2013. Reproduced with permission from Royal Society of Chemistry. C: [308], Copyright 2015. Reproduced with permission from John Wiley and Sons Inc. D: [309], Copyright 2013. Reproduced with permission from John Wiley and Sons Inc.

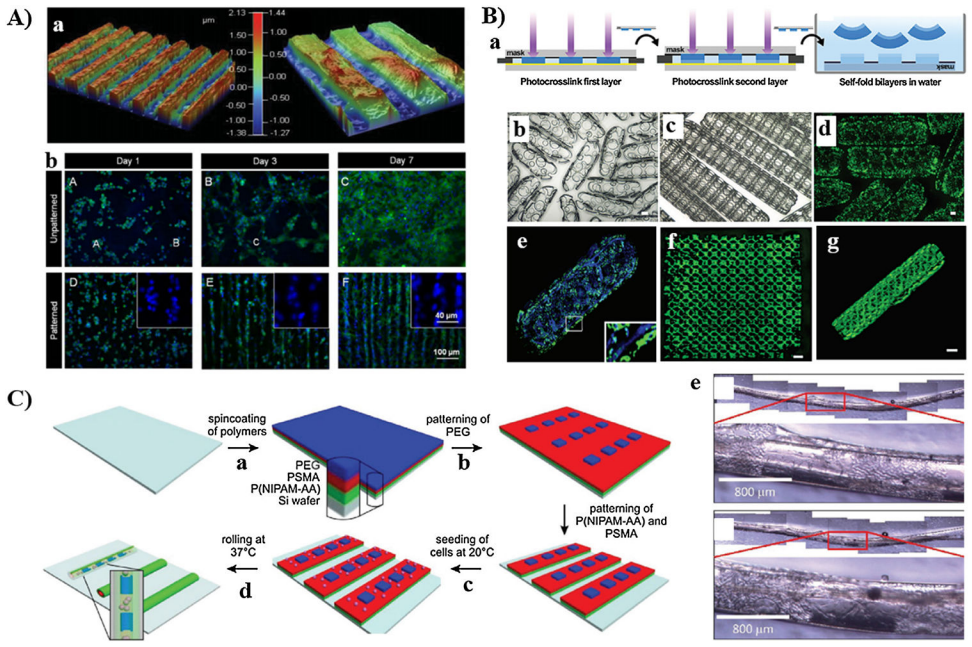

Fig. 12.

Integration of smart materials with photolithography: (A) Development of photopatterned GelMA hydrogel by spatial degradation of photocleavabie oNB ester linkages (a); DAPI (blue)/α-actinin (green) staining of cardiomyocytes cultured on non-patterned (top images) and patterned GelMA (bottom images) at days 1, 3, and 7 (b). (B) 4D biofabrication of self-folding PEG bilayers: (a) irradiation through photomask to crosslink the first and second PEG diacrylate layers of different molecular weights; self-folding of PEG bilayers into small (b) and large (c) cylindrical hydrogels with patterned holes; (d) calcein AM staining of fibroblast cells encapsulated within cylindrical cell-laden hydrogel; (e) Multi-culture of Hoechest-stained (blue) and calcein Am-stained (green) fibroblast within the hydrogel cylinder; (f and g) calcein AM staining of β-TC-6 cells encapsulated on planar PEG monolayer and cylindrical PEG bilayers, respectively. (C) Development of micropatterned trilayers: (a) sequential deposition of poly(NIPAM-*co*-AA) and PSMA on Si wafer; (b) photopatterning of PEG macromer; (c) seeding of F3T3 cells at room temperature; (d) folding of trilayers into tubular structure; (e) bright field images depicting spatial patterning of F3T3 cells inside the 3D rolled tubes. A: [320], Copyright 2014. Reproduced with permission from John Wiley and Sons Inc. B: [324], Copyright 2013. Reproduced with permission from John Wiley and Sons Inc. C: [325], Copyright 2018. Reproduced with permission from John Wiley and Sons Inc.

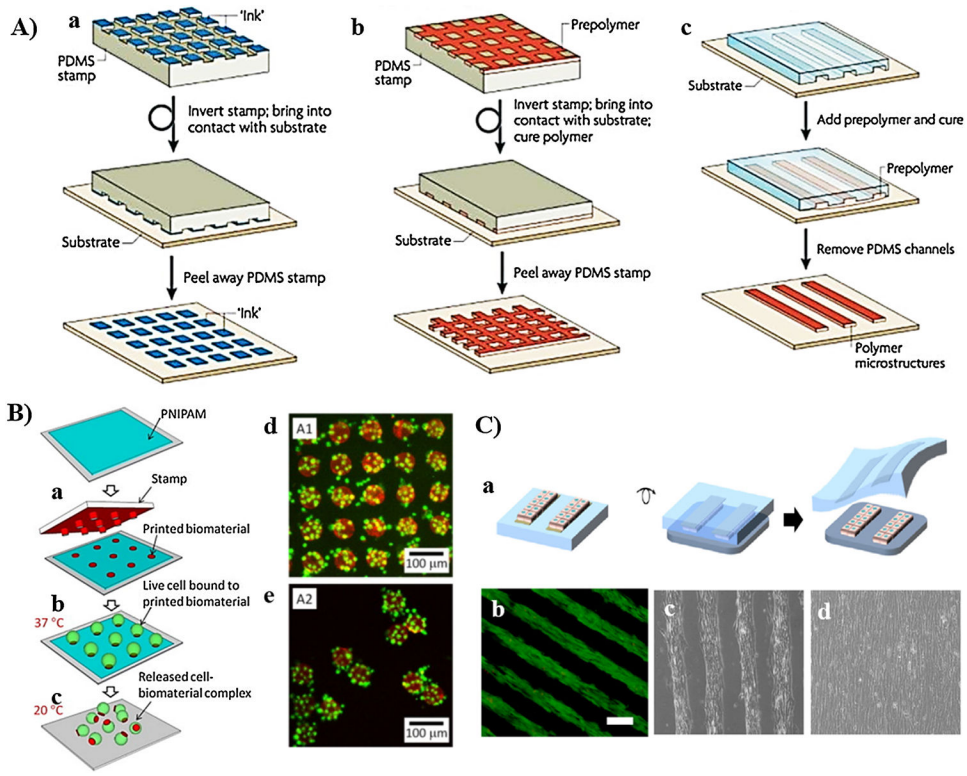

Fig. 13.

(A) Pattern generation using soft lithographic techniques: (a) microcontact printing; (b) microfluidic channels; (c) micromolding. (B) Functionalization of cells using microcontact printed nano-/microparticles on PNIPAM-coated glass: (a) transfer of nano-/microparticles from PDMS stamp to PNIPAM; (b) seeding of cells on the printed particles; (c) detachment of functionalized cells by decreasing temperature and dissolution of PNIPAM; fluorescence images of mESCs (green) seeded on the pattern of the particles (orange) before (d) and after (e) detachment. (C) Translocation of HDFBs cell strips from thermo-responsive tetronic hydrogel patterned with polydopamine to FN-coated glass by decreasing temperature (a), live-dead and phase images of the translocated HDFBs strips on glass (b, c); migration of cells after 48 h of translocation (d). A: [327], Copyright 2007. Reproduced with permission from Nature publishing group. B: [329], Copyright 2014. Reproduced with permission from Elsevier Inc. C: [332], Copyright 2017. Reproduced with permission from Elsevier Inc.

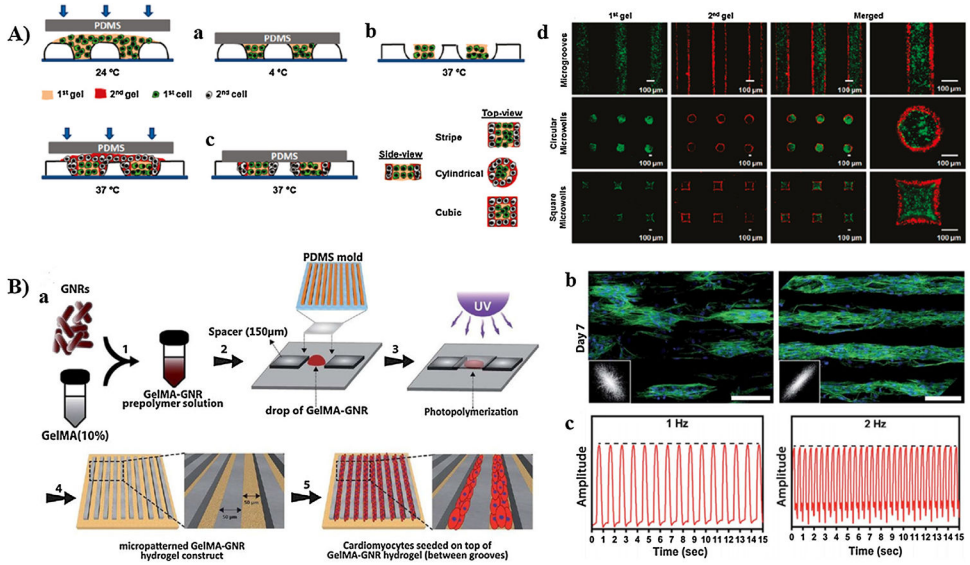

Fig. 14.

(A) Development of multicomponent hydrogels using stimuli-responsive PNIPAM-based micromold: (a) crosslinking of first gel at 4 °C; (b) shrinking of PNIPAM mold at 37 °C to create more space; (c) filling the new space with second gel and crosslinking at 37 °C; (d) patterning of two different microparticles using micromolds of circular, square, and microgroove shapes. (B) Development of electroactive micropatterned hydrogel via photocrosslinking of GelMA-GNR solution in micropatterned PDMS mold, and then seeding cardiomyocytes on microgroove hydrogel (a); F-actin staining of cardiac tissues at day 7 on non-electroactive GelMA (left image) and electroactive GelMA-GNR (right image), respectively (b); beating behavior of cardiac tissues on GelMA-GNR at 1 Hz (left image) and 2 Hz (right image), respectively (c). A: [49], Copyright 2011. Reproduced with permission from American Chemical Society. B: [340], Copyright 2017. Reproduced with permission from Royal Society of Chemistry.

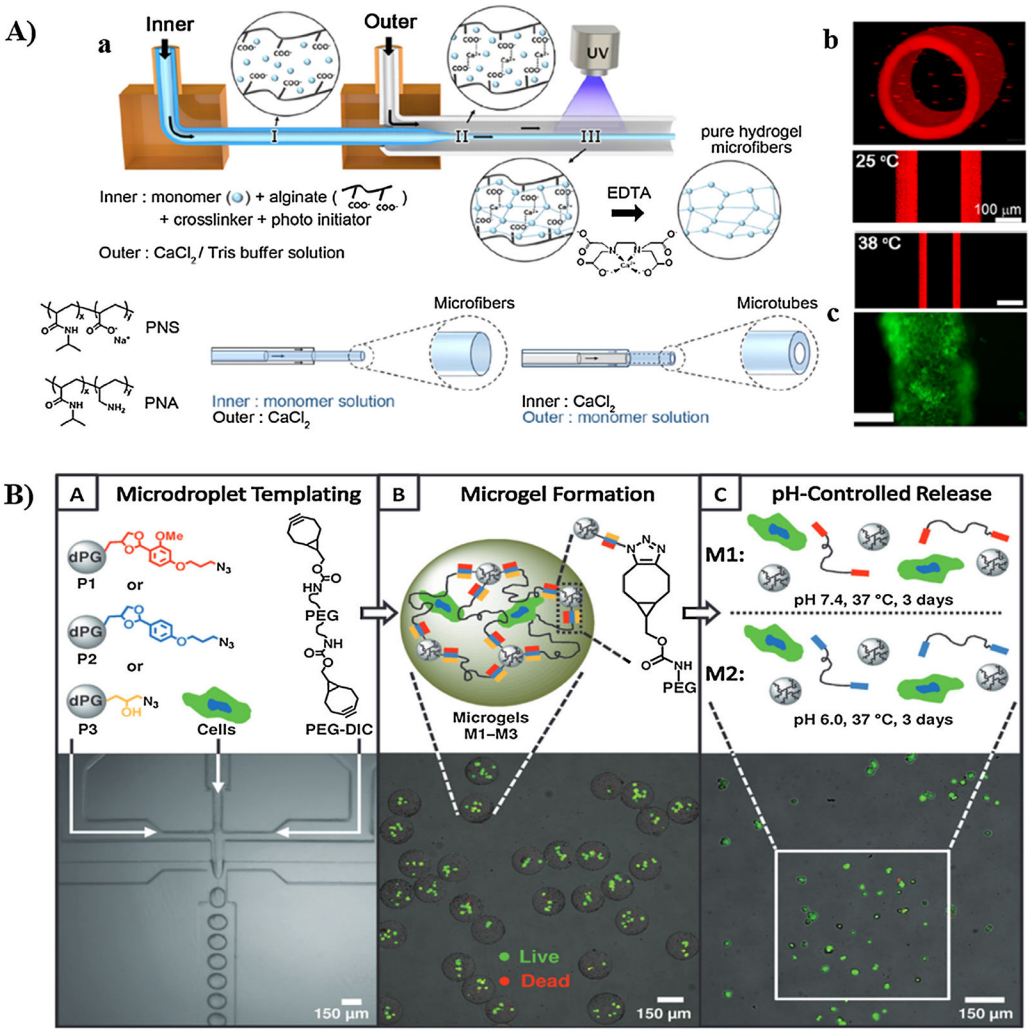

Fig. 15.

Integration of stimuli-responsive polymers with microfluidic technique: (A) Development of thermo-responsive microfibers/tubes by the coaxial flow of inner and outer solutions (a); reversible changes of tube diameters with temperature (b); fluorescence image of Hep G2 cells cultured on microfibers (c). (B) Development of pH-responsive cell-loaded microgels (a); live-dead image of NIH 3T3 cells encapsulated within microgels (b); pH-triggered degradation of microgels, and hence release of NIH 3T3 cells (c). A: [47], Copyright 2018. Reproduced with permission from American Chemical Society. B: [348], Copyright 2013. Reproduced with permission from John Wiley and Sons Inc.

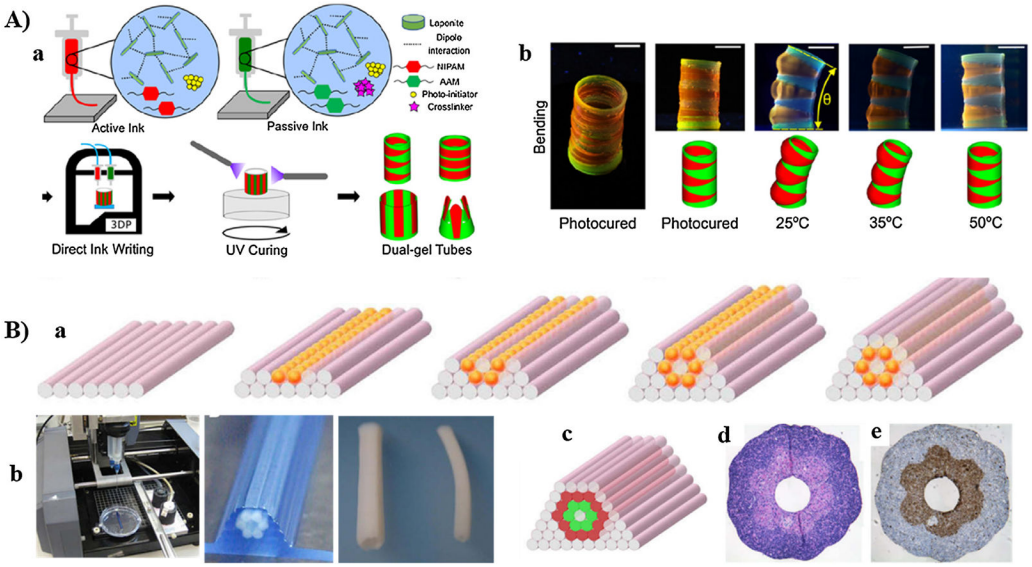

Fig. 16.

(A) 4D printing of thermo-responsive bioinspired tubes (a); bending of the tubes at different temperatures (b). (B) Development of vascular construct using thermo-responsive agarose template: (a) layer-by-layer deposition of agarose rods and cells; (b) fabrication of hollow tubular construct of pig smooth muscle cells. A: [46], Copyright 2019. Reproduced with permission from American Chemical Society. B: [366], Copyright 2009. Reproduced with permission from Elsevier Inc.

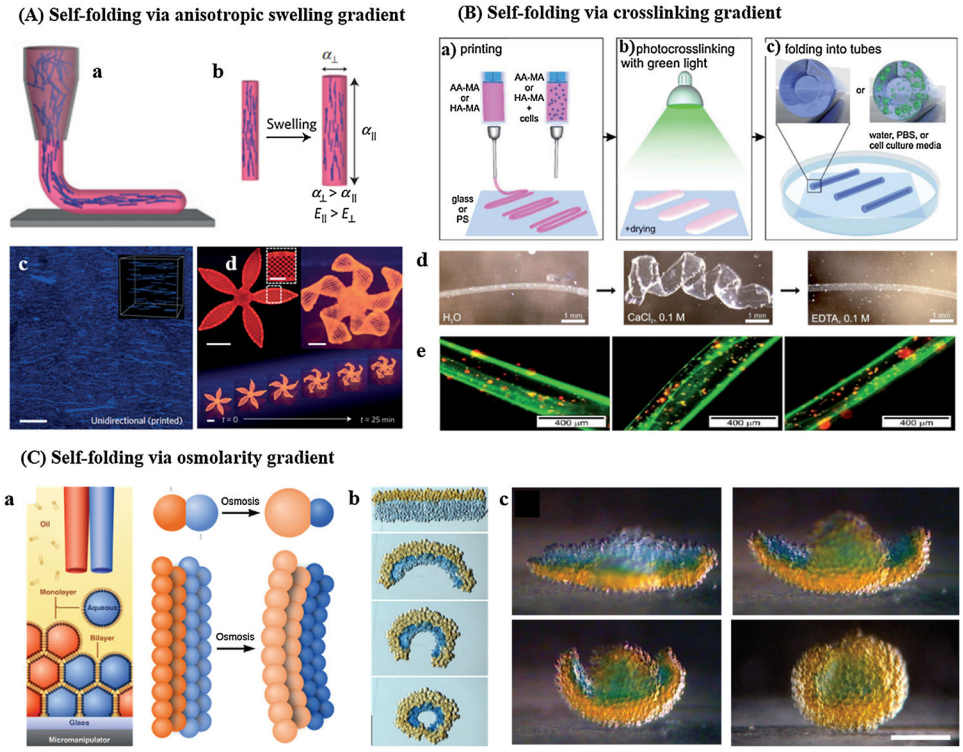

Fig. 17.

4D bioprinting of shape-morphing structures capable of self-transformation with intrinsic stimuli. (A) Biomimetic 4D printing of self-folding objects via anisotropic swelling: (a) 4D printing induce shear-induced alignment of cellulose microfibers; (b) anisotropic swelling in the longitudinal direction; (c) Blue staining of aligned printed fibers; (d) anisotropic swelling trigger folding of the printed pattern into the flower-shaped structure. (B) 4D biofabrication of Ca^{2+} responsive cell-laden hollow tubes: (a) printing of AA-MA or HA-MA in presence/absence of cells; (b) crosslinking of the printed films via irradiation with visible light; (c) spontaneous folding into tubular structures in aqueous solution; (d) reversible unfolding (middle image)/folding (right image) in using Ca^{2+} and EDTA, respectively; (e) live/dead assay of cells encapsulated into self-folded tubes after 1 (left image), 2 (middle image), and 7 (right image) days of culture. (C) Self-folding via osmolarity gradient: (a) printing of droplet network using lipid-coated aqueous droplets of different osmolarities to trigger bending via swelling/shrinking; (b) and (c) self-folding of the printed strip and slower-shaped bilayers driven by different osmolarities, respectively. A: [367], Copyright 2016. Reproduced with permission from Nature publishing group. B: [368], Copyright 2017. Reproduced with permission from John Wiley and Sons Inc. C: [369], Copyright 2013. Reproduced with permission from the American Association for the Advancement of Science.